DEVELOPMENT AND APPLICATION OF AN INTERACTIVE INTEGRATED SYSTEM FOR MODELING SALINE WATER INTRUSION IN GROUNDWATER

by

Ming-Shu Tsou

Kansas Geological Survey
Open-file Report
98-21

Disclaimer

DEVELOPMENT AND APPLICATION OF AN INTERACTIVE INTEGRATED SYSTEM FOR MODELING SALINE WATER INTRUSION IN GROUNDWATER

by

Ming-Shu Tsou

B. S., Tamkang University, Taiwan, 1990
M. S., National Taiwan University, Taiwan, 1992

Submitted to the Department of Civil Engineering and the Faculty of the Graduate School of the University of Kansas in partial fulfillment of the requirement for the degree of Doctor of Philosophy.

Professor in Charge

Committee Members

Date Defended: March 31, 1998

ABSTRACT

The Arkansas River entering the western border of Kansas from Colorado is one of the most saline rivers in the United States. Most of the saline water entering Kansas infiltrates from the river channel and irrigation diversions into the alluvial and Ogallala aquifers, referred to as the High Plains aquifer. The river water with high sulfate concentration enters the aquifer and migrates outward and downward in the High Plains aquifer and pollutes many wells located in the area. However, the exact mechanism of the spreading of the saline water from the upper aquifer to the lower aquifer and the severity of the pollution is not well understood and needs investigation for long-term management of the aquifer system.

Through the years, infiltration of saline river and ditch irrigation water has produced highly polluted, shallow perched water with sulfate concentrations generally in the range of 2000 mg/L. One path for the saline water in the perched aquifer to reach the underlying Ogallala aquifer is through the leaky clay layer under the perched zone. The other possible path for the perched saline water to reach the freshwater of the Ogallala is through the unsealed gravel packs of irrigation wells. These possible mechanisms of saline water intrusion are investigated based on a conceptual model which is solved numerically. A sensitivity analysis is conducted for estimating the effects of uncertainties in the model parameters on the numerical results.

The lithologic data available are incorporated in the inverse solution procedure for parameter identification. Based on the lithologic data, the three-dimensional structure of the aquifer can be estimated using spatial interpolation. The unknown model parameters, namely, hydraulic conductivity and specific yield, in the formulation are directly related to different geological materials existing in the aquifer. Thus, the nonuniqueness of the estimated set of parameters in the inverse problem can be mitigated.

A general purpose system for modeling groundwater is developed. The system operates in the GIS environment and integrates spatial databases (ARC/INFO), groundwater models, and parameter identification for model calibration and simulation through a graphical user interface (GUI) customized within ARCVIEW. The advantages of this system are: 1. The system is interactive and user-friendly. 2. Laborious and time-consuming tasks in data handling are avoided. 3. Results are visually displayed for comparison. 4. The system can easily include any other numerical models for solving problems of user's interest.

The integrated system is applied to an investigation of the saline water intrusion into groundwater near Deerfield, Kansas. Since no field data are available at the present time for model validation, numerical results obtained can only be viewed as helpful suggestions in identification of the relative importance of the mechanisms for the contaminant spreading in the groundwater and the effect of various model parameters on the contaminant transport.

DEDICATION

To my parents, my wife and, especially, Shakyamuni Buddha who shows me a path to ultimate happiness - " True sincerity, purity of mind, compassion and be mindful of Amitabha Buddha.".

ACKNOWLEDGMENTS

I wish to express my sincere appreciation to Dr. Yun-Sheng Yu and Dr. Donald O. Whittemore for their time, advice, and encouragement throughout this study. Without Dr. Yu's invaluable guidance and patience, this dissertation would not be completed. Dr. Whittemore's support and trust are greatly acknowledged.

Appreciation is extended to Dr. Ernest C. Pogge, Dr. A. David Parr, and Dr. Bruce M. McEnroe for serving as the committee members. The financial support by Kansas Geological Survey and the assistance of Dr. Ricardo A. Olea, Dr. Xiaodong Jian, Dr. Tainshing Ma, Jinwu Ma, Tiraz Birdie, Dave P. Young and Julie Grauer are also acknowledged.

Finally, my deepest appreciation goes to my parents and my wife, Mei-Hui, for their encouragement and understanding during my study. Also, I would like to express my gratitude to my brother and my sisters for their moral support.

Contents

List of Figures

List of Tables

I. INTRODUCTION

The Arkansas River entering the western border of Kansas from Colorado is one of the most saline rivers in the United States. Figure 1.1 shows a plot of sulfate concentration versus river discharge near Coolidge located in Kansas near the border with Colorado. The high sulfate concentration reaches a maximum of 2500 mg/L at low discharge. The average discharge near Coolidge is about 5.72 m^3/sec (U.S.G.S. Water Resources Data, 1995). The flow has varied widely from 4474 m^3/sec in 1965 to many days with no flow in 1903, 1954, 1960. At the average discharge, the corresponding sulfate concentration is usually greater than 2000 mg/L. Most of the saline water entering Kansas infiltrates from the river channel and irrigation diversions into the alluvial and Ogallala aquifers, referred to as the High Plains aquifer. The saline river water enters the aquifer and migrates outward and downward in the High Plains aquifer and pollutes many wells located in the area. The saline river water is the main source of high sulfate concentration to the High Plains aquifer (Whittemore et al., 1996). However, the exact mechanism of the spreading of the saline water from the upper aquifer to the lower aquifer and the severity of the pollution is not well understood and needs investigation for long-term management of the aquifer system.

Through the years, infiltration of saline river and ditch irrigation water has polluted shallow alluvial aquifer to give sulfate concentrations generally in the range of 2000 mg/L. This is much greater than the U.S. EPA recommended (250 mg/L) and

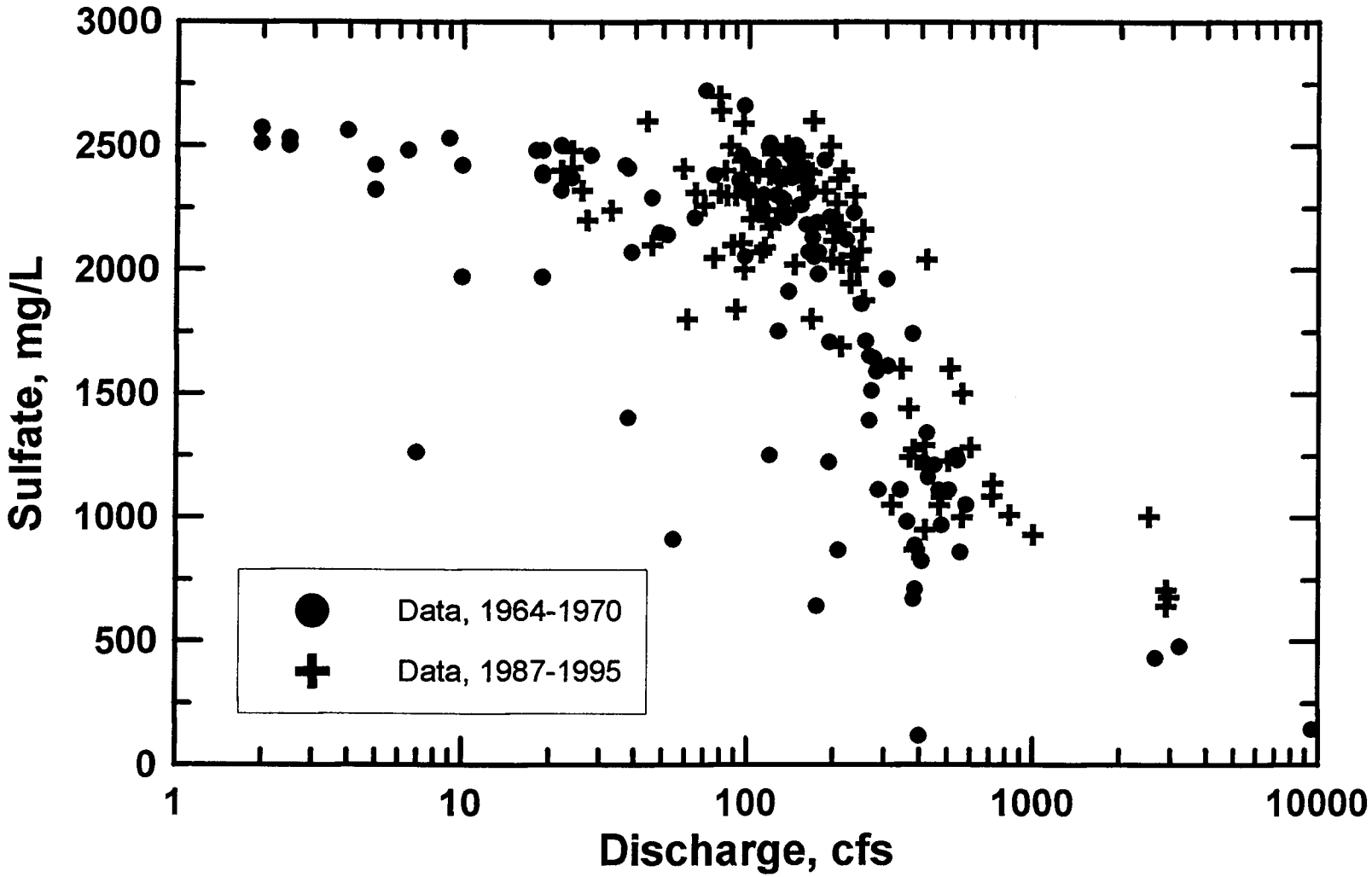

Figure 1.1 Sulfate concentration versus discharge for the Arkansas River near Coolidge, Kansas.

proposed maximum contaminant limit (500 mg/L) for sulfate concentration in drinking water. Because of the high salinity of water in the upper aquifer, groundwater has been mainly withdrawn from the deeper Ogallala aquifer within the river valley in recent decades.

The low permeability clays underlies the alluvial aquifer are present in parts of the upper Ogallala aquifer. This low-permeability material restricts the infiltration of the saline water to the deeper Ogallala aquifer. Consequently, perched saline water exists in some areas above the main body of the Ogallala aquifer. Discontinuous clay layers also occur within the main aquifer and further retard the downward movement of saline water (Whittemore and Butler, 1997).

It is known that most irrigation wells in the region have been installed using reverse rotary drilling. Gravel packs are placed in the annular space between the well casing and the outer borehole surface through the screened interval. Gravel packs often extend upwards across the clay and silty clay layers as shown in Figure 1.2. Except for public water supply wells and more recently drilled domestic wells, grout seals in the well annulus are either not present or extended only to 10 to 20 feet below the ground surface. The upper alluvial aquifer is usually between 20 and 50 feet thick. Thus, the saline water in the perched aquifer can flow down the gravel pack and intrude the Ogallala aquifer (Whittemore and Butler, 1997). The borehole skin has a permeability lower than the aquifer sediments because of the presence of the drilling mud. The low-permeability skin initially extends along the entire borehole.

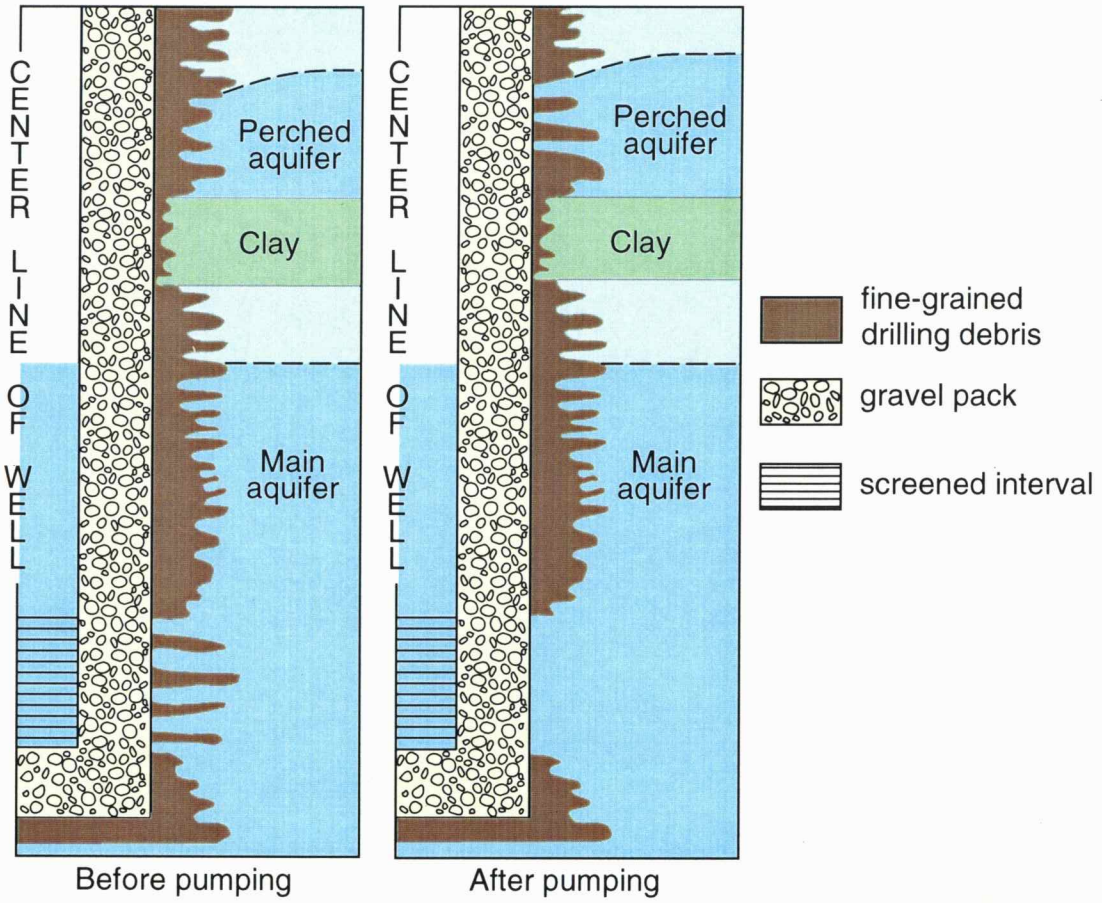

Figure 1.2 Before pumping and after pumping in a water supply well.

However, most of the mud skin along the screened interval is removed after pumping started. Figure 1.2 is a schematic drawing showing before and after a well being used for water supply. As a result, the highly saline water in the upper aquifer can flow directly into the Ogalla aquifer through the screened interval. It has been observed that some areas with gravel-packed wells have high salinity in the deeper portion of the Ogallala aquifer and lower concentration in the upper portion depending on the location of the screened interval. The other possible path for the saline water in the perched aquifer to reach the Ogallala aquifer is through the leaky clay layer. A conceptual model is proposed in this study to study quantitatively the saline water intrusion from the upper perched water into the fresh water of the Ogallala aquifer.

This study also develops a general purpose interactive system to facilitate groundwater modeling in the GIS environment with a user interface. The user interface is customized within ARCVIEW as the command control to integrate ARC/INFO, numerical groundwater models, and a parameter-identification method as a decision support system for groundwater management.

Due to the lack of reliable field data on solute concentration, the study area is limited to a small region of Deerfield (Figure 1.3). The lack of reliable field data makes model calibration and validation very difficult if not impossible. Hopefully, field data will be collected in the near future for evaluating the uncertainty of model results for further improvement.

The specific objectives of the research are:

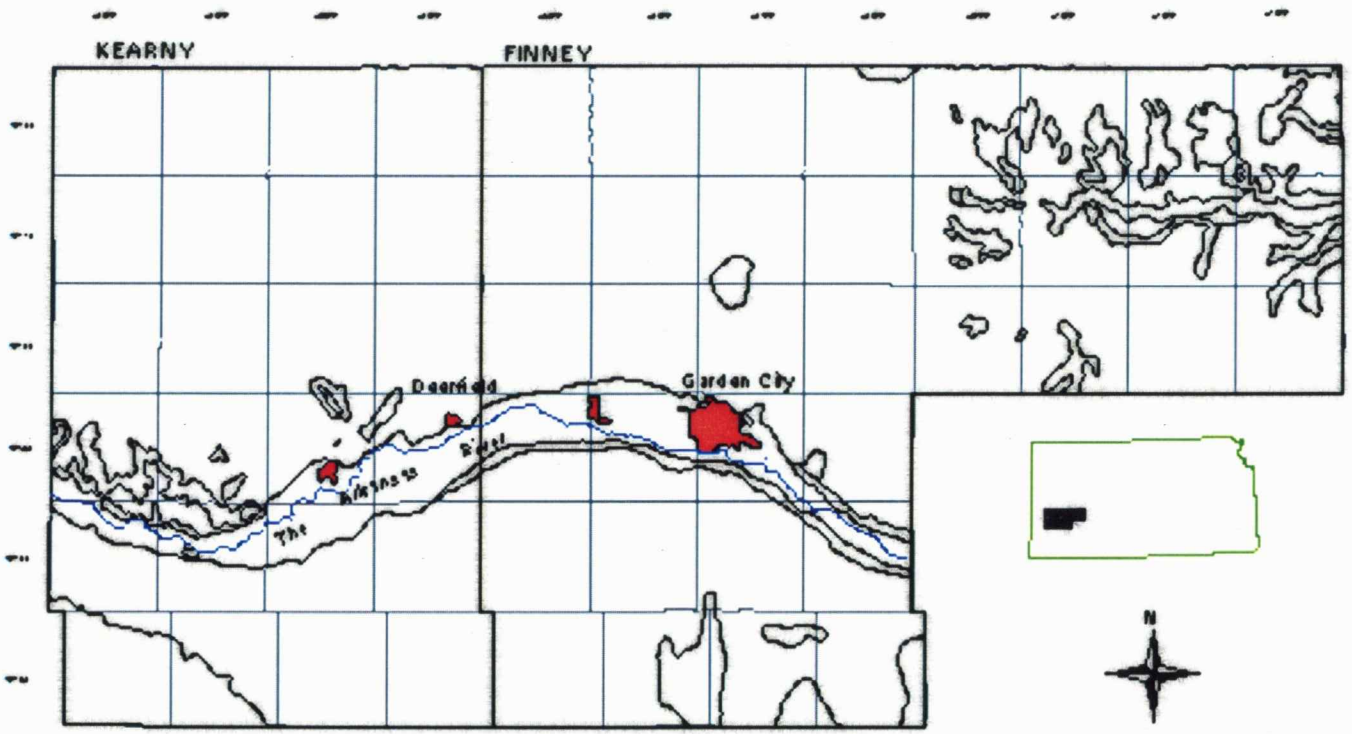

Figure 1.3 The location of the Deerfield area.

1. To determine the time variation of the polluted area in the freshwater aquifer for the conceptual model of the saline water intrusion using numerical models and to make a sensitivity analysis of the effects of model parameters on the polluted area.

2. To identify model parameters using an inverse approach incorporating available lithologic and groundwater level data, and spatial interpolation.

3. To develop an integrated system which consists of a geographic information system (GIS), numerical models, a parameter-identification method, and a graphical user interface (GUI) to enable modeling in an interactive mode.

4. To apply the integrated system to estimate piezometric heads and solute transport in the High Plains aquifer near Deerfield under various conditions.

II. LITERATURE REVIEW

Mathematical models for groundwater flow and contaminant transport have become powerful tools to evaluate and manage groundwater resources in recent decades. In a control theoretic approach, modeling dynamic systems comprises three fundamental steps: system characterization, system classification, and system identification. System identification includes model structure identification and parameter identification. The latter deals with parameter identifiability, parameterization, methods of parameter estimation, uncertainty in the estimated values of parameters, and uncertainty associated with prediction of the future behavior of the system (Yu, 1991). Groundwater flow and solute transport models relevant to this study are reviewed in this chapter. Some important publications on the application of GIS to water resources are also reviewed.

2.1 Groundwater Flow and Solute Transport Models

Solute-transport simulation is widely used to assess the alternative groundwater developments, the environmental impact and the design of groundwater contamination remediation programs.

Mangold and Tsang (1991) presented a review of 56 major numerical codes along with descriptions of the methods of analysis and their capabilities. These codes

can be broadly classified as hydrologic transport models, geochemical models, and hydrochemial models.

If the velocity field of the groundwater flow is not affected by the solute concentration, then the velocity field can be calculated by using an existing groundwater flow model such as MODFLOW. The resulting velocity field can be used in the solute transport model such as MT3D for computing the solute concentration. However, the major uncertainty involves the parameter estimation, in particular, the dispersivities involved in the solute transport model. The U.S. Bureau of Reclamation (1993) investigated the water-quality degradation of the Equus Beds aquifer in south-central Kansas through the conjunctive use of MODFLOW and MT3D. The objective was to determine how aquifer use affects the distribution of chloride. Ahlfeld and Zafirakou (1994) applied MODFLOW and MT3D to simulate groundwater flow and contaminant transport and, combined with a linear optimization technique, to solve the groundwater contaminant remediation problem.

If the velocity field is affected by the solute concentration, a coupled approach must be taken. Ma (1996) studied the saltwater intrusion into the Great Bend aquifer in south-central Kansas by using the existing software SWIFT II (Reeves et al, 1986) which includes the effect of density gradient. The saltwater intrusion in his study is due to the irrigation pumping which results in the upconing of deeper saline water in the aquifer. The maximum chloride concentration of the saline water is 28,000 mg/L

and the corresponding density is 1036 kg/m^3. Therefore, the effect of density gradient on the velocity field is important and must be included in modeling.

In this study, the maximum sulfate concentration is around 2,500 mg/L and the concentration of total dissolved solids is approximately 3500 mg/L. The estimated density of this saline water is 1002.5 kg/m^3 which is only about 0.25 percent higher than the pure water. In comparison with Ma's case, the density of the saline water in this study is not significant, thus the gravitational effect due to density gradient on the groundwater motion can be neglected. The velocity field computed using MODFLOW can be used in the solute transport model MT3D for computing the salinity distribution in the aquifer.

2.2 Parameterization

Groundwater flow and solute transport model parameters are continuous functions in space, hence the dimension of parameters can be infinite. Parameterization is a procedure to reduce the parameter dimension for use in numerical schemes and has a significant effect on the "well-posedness" of the inverse problem. The methods for reducing parameter dimension can be classified as (Sun, 1994): (1) the zonation method, (2) the interpolation method, (3) the stochastic-field method, and (4) the geological structure method.

The zonation method is the most widely used in practical application. In this approach, the flow region may be divided into a number of homogeneous and

isotropic zones. In each zone, the parameter(s) is constant. However, dividing the zones optimally is a difficult problem. Sun and Yeh (1985) noted that an incorrect zonation pattern can lead to large errors in estimated parameter values. One way to improve the zonation method is to estimate the parameter structure and parameter values to avoid both overparameterization and a priori zonation. Eppstein and Dougherty (1996) presented a method to simultaneously estimate transimissivities and zonation structure by combining an extended Kalman filter and an iterative partitional cluster algorithm.

Two common interpolation methods are found in groundwater literature. One is the finite-element interpolation method, and the other is the geostatistical interpolation method. For the finite-element interpolation method, it is extremely difficult to optimally determine the locations of nodes. The geostatiscal interpolation method is to determine the unknown distributed parameter by employing kriging and pilot points (de Marsily et al., 1984; Keidser and Rosbjerg, 1991; LaVenue and Pickens, 1992). However, to obtain reliable kriging results, relatively large sample size is needed that is generally not available in dealing with practical problems.

In the stochastic-field method, the unknown parameter is regarded as a random variable described by some statistical parameters such as the mean and the covariance (Hoeksema and Kitanids, 1984; Dagan and Rubin, 1988; Sun and Yeh, 1992). However, the inverse solution hinges on the appropriate statistical

assumptions and the structure of covariance functions. Justification of using such assumptions is a difficult task.

The common weakness of the first three methods is that the valuable geological structure information obtained from well logs is not directly included in parameter estimation. Sun et al. (1995) proposed the geological structure method which takes the local geological information in parameter estimation and is more reasonable for three-dimensional modeling. This method will be discussed in detail in Chapter IV and will be used in this study.

2.3 Model Parameter Identification

The problem of aquifer parameter identification has been studied extensively during the last several decades. The inverse problem of parameter identification concerns the optimal determination of the model parameters which have physical significance but are difficult to measure. These parameters may be inferred from the observations of the dependent variable of the governing equation. A typical example is the identification of hydraulic conductivity from the observations of piezometric head. A paper by Yeh (1986) reviews the literature on this topic. Various techniques have been developed to solve the inverse problem of parameter identification. McLaughlin and Townley (1997) presents a functional formulation of the inverse problem which is general to accommodate commonly used inverse algorithms.

Neuman (1973) classified the techniques as the direct or indirect approach. The direct method uses the equation error criterion in formulating the inverse problem while the indirect method uses the output error criterion in the formulation. The equation error criterion requires substantially more field data for the dependent variable than those for the output error criterion. Therefore, the indirect method has been mostly used in groundwater studies. The indirect method is to minimize a function of the discrepancies between calculated and observed output by using mathematical optimization techniques. Publications using the indirect method for estimating groundwater flow parameters have appeared in various journals (Yeh, 1986 and others). However, few published works have been done for coupled flow and solute transport problems.

Strecker and Chu (1986) combined the method of characteristics (MOC) with quadratic programming to estimate both flow and transport parameters. In order to avoid the numerical instability, they separated the estimation into two stages. In the first stage the transmissivity field was estimated using piezometric head data only, and in the second stage the dispersivity coefficients were estimated from measured solute concentration incorporated with the previously estimated transmissivity. The concentration data are a function of transmissivity, thus it is more reasonable to inverse transmissivities based on both head and concentration data in the first stage. Wagner and Gorelick (1987) presented a weighted least-squares analysis for

estimating flow and transport parameters simultaneously and also discussed parameter uncertainty for a hypothetical two-dimensional aquifer system.

Keidser and Rosbjerg (1991) extended the two-stage approach to a two-stage feedback procedure. The model parameters were divided into flow (transmissivities) and transport (dispersivities and initial concentration of sources) parameters. In the first stage they used both measured piezometric head and concentration to estimate transmissivities, given initial values of the source concentration and the dispersivities. In the second stage, the solute transport parameters were estimated by using estimated transmissivities in the first stage and the concentration data. By repeating the optimization of the first stage, the final estimates of transmissivities were obtained. Minimization of the formulated objective function for both stages were performed using Levenberg-Marquardt's algorithm.

Wagner (1992) proposed a methodology which combined groundwater flow and solute transport simulation based on the maximum likelihood estimation without prior information. Xiang et al. (1993) estimated coupled flow and solute transport parameters for steady flow. They proposed a weighted L_1-norm as the error measure between the vector of the observed piezometric heads and concentrations and the corresponding vector of the computed heads and concentrations. They applied a sensitivity equation method to minimize the error. Two hypothetical groundwater parameter estimation problems were presented in their applications.

2.4 GIS-Modeling System

The input data of groundwater models vary with space and time. For a large groundwater system, a large amount of input data must be handled for numerical models. In addition, an iterative procedure is generally needed to assess the adequacy and accuracy of hydrogeological parameters and boundary conditions, thus visual comparison between simulated results and measurements is desirable for adjusting the parameters in each simulation. Clearly, a geographic information system (GIS) provides an integrated platform to manage, analyze and display disparate data and can greatly facilitate the modeling effort in data compilation, model calibration, and display of model parameters and results. Furthermore, GIS can also be used to generate valuable information for decision-making through its ability to spatially overlay and process data.

Various applications of GIS in water resources have been published in the Proceedings of the Symposium on "Geographic Information Systems and Water Resources" (Harlin and Lanfear, 1993). Another Proceedings of the Symposium on "Environmental modeling with GIS" (GoodChild et al., 1993) presents the integration of GIS and environmental simulation models. Devantier and Feldman (1993) reviewed several applications in hydrologic modeling including floodplain hydrology, erosion prediction/control, and water-quality prediction/control. Recently, the development of an integrated GIS with groundwater models has attracted the attention of many researchers. Watkins et al. (1996) described GIS applications in groundwater

flow modeling and reviewed some existing programs which interface GIS and groundwater models. The simulation-GIS systems can be broadly classified into two types: (1) integrated GIS-groundwater models, and (2) groundwater models embedded in GIS.

The first approach uses a set of programs or an interface to transfer data between GIS and groundwater models. In other words, the data stored in a GIS database are transferred into input files of groundwater models and output data of the models are transferred back into the GIS database after simulation. The disadvantage of this approach is that one set of data is stored twice, one in the GIS database and the other in ASCII files. This approach requires minimum modification in GIS and groundwater models to avoid the errors in modifying GIS source code and/or groundwater models. Hence, it is widely adopted in many applications because of its simplicity. This approach can be enhanced by modifying the groundwater models to directly read model inputs from GIS data files such as "coverages" in ARC/INFO instead of original ASCII files. Thus, only a GIS database is used and no data-transfer program is required. An example is MODFLOWARC (Orzol and McGrath 1992).

The work by Rifai et al.(1993) and El-Kadi et al.(1994), respectively, basically integrated GIS with some existing groundwater models through data transfer and a user interface. Rifai et al. (1993) integrated a GIS software SYSTEM 9 with a groundwater model WHPA (Blandford and Huyakorn, 1990) for delineating wellhead protection areas around public water-supply wells. They developed a

graphical user interface (GUI) in C- language for user interaction. El-Kadi et al. (1994) integrated a GIS software MAPINFO with a two-dimensional flow and transport model known as MOC (Konikow and Bredehoeft, 1978) and provided a customized graphical user interface by using MAPBASIC language included in MAPINFO.

The second approach is to embed the equations governing the groundwater flow and solute transport into GIS as intrinsic functions through modifying the GIS source code or writing macro programs to perform numerical calculations (Watkins et al., 1996). There is no data conversion in this approach. However, this approach requires a great deal of modification and it is a difficult task to incorporate complicated numerical procedures into GIS as intrinsic functions. As an example, McKinney and Tsai (1993) wrote macro programs to solve sets of finite-difference equations in a raster system. The different levels of discretization were applied in their study in order to minimize numerical errors and accelerate convergence. Tim et al. (1996) embedded three simplified formulas into the ARC/INFO software to calculate three kinds of indices which indicate the susceptibility of groundwater to contamination by pesticides without involving any groundwater model simulation. They developed a GUI by using arc macro language (AML) included in ARC/INFO to facilitate the rapid appraisal of groundwater vulnerability.

In this study, the first approach (integrated GIS-groundwater model) is adopted because of its flexibility and simplicity. Two GIS softwares ARC/INFO and

ARCVIEW are integrated with groundwater models MODFLOW and MT3D and a parameter identification method. ARCVIEW is customized to serve as the user interface of the integrated system as described in Chapter V.

III. THE SALINE WATER INTRUSION - A CONCEPTUAL MODEL

3.1 A Conceptual Model for Saline Water Intrusion

As described in Chapter I, the saline water in the upper unconfined aquifer can intrude to the freshwater of the lower unconfined Ogallala aquifer by two possible avenues: (1) through the leaky clay layer that separates the two unconfined aquifers, and (2) through the unsealed gravel packs of irrigation wells that are abandoned or that are not pumping such as during the off-irrigation season. Although chemical data exist for for many wells, little field data are available for determination of the relative importance of the two intrusion mechanisms. Therefore, a conceptual model is proposed based on which numerical solution of the solute transport can be obtained to give some estimates of the polluted area as a function of time.

The conceptual model is based on field observations of the spreading of the saline water in the freshwater of the Ogallala aquifer in the Arkansas River corridor in Kearny and Finney counties, southwestern Kansas. The upper perched water underlying an irrigated field in that area is mainly derived from the intrusion of saline river waterwhich is diverted for irrigation. Observed sulfate concentration are in the range of about 2000 mg/L in the perched aquifer. This concentration is also assumed for the salinity of the perched water underlying the ditch-irrigated field. In the conceptual model, the saline water from the non-pumping irrigation well is considered as a line source whereas the saline water passing through the leaky clay

layer is considered as a nonpoint source with a uniform rate of infiltration. The saline water intrusion from the line source and the combination of the line source and the nonpoint source will be modeled separately to delineate the effects of the two different mechanisms of saline water intrusion.

In the conceptual model, a 120-m thick aquifer is divided into eight layers each 15 m thick, Fig. 3.1. The modeled area is 4400 m by 800 m with a grid of 200 columns and 44 rows as shown in Fig. 3.2. Two grid systems are used to meet the requirement for accuracy of numerical solution. Near the point source, a fine grid of 10-m squares is used. Coarse grids of 25-m squares and 10 m by 25 m rectangles are used in regions farther away from the source. The groundwater flow is uniform and to the east. A municipal water-supply well is placed 800 m downstream from the irrigation well. The western and eastern boundaries are assumed to have constant piezometric heads equal to 910 m and 895.4 m above the mean sea level, respectively,to represent as estimated field conditions near the town of Deerfield in Kearny county. The northern and southern boundaries of the modeled area are assumed to have no flow. The background salinity of the fresh groundwater is 30 mg/L.

The saline water in the upper perched zone flows down the unsealed gravel pack of the non-pumping irrigation well by gravity at a steady rate and enters the lower aquifer radially. The estimated steady flowrate of the saline water based on the Theim equation (Fetter, 1994) is about 200 m^3/day or 36 gpm based on the hydraulic

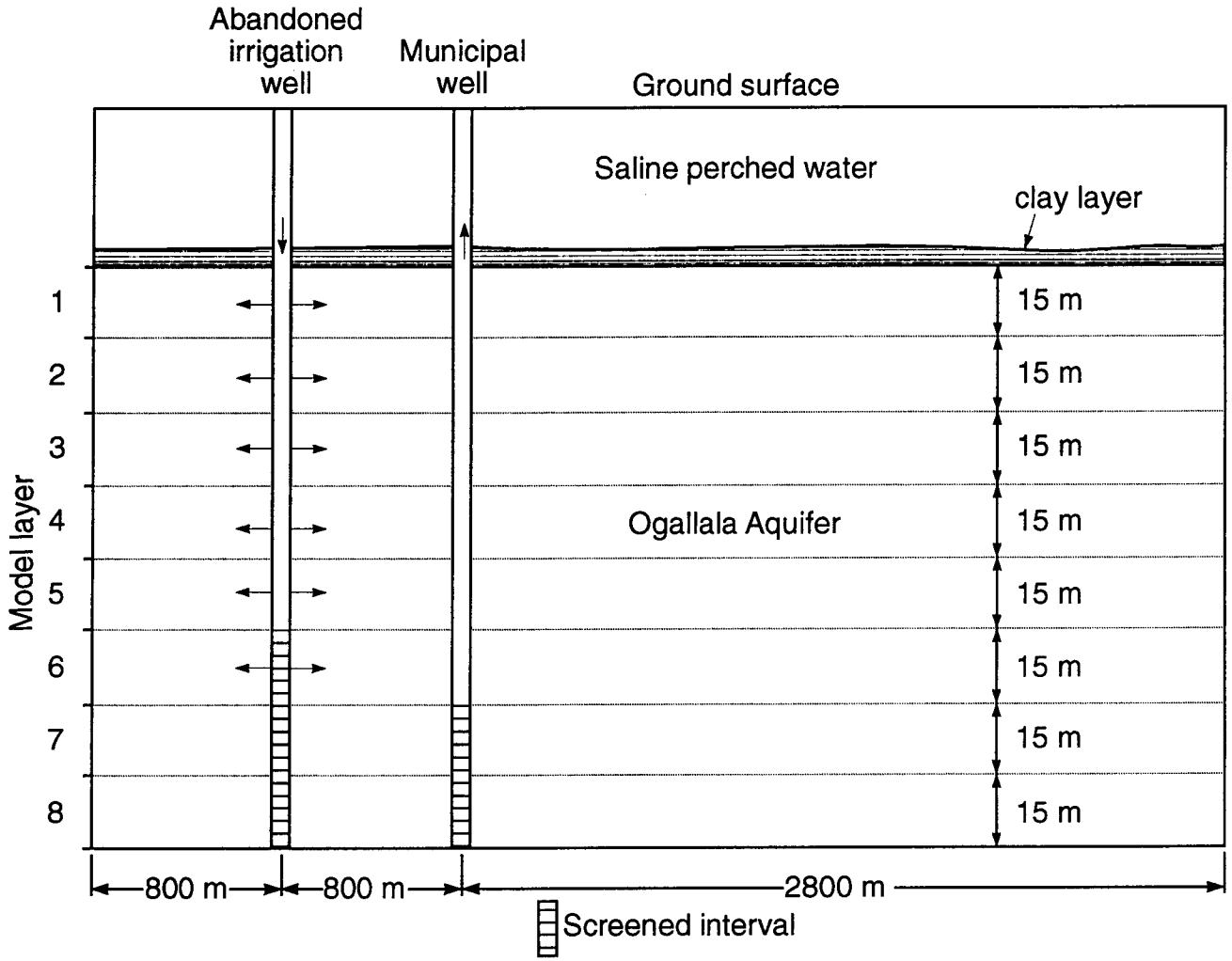

Figure 3.1 E-W cross secton showing saline perched water entering an abandoned well as a line source of polluted water into the Ogallala aquifer

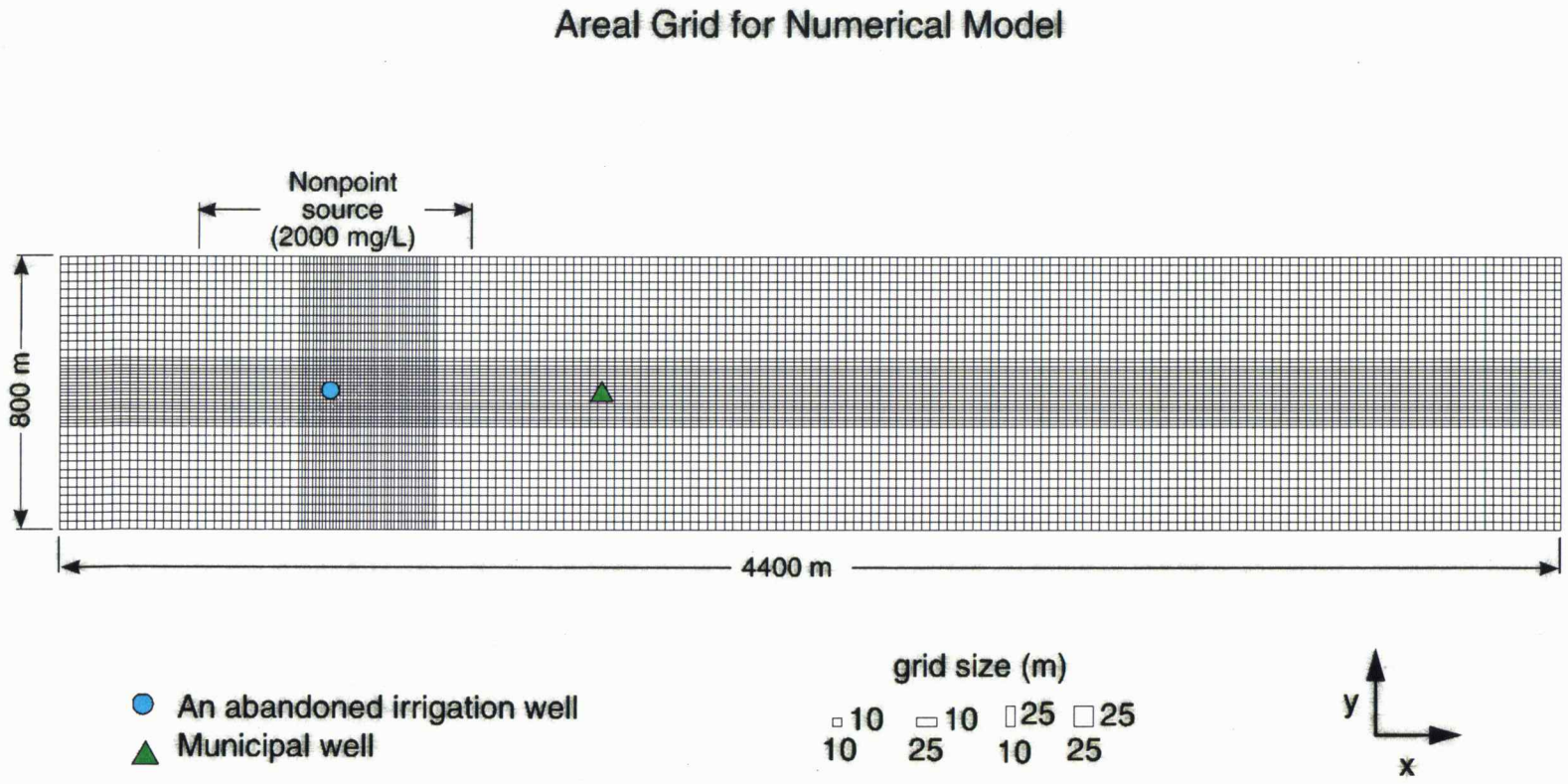

Figure 3.2 Areal view of the grid system for the numerical model.

heads and the radius over which the head drop occurs as assumed for this calculation. The velocity of saline water seeping through the leaky clay layer is estimated to be 0.1 m/year. The sulfate concentration of the upper perched water outside the ditch-irrigated field is assumed to be 60 mg/L and seep downwards at an estimated velocity of 0.01 m/year.

3.2 Groundwater Flow and Contaminant Transport Equations

Equations governing the groundwater flow and contaminant transport are briefly described in the following section. The publically available software MODFLOW (1988) and MT3D (1992) solve these equations numerically and are usedfor simulating the saline water migration in the conceptual model. Results for these models for a point-source contamination plume have been shown to agree with an analytical solution (Zheng, 1992).

3.2.1 Groundwater Flow Equation

The groundwater flow is governed by Darcy's law and the law of conservation of mass. For three-dimensional, unsteady flow, the piezometric head h is usually chosen as the dependent variable and the governing equation can be written as (see, for example, Rushton and Redshaw, 1979):

$$\frac{\partial}{\partial x}\left(K_x \frac{\partial h}{\partial x}\right)+\frac{\partial}{\partial y}\left(K_y \frac{\partial h}{\partial y}\right)+\frac{\partial}{\partial z}\left(K_z \frac{\partial h}{\partial z}\right)-W=S_s \frac{\partial h}{\partial t} \qquad (3.1)$$

where K_x, K_y, K_z are, respectively, hydraulic conductivities in the principle axes directions of x, y and z, h(x, y, z, t) is the piezometric head, W is the volume flow rate per unit volume for a source (positive) or a sink (negative), S_s is the specific storage of the porous material defined as the volume of water released from storage per unit change in piezometric head per unit volume of aquifer material, t is the time. The coordinate axes x and y are in a horizontal plane and the z-axis is vertically downward.

The velocity components in Eq. 3.1 are given by Darcy's law

$$v_x = -K_x \frac{\partial h}{\partial x} \, , \; v_y = -K_y \frac{\partial h}{\partial y} \, , \; v_z = -K_z \frac{\partial h}{\partial z} \tag{3.2}$$

In general, S_s, K_x, K_y, and K_z are functions of x, y, and z and W is a function of x, y, z, and t. Equation 3.1 describes the movement of groundwater with constant density in a heterogeneous and anisotropic medium, provided that x, y, and z are the principal axes of the hydraulic conductivity tensor.

Equation 3.1 together with specified boundary and initial conditions forms the mathematical model for groundwater flow. The numerical solution is usually obtained by either finite difference or finite element methods. In MODFLOW, the block-centered finite-difference method is used to solve numerically Eq. 3.1. The algorithm is described in detail by McDonald and Harbaugh (1988).

3.2.2 Solute Transport Equation

The equation governing the unsteady, three-dimensional, solute transport in groundwater without chemical reactions can be written as follows (Zheng, 1992):

$$\frac{\partial C}{\partial t} = \frac{\partial}{\partial x}\left(D_x \frac{\partial C}{\partial x}\right) + \frac{\partial}{\partial y}\left(D_y \frac{\partial C}{\partial y}\right) + \frac{\partial}{\partial z}\left(D_z \frac{\partial C}{\partial z}\right)$$

$$-\left[\frac{\partial}{\partial x}(u_x C) + \frac{\partial}{\partial y}(u_y C) + \frac{\partial}{\partial z}(u_z C)\right] + \frac{W}{\theta} C_s \qquad (3.3)$$

where C is the solute concentration (ML^{-3}), D_x, D_y, D_z are, respectively, the hydrodynamic dispersion coefficients in the direction of the principal axes x, y, z, respectively (L^2T^{-1}); θ is the effective porosity of the porous medium, u_x, u_y, u_z are the velocity components in x, y, z directions, respectively; C_s is the concentration of the source or sink (ML^{-3}).

The three terms on the right side of Eq. 3.3 are from left to right: the dispersion terms, the advection term, and the sink or source term. For an isotropic porous media, D_x, D_y and D_z can be defined as follows (Burnett and Frind, 1987):

$$D_x = \alpha_x \frac{u_x^2}{|u|} + \alpha_y \frac{u_y^2}{|u|} + \alpha_z \frac{u_z^2}{|u|} + D^* \qquad (3.4a)$$

$$D_y = \alpha_x \frac{u_y^2}{|u|} + \alpha_y \frac{u_x^2}{|u|} + \alpha_z \frac{u_z^2}{|u|} + D^* \tag{3.4b}$$

$$D_z = \alpha_x \frac{u_z^2}{|u|} + \alpha_y \frac{u_x^2}{|u|} + \alpha_z \frac{u_y^2}{|u|} + D^* \tag{3.4c}$$

where

α_x = the longitudinal dispersivity (L),

α_y = the horizontal transverse dispersivity (L),

α_z = the vertical transverse dispersivity (L),

$|u| = \left(u_x^2 + u_y^2 + u_z^2\right)^{1/2}$, the magnitude of the velocity vector (LT^{-1}),

D^* = the effective molecular diffusion coefficient (L^2T^{-1}).

Equation 3.3 can also be written as

$$\frac{DC}{Dt} = \frac{\partial}{\partial x}\left(D_x \frac{\partial C}{\partial x}\right) + \frac{\partial}{\partial y}\left(D_y \frac{\partial C}{\partial y}\right) + \frac{\partial}{\partial z}\left(D_z \frac{\partial C}{\partial z}\right) - \frac{W}{\theta}(C - C_s) \tag{3.5}$$

where $\frac{DC}{Dt} = \frac{\partial C}{\partial t} + u_x \frac{\partial C}{\partial x} + u_y \frac{\partial C}{\partial y} + u_z \frac{\partial C}{\partial z}$ indicates that the time rate of change is calculated the pathline of a contaminant particle (or a characteristic curve of the velocity field). By introducing the finite-difference algorithm, the substantial derivative in an Eulerian grid system becomes

$$\frac{D C}{D t} = \frac{C_m^{n+1} - C_m^{n^*}}{\Delta t} \tag{3.6}$$

so that Eq. 3.4 becomes

$$C_m^{n+1} = C_m^{n^*} + \Delta t \times \left[\text{RHS of Eq. 3.4}\right] \tag{3.7}$$

where

C_m^{n+1} = the average solute concentration for cell m at the new time level (n+1),

$C_m^{n^*}$ = the average solute concentration for cell m at the new time level (n+1) due to advection alone, also refer to as the intermediate time level (n^*),

Δt = the time increment.

Equation 3.7 constitutes the basic equation of the mixed Eulerian-Lagrangian algorithm by solving the advection term with a Lagrangian scheme and the dispersion term with an Eulerian scheme. In MT3D, the Lagrangian approach employs the method of characteristics by using the particle tracking technique and the Eulerian approach utilizes the block-centered finite-difference method. If the velocity field is not affected by the density gradient, then the velocity components obtained from the solution of Eq. 3.1 can be used in the transport equation. Since in this study, the

salinity (density) of the groundwater is not large enough to affect the velocity field, the velocity components determined from MODFLOW are used for solving the transport equation.

3.3 Model Parameters

No field data for the hydraulic conductivity and specific yield are available. Therefore, water well-log data around Deerfield are used to estimate these model parameters. The sediment composition indicated by the well logs is classified into five categories listed in Table. 3.1. For each sediment category, the values of hydraulic conductivity and specific yield are taken from those given in textbooks (Freeze and Cherry, 1979; Fetter, 1994). The general lithologic character was averaged to give uniform values for the horizontal hydraulic conductivity and specific yield of 40 m/day and 0.2, respectively. This hydraulic conductivity compares with that of 28 m/day for the lower aquifer of a regional flow model in the Arkansas River corridor by Dunlap et al. (1985). Dunlap et al. also estimated their value based on an evaluation of lithologic information in well logs. A value of 25 m/day is also used for the horizontal hydraulic conductivity to determine the sensitivity of the contaminant spreading to this parameter. The vertical hydraulic conductivity is also assumed to be uniform with a value of 0.015 m/day. A different value of 0.15 m/day for the vertical hydraulic conductivity is also used in the simulation for sensitivity analysis.

Table 3.1 Hydraulic conductivity and specific yield for five geological materials in the unconfined aquifer.

Material category	Geological materials	Hydraulic conductivity (m/day)	Specific yield
1	Fine gravel and very coarse sand	8.6E1 - 8.6E3	0.12 - 0.35
2	Coarse sand and medium sand	8.6E0 - 8.6E2	0.15 - 0.35
3	Fine sand and silty sand	8.6E-2 - 8.6E1	0.1 - 0.28
4	Silt and sandy clay	8.6E-4 - 8.6E-1	0.03 - 0.19
5	Silty clay and clay	8.6E-6 - 8.6E-4	0 - 0.05

Based on some typical values given in the literature, an effective porosity of 25% is selected. The value of the longitudinal dispersivity is selected to be 1 m based on the field data analyzed by Gelhar et al. (1992). A different value of the longitudinal dispersivity of 10 m is also used in the simulation for sensitivity analysis. The vertical transverse dispersivity is typically an order of magnitude smaller than the horizontal transverse dispersivity (Gelhar et al, 1992). However, the horizontal transverse dispersivity and the vertical transverse dispersivity are both set as 0.1 m in this model because, for the grid sizes of 10 m and 25 m used in the numerical model, the data plotted by Gelhar et al. (1992) indicate that the vertical transverse dispersivity can be close to the horizontal transverse dispersivity.

The time step of 10 days is selected to meet the Courant criterion for numerical stability in groundwater flow simulation. The criterion corresponding to the x coordinate direction is as follows

$$\text{Courant No.} = \frac{u_x \, \Delta t}{\Delta x} \leq 1. \tag{3.8}$$

Around the point source, u_x is about 0.4 m/day and Δx is 10 m. Thus, the time step Δt of 10 days meets the criterion in the x-direction. The same criterion is also applied to the y and z coordinate directions. For the solute transport simulation, the transport step criterion is expressed as follows (Redell and Sunada, 1970)

$$\left[\frac{D_x}{\Delta x^2}+\frac{D_y}{\Delta y^2}+\frac{D_z}{\Delta z^2}\right]\Delta t \leq 0.5 \qquad (3.9)$$

The criterion is calculated to determine the appropriate stepsize for solving the dispersion term. The values of the parameters used in the numerical solution are summarized in Table 3.2.

3.4 Saline Water Intrusion from A Single Non-Pumping Irrigation Well

A typical irrigation well in the study area generally pumps water from the deeper portion of the aquifer through a 45-meter well screen. When an irrigation well is not pumping, the perched saline water can flow downward through the unsealed gravel pack well into the lower aquifer and pollute the freshwater in the deeper portion of the aquifer. In the conceptual model, the non-pumping irrigation well is screened from 75 to 120 meters (layer 6 to 8) below the confining clay layer. The major portion of the saline water is expected to enter the lower aquifer through the well screen and a minor portion would enter layers 1 through 5 because of the larger resistance of the mud skin remaining around the borehole of the well from above the screened interval to the top of the gravel pack. Accordingly, the total saline water flowrate of 200 m^3/day is distributed as follows: 75% in layer 6 and 5% in each of layers 1 through 5.

Table 3-2 : Values of variables and parameters used in the numerical simulation.

Aquifer and other parameters	
horizontal hydraulic conductivity	$K_x = K_y =$ 40 m/day and 25 m/day
vertical hydraulic conductivity	$K_z =$ 0.015 , 0.15 and 1.5 m/day
specific yield	S = 0.2
storage coefficient	S_c = 0.0002
porosity	θ = 0.25
longitudinal dispersivity	α_x = 1 m and 10 m
horizontal transverse dispersivity	α_y = 0.1 m and 1m
vertical transverse dispersivity	α_z = 0.1 m and 1m
depth from ground surface to bedrock	120 m
pumpage for municipal well	2180 m^3 / day
background sulfate concentration	30 mg/L
time step	10 days
total simulation time	15 years

For sensitivity analysis, computations are carried out for different combinations of the line source of contaminant from the non-pumping irrigation well, the nonpoint source through the leaky clay layer, and different values of model parameters such as hydraulic conductivity and dispersivities. For each case, the salinity distribution is computed for a period of 15 years with a time step of 10 days. In particular, since the maximum sulfate concentration recommended for drinking water is 250 mg/L, the time variation of the area covered by the saline water of 250 mg/L or larger is computed. The focus of the computations is the area with a sulfate content equal to or larger than 250 mg/L in the sixth layer because that is the layer receiving the main portion of the saline water intrusion. The computed results are presented and discussed in the following sections. In the discussion, the polluted area refers to the area enclosed by saline water with salinity equal to or larger than 250 mg/L.

The computed isolines of salinity in the plume at the end of the 15th year of simulation in Layers 1, 3, 6, and 8 are shown in Fig. 3.3. The maximum salinity at the source is 2000 mg/L and the background salinity is 30 mg/L. The general shape of the plumes suggests that the convective process dominates the dispersive process in the contaminant transport.

Figure 3.4a shows the temporal variation of the polluted area due to the line source of contaminant for three different values of vertical hydraulic conductivity: 0.015 m/day, 0.15 m/day and 1.5 m/day. In general, the change in the polluted area

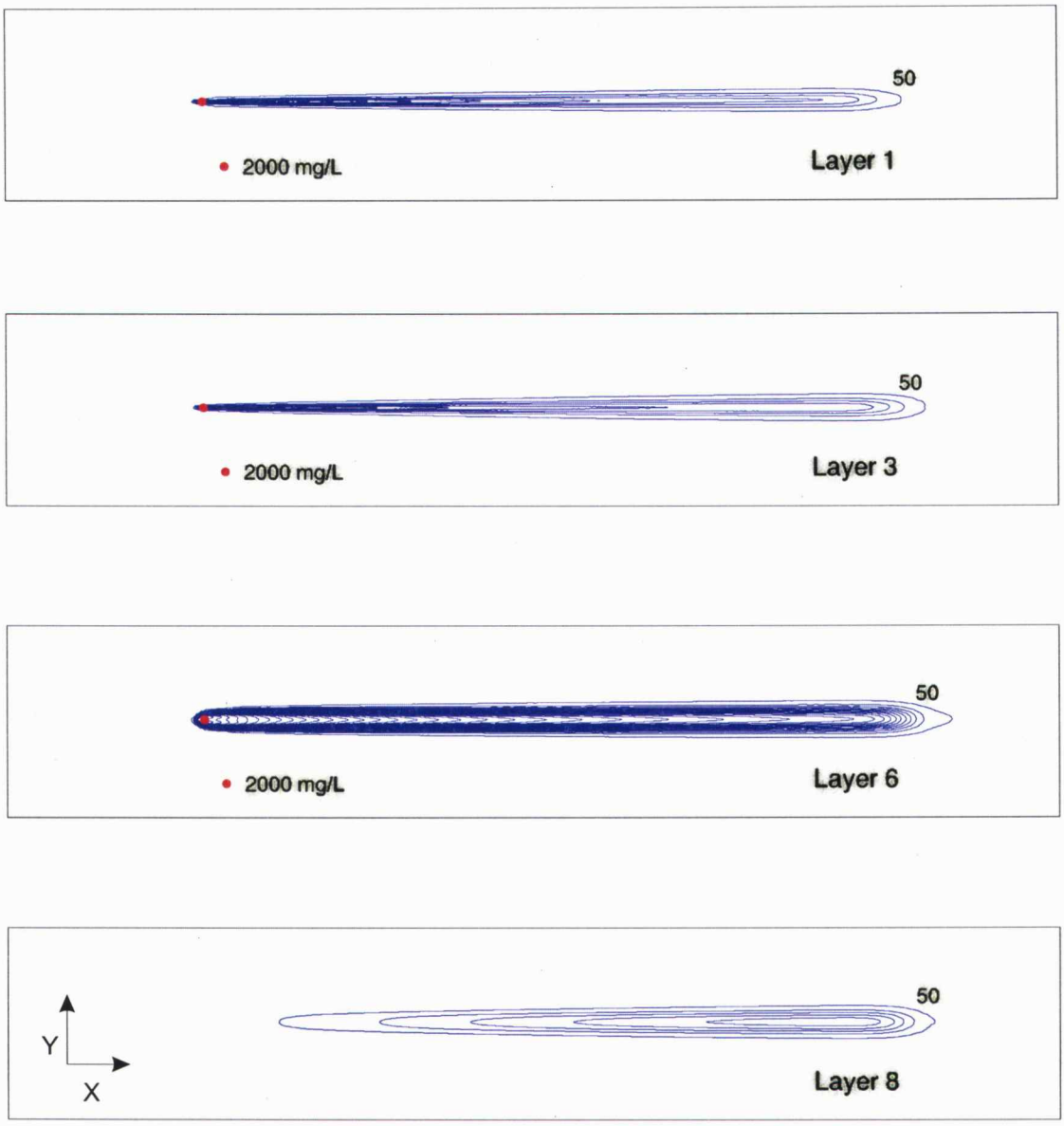

Figure 3.3 Saline water plumes in layers 1, 3, 6, 8 after the computation of 15 years.

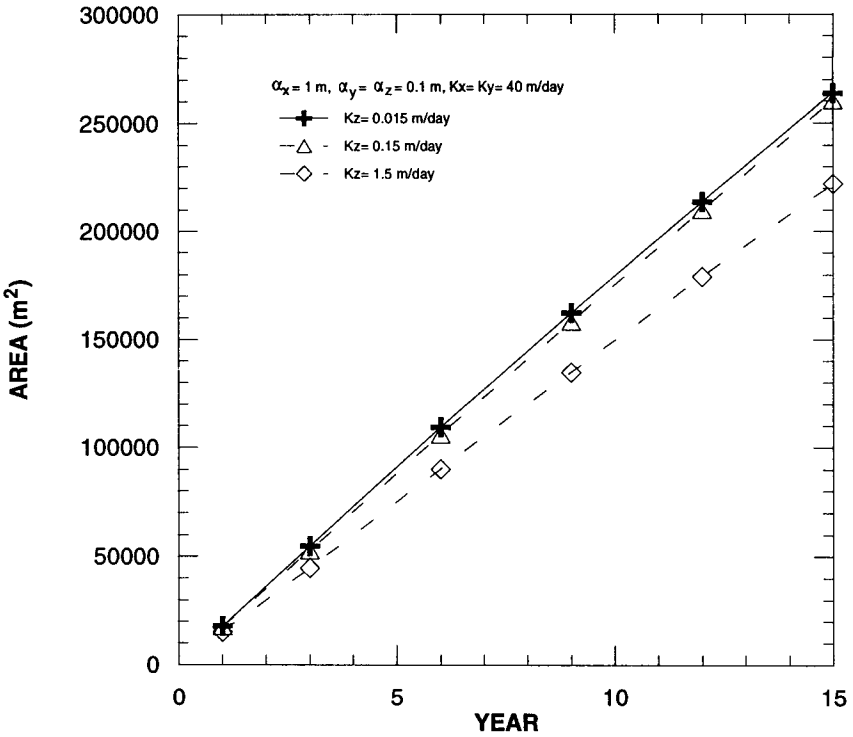

Figure 3.4a Effect of vertical hydraulic conductivity on the polluted area in the 6th layer from line source only.

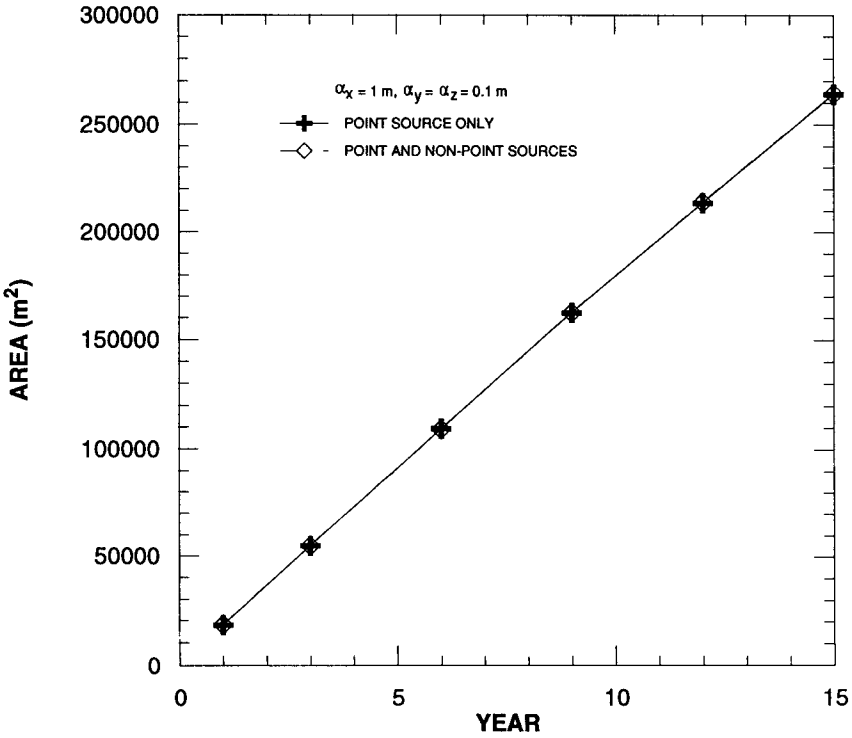

Figure 3.4b Effect of combined point and non-point sources on the polluted area in the 6th layer with Kv= 0.015.

versus time close to linear. As the vertical hydraulic conductivity increases, apparently an increase in the net outflux of polluted water from the sixth layer into the underlying layers occurs. This results in the decrease in the polluted area in the sixth layer as shown in Fig. 3.4a. The reduction in polluted area as K_z increases from 0.015 m/day to 0.15 m/day is not as significant as that for K_z = 1.5 m/day

The water in the upper five layers are less polluted than the sixth layer because the proportion of saline water entering these layers is smaller. Clearly, the time variation of the polluted area depends on the vertical distribution of the line source of the contaminant. The effect of a different distribution of saline water inflow to various layers is not investigated. The distribution assumed in this study is assumed to be a probable scenario. At the end of the 15th year of simulation, the polluted area for K_v = 0.015 m/day is close to 0.25 square kilometers in the sixth layer. With the number of abandoned, unsealed, and operable irrigation wells in the irrigation district close to four wells per square kilometer, saline water intrusion through the unsealed gravel packs of irrigation wells could be very substaintial.

Figure 3.4b is a plot of the time variation of the polluted area for the combined line source and non-point source of contaminant through the leaky clay layer for K_v = 0.015 m/day. Because of the low rate assumed for the seepage of saline water through the clay layer (0.1 m/year), the effect of the non-point source of contaminant on the polluted area in the sixth layer during the 15-year simulation is very samll. The effect of changing the horizontal hydraulic conductivity from 40 m/day to 25 m/day on the

polluted area is shown in Fig. 3.5. As the horizontal hydraulic conductivity decreases, the spreading of the intruding saline water is also reduced. The polluted area for the horizontal hydraulic conductivity equal to 25 m/day is lower than that for $K_x = K_y =$ 40 m/day because the smaller hydraulic conductivity leads to the smaller spreading area of contaminant.

Break-through curves at four different locations along the x-axis in the sixth layer are shown in Fig. 3.6. All four curves start with a background salinity of 30 mg/L and approach an equilibrium value that decreases with distance from the source. The equilibrium condition is reached when the influx and outflux of salinity to the grid are in balance at the location. Break-through curves in the 7th and 8th layers at the location of the municipal water-supply well are shown in Fig. 3.7. In the 7th layer, the equilibrium salinity is a little above 400 mg/L whereas in the 8th layer its value is close to 100 mg/L. Since the pumped water is a mixture of water in these two layers, the salinity of pumped water would be between these values.

The Peclet number equal to 10 is used in the computation for Figs. 3.4a and 3.4b. The Peclet number is defined as:

$$Pe_x = \frac{u_x \Delta x}{D_x} \tag{3.10}$$

The effects of different values of the Peclet number on the polluted area are presented in Figs. 3.8a and b for the line source only. When the horizontal transverse

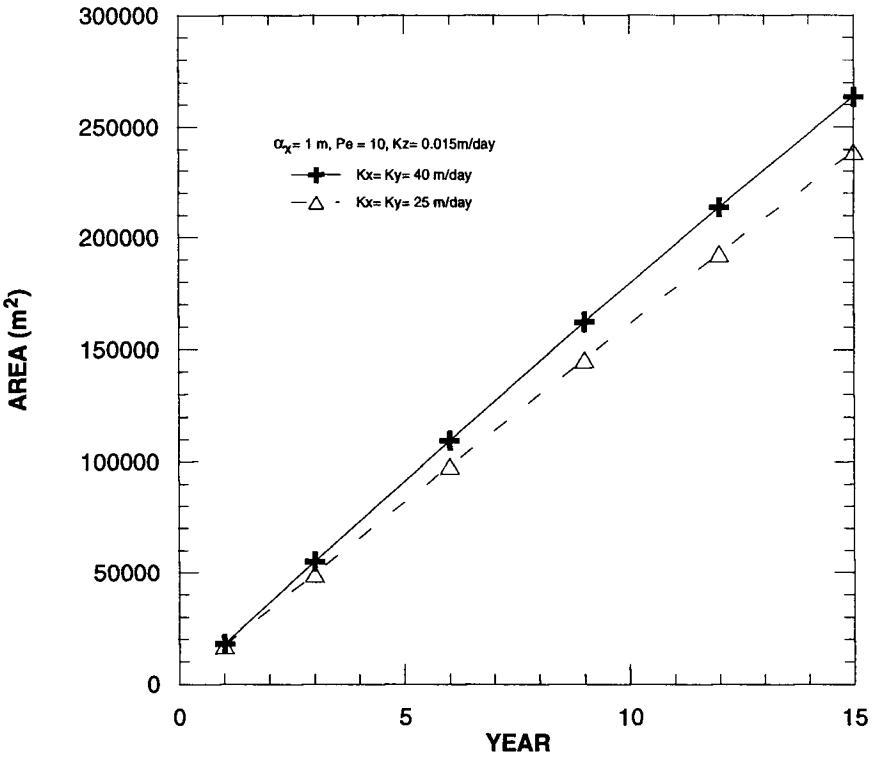

Figure 3.5 Effect of horizontal hydraulic conductivity on the polluted area in layer 6.

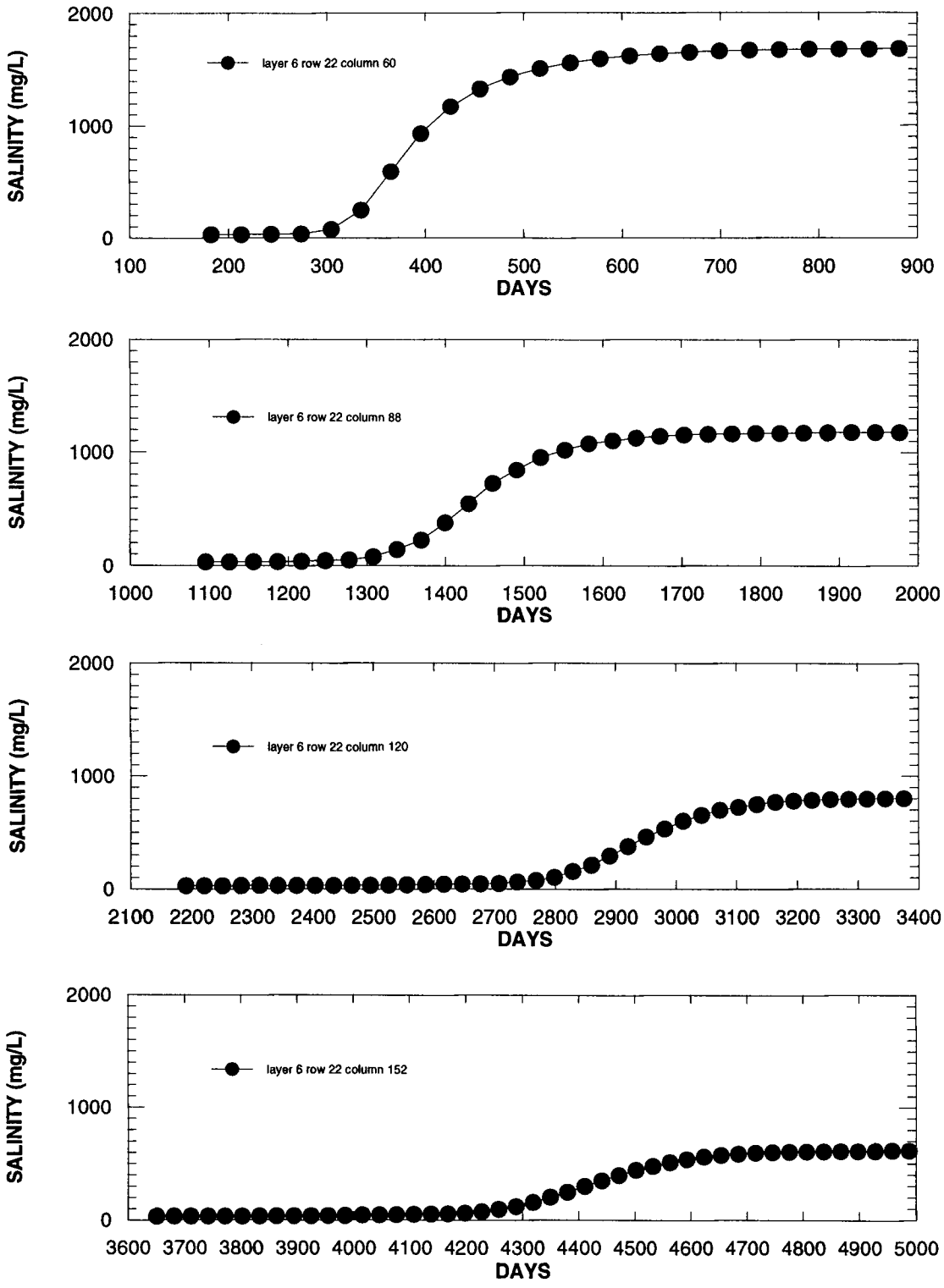

Figure 3.6 Break-through curves at four different locations along the x-axis in layer 6.

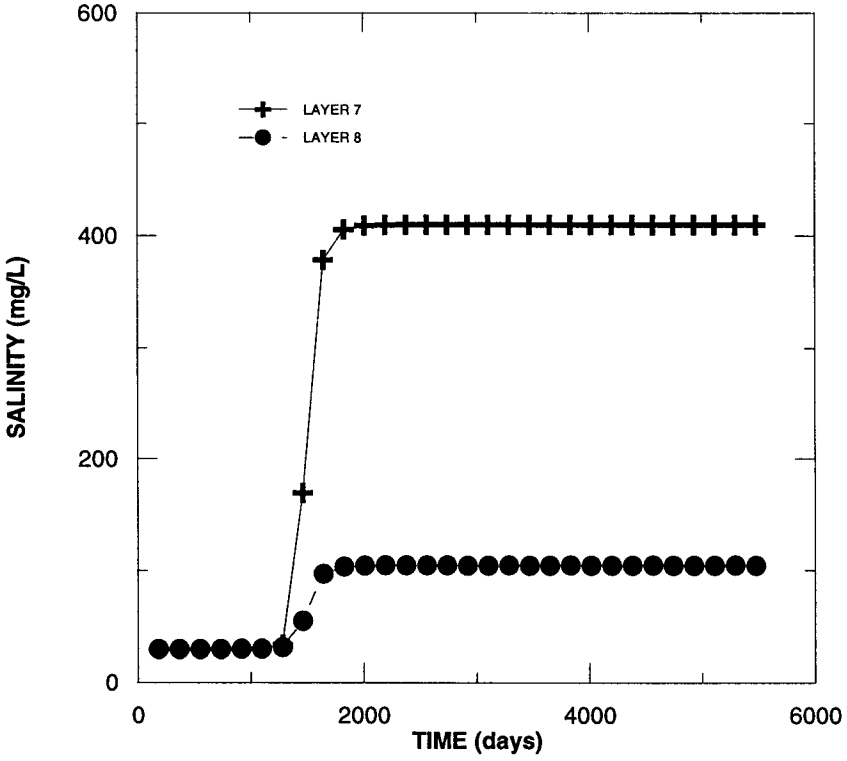

Figure 3.7 Salinity vs time at the location of the municipal well with line source only and Kz=0.15, Pe= 10.

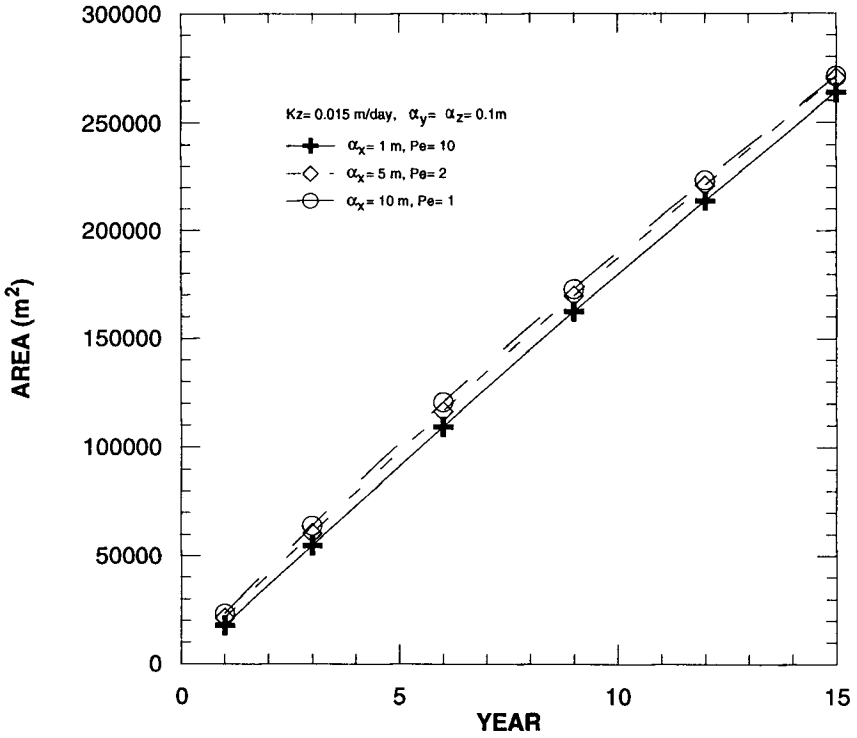

Figure 3.8a Effects of longitudinal dispersivity on the polluted area in the 6th layer from line source only.

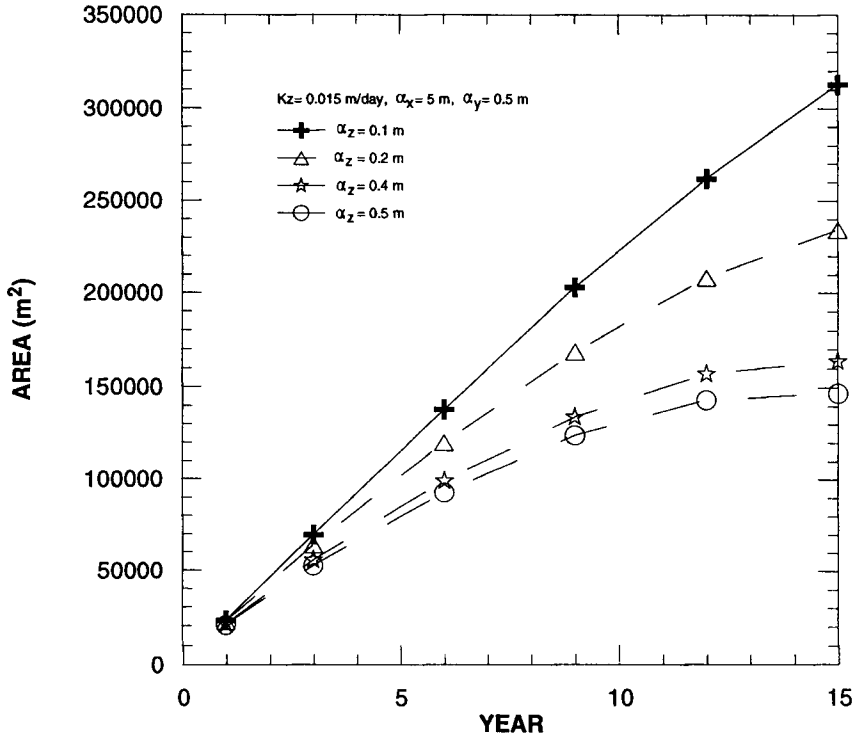

Figure 3.8b Effects of vertical transverse dispersivity on the polluted area in the 6th layer from line source only.

dispersivity and the vertical transverse dispersivity are kept constant at 0.1 m, the effect of changing the longitudinal dispersivity from 1 m to 10 m (Peclet number from 10 to 1) on the polluted are is illustrated in Fig. 3.8a. As the Peclet number decreases, the dispersive process tends to become a more dominating factor versus the convective process. Therefore, it is expected that the polluted area with salinity equal to or larger than 250 mg/L in layer 6 would increase at a given time. Although Fig. 3.8a shows this, the change is not substantial. However, if the Peclet number based on the longitudinal dispersivity and the horizontal transverse dispersivity are both kept constant but the vertical transverse dispersivity is changed from 0.1m to 0.5 m, a substantial decrease in the polluted area at a given time is observed (Fig. 3.8b). In addition, as α_z increases from 0.1m to 0.5 m, the increase in the polluted area with time becomes more curvlinear. For α_z = 0.5 m, the curve gradually approaches an equilibrium value with time. The reduction of the polluted area with salinity equal to or larger than 250 mg/L at a given time is likely due to larger downward dispersion of saline water in the sixth layer to the seventh layer.

IV. PARAMETER IDENTIFICATION

The parameterization method presented here is used to incorporate lithologic well-log data into the inverse solution procedure for groundwater modeling. The unknown model parameters, namely, hydraulic conductivity and storage coefficient, are directly related to the different geological materials found in the aquifer. For this reason, the parameter dimension can be determined by the number of geological materials instead of the number of grid points in a numerical model. If the number of grid points is used, nonuniqueness of the estimated set of parameters is often to be expected because the number of grid points generally far exceeds the number of observation sites.

The lithologic well logs are analyzed to determine the composition of geological materials and the thickness of each material for each well log. By using the well-log data, the local geological information at each model grid point is estimated through spatial interpolation. Then, the information can be incorporated into the inverse problem. The optimal hydraulic conductivities or storage coefficients of geological materials can be estimated by solving the inverse problem. Finally, the hydrogeological parameters at each grid point can be obtained by using the method described in the following sections. The application of the method in the study area of Deerfield is presented in Chapter VI.

4.1 Estimating the Thickness of Geological Materials

A sample lithologic well log is shown in Fig. 4.1, in which different geological materials and their thickness below the ground surface at the well location are identified. Let an aquifer system be discretized into a number of model layers (Fig. 4.2) and the thickness distribution of the ith geological material within a model layer be designated as $b_i(x,y)$ for i = 1, 2, ... , N, N being the number of geological materials within a model layer. The value of $b_i(x,y)$ at an unsampled site is estimated using two different spatial interpolation techniques: TIN (triangulated irregular network) and universal kriging for comparison.

4.1.1 TIN

TIN (triangulated irregular network) is a type of surface modeling algorithm used in ARC/INFO. The TIN data structure has two basic elements: points with x, y, z values and a series of lines joining these points to form triangles. Each triangular plane depends on three nearby sample points. The equation of the plane can be expressed as (Isaaks and Srivastava, 1989):

$$z = ux + vy + w \tag{4.1}$$

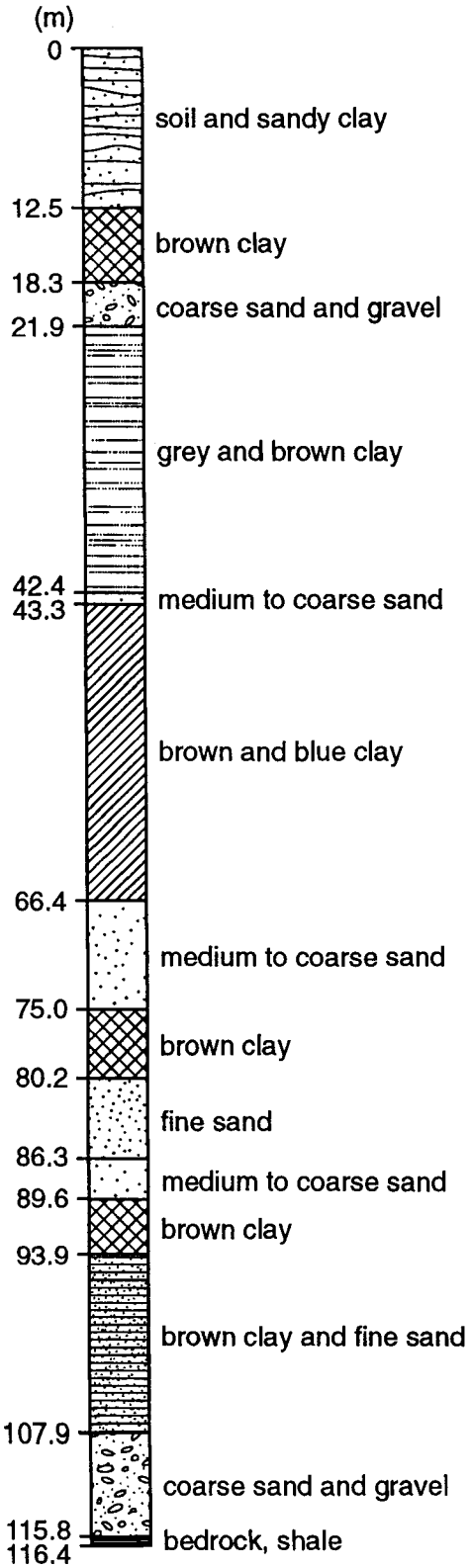

Figure 4.1 A sample lithologic well log

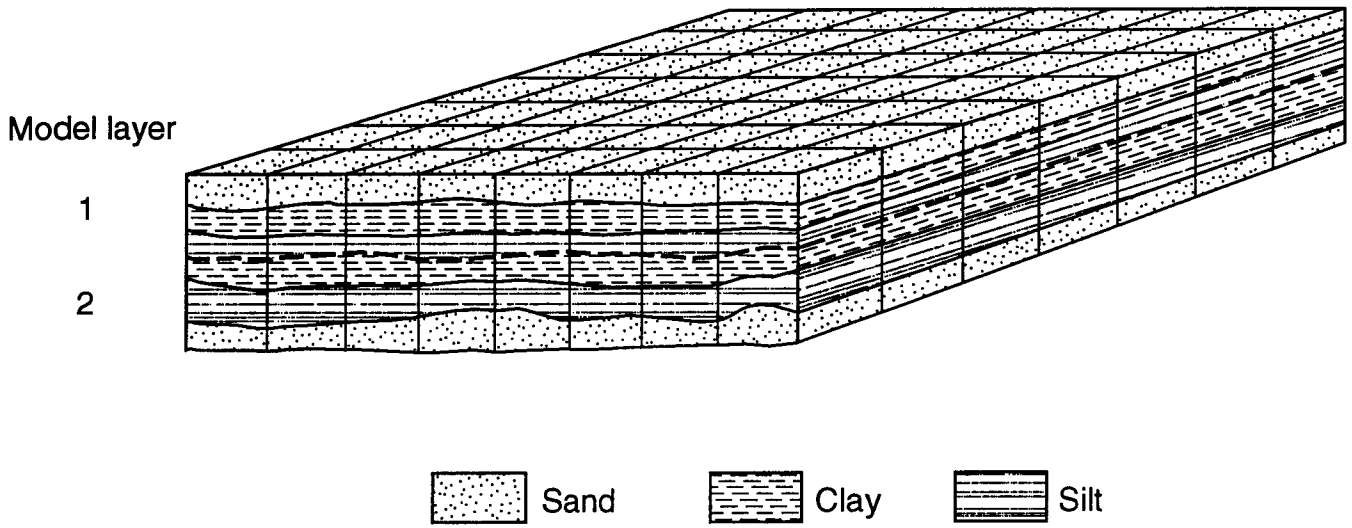

Figure 4.2 Spatial discretization of an aquifer system.

Given the coordinates (x_1,y_1), (x_2,y_2) and (x_3,y_3) and the sample values z_1, z_2 and z_3 of three nearby sample points, the coefficients u, v and w can be obtained by solving the following system of equations:

$$ux_1 + vy_1 + w = z_1 \tag{4.2a}$$

$$ux_2 + vy_2 + w = z_2 \tag{4.2b}$$

$$ux_3 + vy_3 + w = z_3 \tag{4.2c}$$

Based on the equation of the plane, the value at any location within the plane can be estimated by substituting the appropriate x and y values. Obviously, this method cannot be used for extrapolation purposes. The TIN triangulation is based on the Delaunay triangulation which produces triangles that are as close to equilateral as possible and satisfies the requirement that a circle drawn through the three points of a triangle contains no other point. In other words, all sample points are connected with their two nearest points to form triangles.

TIN interpolation is widely used in ARC/INFO because of its simplicity and convenience. The thickness $b_i(x,y)$ is estimated by using TIN.

4.1.2 Universal kriging

The universal kriging is also used to find the best linear unbiased estimate of the thickness distribution $b_i(x,y)$ of the ith geological material within a model layer. Let $b_i(x,y)$ be a nonstationary spatial random function with a trend given as

$$b_i(x,y) = m_i(x,y) + r_i(x,y) \tag{4.3}$$

where

$m_i(x,y) = E\{b_i(x,y)\}$, the trend,

$r_i(x,y)$ = the residual.

The trend is a gently varying deterministic function which is usually modeled as a low order polynomial of the coordinates x and y, for example,

$$m_i(x,y) = \alpha_0 + \alpha_1 x + \alpha_2 y \tag{4.4a}$$

or

$$m_i(x,y) = \sum_{k=0}^{L} \alpha_k p_k(x,y) \tag{4.4b}$$

where the p(x,y) are the polynomials in x and y. The residual $r_i(x,y)$ is commonly modeled as a stationary random function

The universal kriging estimator is written as:

$$b_i^*(x,y) = \sum_{j=1}^{M} \lambda_j b_i(x_j, y_j) \tag{4.5}$$

and the kriging system is as follows:

$$\begin{cases} \sum_{l=1}^{M} \lambda_l \gamma(x_j - x_l, y_j - y_l) + \sum_{k=0}^{L} \mu_k p_k(x_j, y_j) = \gamma(x_j - x_0, y_j - y_0), \\ \qquad\qquad\qquad\qquad\qquad\qquad\qquad\qquad\qquad\qquad j = 1, \ldots, M \\ \sum_{l=1}^{M} \lambda_l p_k(x_l, y_l) = p_k(x, y), \; k = 0, \ldots, L \end{cases} \tag{4.6}$$

where

M = the number of well logs,

γ = the semivariogram,

λ = the kriging weights,

μ = the (L+1) Largrange multipliers associated to the (L+1) constraints on the weights.

The solution of Eq. 5.6 gives the λ_l for calculating $b_i^*(x,y)$ using Eq. 5.5 and the μ_k for calculating the estimation variance using the following equation

$$\text{Var}\,[b_i^*(x_0, y_0) - b_i(x_0, y_0)] = \sum_{j=1}^{M} \lambda_j \gamma(x_j - x_0, y_j - x_0) + \sum_{k=0}^{L} \mu_k p_k(x_{0,} y_0) \tag{4.7}$$

The computation can be performed using the software KTB3D in GSLIB (Deutsch and Journel, 1992). The thickness-weighted hydraulic conductivity and storativity of a rectangular block can then be estimated.

4.2 Block Parameter Estimation

After the thickness distribution for each geological layer is estimated, the parameterization for the unknown parameters can be generated. Suppose that the hydraulic conductivity and storativity are to be estimated and that m geological materials exist in the aquifer. The hydraulic conductivity and storativity related to each of the m geological materials can be represented as K_1, K_2, ..., K_m and S_1, S_2, ..., S_m, respectively. These values are defined as unknown parameters.

An aquifer system is discretized into a number of rectangular blocks with the center representing the grid node (Fig. 4.2). Each block may contain some or all of the m geological materials with varying thickness. The thickness-weighted distributed parameters K_H, K_V, and S can then be estimated for each block (Fig. 4.3) by the following equations:

$$K_H(x_{ijk}) = \sum_{n=1}^{N_{ijk}} b_{ijk}^n K_{ijk}^n / b_{ijk} \tag{4.8}$$

$$K_V(x_{ijk}) = b_{ijk} / \sum_{n=1}^{N_{ijk}} \left(b_{ijk}^n / K_{ijk}^n \right) \tag{4.9}$$

$$S(x_{ijk}) = \sum_{n=1}^{N_{ijk}} b_{ijk}^n S_{ijk}^n / b_{ijk} \tag{4.10}$$

where

$K_H = K_x = K_y$, the horizontal hydraulic conductivities in x and y directions are assumed to be equal,

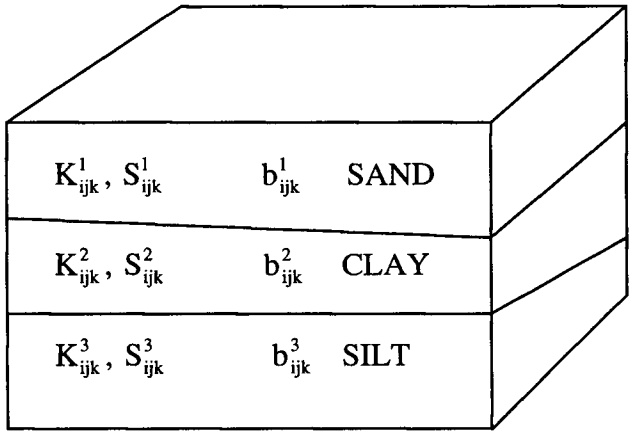

Figure 4.3 An example for three geological materials in a block (ijk).

$K_V = K_z$, the vertical hydraulic conductivity,

x_{ijk} = the identification of a block in which i, j, and k indicate the number of the row, the column, and the model layer, respectively,

N_{ijk} = the number of geological materials in the block,

b_{ijk}^n = the thickness of the nth material in the block, where n = 1, 2, ... , N,

$$b_{ijk} = \sum_{n=1}^{N_{ijk}} b_{ijk}^n ,$$

K_{ijk}^n = the hydraulic conductivity associated with the nth geological material,

S_{ijk}^n = the storativity associated with the nth geological material.

Based on the preceding formulation, the distributed parameters K_H, K_V, and S for the entire modeled aquifer can be represented by K_1, K_2, ..., K_m and S_1, S_2, ..., S_m. The optimal estimates of these unknown parameters can be obtained by solving the inverse problem as described in the following section.

4.3 Estimation of Optimal Parameters

If the field measurements of solute concentration are also available, then the simultaneous estimation of groundwater flow and solute transport parameters can be conducted by minimizing the weighted sum of squared errors between calculated and observed piezometric head and solute concentration data. In this study, the scarcity of

solute concentration data would give unreliable estimates of dispersion parameters. Thus, only the the groundwater flow parameters are estimated.

Let $\mathbf{u}_{obs}$ be a vector of the observed piezometric heads and $\mathbf{u(P)}$ a vector of computed piezometric heads as a function of parameter vector **P.** The vector **e** is the difference between the observed and computed piezometric heads and is a function of **P**.

$$\mathbf{e} = \mathbf{u}_{obs} - \mathbf{u(P)} \tag{4.11}$$

The optimal estimates of model parameters minimize the following constrained weighted squares of errors:

$$Z = \mathbf{e}^T \mathbf{w} \mathbf{e} = (\mathbf{u}_{obs} - \mathbf{u(P)})^T \, w \, (\mathbf{u}_{obs} - \mathbf{u(P)}) \qquad \mathbf{P}_L \leq \mathbf{P} \leq \mathbf{P}_U \tag{4.12}$$

where

T = transpose,

w = a diagonal weighting matrix indicating the reliability of $\mathbf{u}_{obs}$,

$\mathbf{P}_L$ = the estimated lower bounds of the vector **P**,

$\mathbf{P}_U$ = the estimated upper bounds of the vector **P**.

The upper and lower bounds of the hydraulic conductivity and the storativity for geological materials can be found in textbooks (See, for example, Freeze and Cherry, 1979). For instance,

$$10^{-2} < K_{sand} < 10^{-5} \text{ (m/sec)} \tag{4.13}$$

$$10^{-9} < K_{clay} < 10^{-12} \text{ (m/sec)} \tag{4.14}$$

The objective function, Eq. (4.12), subject to constraints 4.13 and 4.14, forms a nonlinear optimization problem. The optimal estimate of **P** can be obtained by solving the nonlinear optimization problem through an iterative procedure as follows. The gradient vector **g** of the objective function can be written as

$$\mathbf{g}(\mathbf{P}) = \nabla Z = 2\,\mathbf{J}(\mathbf{P})^{T}\mathbf{we}(\mathbf{P}) \tag{4.15}$$

where **J(P)** is the Jacobian matrix

$$\mathbf{J}(\mathbf{P}) = \begin{bmatrix} \frac{\partial e_1}{\partial p_1} & \frac{\partial e_1}{\partial p_2} & .. & \frac{\partial e_1}{\partial p_s} \\ . & . & & . \\ . & . & & . \\ \frac{\partial e_r}{\partial p_1} & \frac{\partial e_r}{\partial p_2} & .. & \frac{\partial e_r}{\partial p_s} \end{bmatrix} \tag{4.16}$$

where r indicates the number of observations and s is the number of model parameters. Each element of the Jacobian matrix represents the derivative of each residual with respect to each parameter. Since the residual is computed based on the

model output and the observation, the derivative in the matrix cannot be directly calculated from some equations describing the residual. Hence, the derivative is approximated by the increment of the residual due to parameter change divided by the increment of the parameter.

Let $\mathbf{P}^{(k+1)}$ be the (k+1)st iteration value of $\mathbf{P}$. The gradient at $\mathbf{P}^{(k+1)}$ is approximated by

$$\mathbf{g}[\mathbf{P}^{(k+1)}] \approx \mathbf{g}[\mathbf{P}^{(k)}] + \mathbf{H}[\mathbf{P}^{(k)}]\,\Delta\,\mathbf{P} \tag{4.17}$$

where $\mathbf{H}$ is the Hessian matrix and $\Delta\,\mathbf{P} = \mathbf{P}^{(k+1)} - \mathbf{P}^{(k)}$, referred as parameter upgrade vector. The necessary condition for a minimum to exist at $\mathbf{P}^{(k+1)}$ is $\mathbf{g}[\mathbf{P}^{(k+1)}] \approx 0$. Thus, from equation (4.17) the following is obtained

$$\Delta\,\mathbf{P} = \mathbf{H}[\mathbf{P}^{(k)}]^{-1}\,\mathbf{g}[\mathbf{P}^{(k)}] \tag{4.18}$$

Based on the Gauss-Newton method, the Hessian matrix can be approximated by

$$\mathbf{H} \approx 2\,\mathbf{J}^{T}\mathbf{w}\,\mathbf{J} \tag{4.19}$$

Equations (4.15), (4.18) and (4.19) lead to the approximation of the parameter upgrade vector

$$\Delta \mathbf{P} = (\mathbf{J}^T \mathbf{w}\, \mathbf{J})^{-1}\, \mathbf{J}^T \mathbf{we} \tag{4.20}$$

Equation (4.20) can be replaced by using the Marquardt (1963) correction

$$\Delta \mathbf{P} = (\mathbf{J}^T \mathbf{w}\, \mathbf{J} + \lambda\, \mathbf{I})^{-1}\, \mathbf{J}^T \mathbf{we} \tag{4.21}$$

where λ is a positive coefficient and $\mathbf{I}$ is the unit matrix. When λ tends to infinity, the minimization approaches a steepest descent search. In contrast, when λ tends to zero, it reduces to the Gauss-Newton method. The algorithm has been applied in several parameter estimation packages. PEST (Doherty, 1994), a model-independent parameter estimation package, is used to solve the inverse problem for parameter estimation. The advantage of PEST is that it can link to any numerical model to estimate model parameters by supplying the starting parameter values and model input files.

In order to obtain reasonable estimates of parameters, the number of parameters must be less than the number of observations. The distributed parameters K_H, K_V, and S over the entire aquifer under study can be obtained from Eqs. 4.8, 4.9, and 4.10 by using the estimated parameter vector from the solution of the inverse problem.

V. INTERACTIVE INTEGRATED MODELING SYSTEM

5.1 System Components

The main objective of developing an integrated modeling system is to provide a user-friendly system that integrates spatial database and analysis (ARC/INFO), groundwater models, and a parameter identification method in the GIS environment, thereby permitting interactive model simulation and calibration through a graphical user interface (GUI). Figure 5.1 is a schematic diagram showing the four components of the integrated system. At the heart of the system are the groundwater models. These models draw on a variety of data from an ARC/INFO database. Parameter Identification (Fig. 5.1) incorporates the geological structure method in the inverse-solution approach and facilitates the model calibration effort. Interactions with the user and presentation of information are through ARCVIEW which is customized by using AVENUE codes. ARC/INFO and ARCVIEW are described in more detail below. An application of the integrated system is presented in Chapter VI. further explanation of the integrated system is in Appendix A.

5.2 ARC/INFO

The geographic information system ARC/INFO stores and generates spatial data which are required as input to execute the numerical models. The spatial data are stored in three different coverages, namely, point, line, and polygon coverages. Data

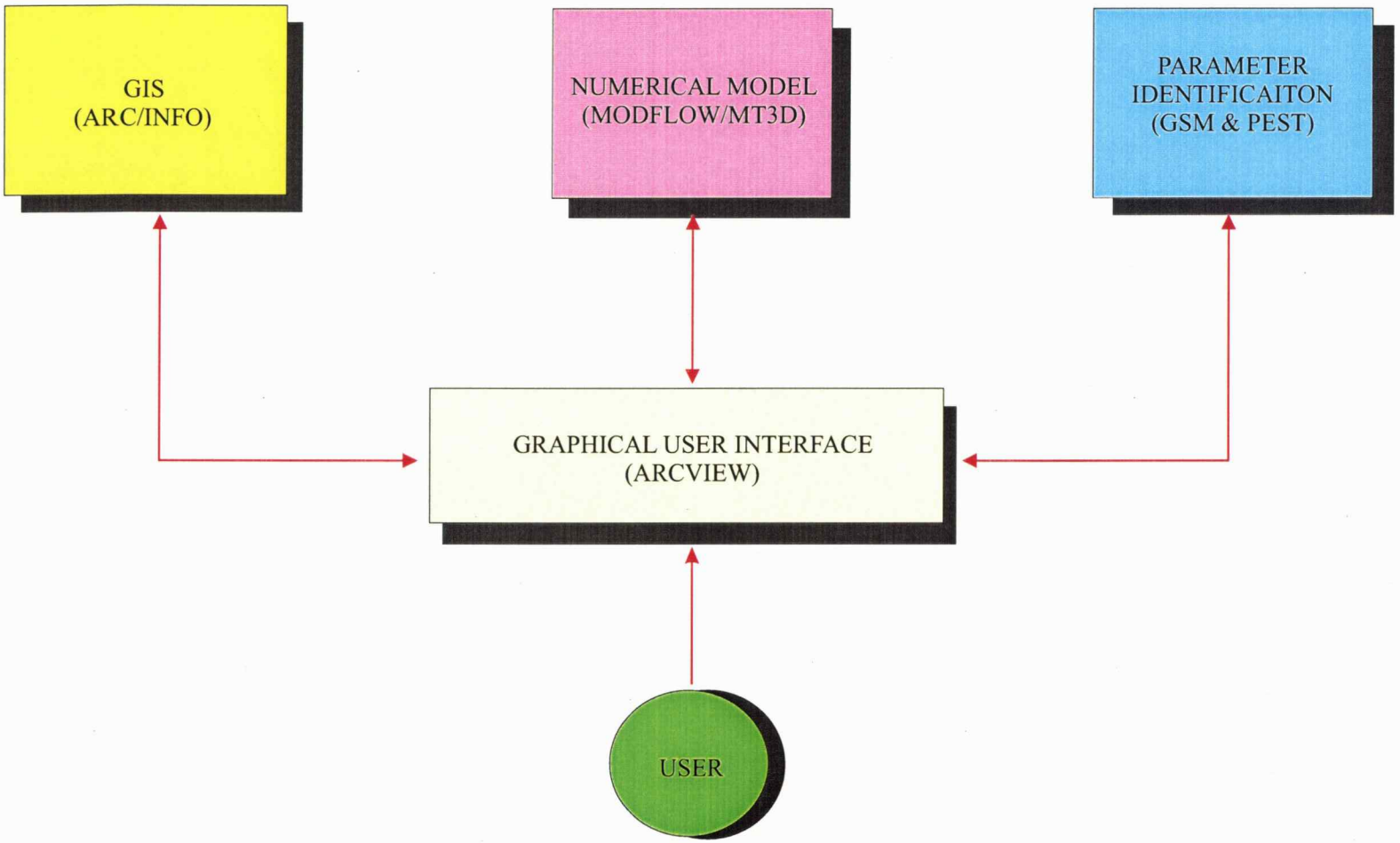

Figure 5.1 Components of the integrated system.

such as rainfall, streamflow, well logs, pumpage, and groundwater level are stored in the point coverages. Data related to rivers and irrigation canals are stored in line coverages. Data such as soil types and irrigated fields, which are related to recharge in the groundwater model, are stored in polygon coverages.

A coverage of ground surface contour can be generated through a triangulated irregular network (TIN), a type of surface modeling used in ARC/INFO, or digitizing based on some point measurements and USGS topographic maps. Also, hydrogeological information such as hydraulic conductivity can be stored as coverages. These data can be transferred into the groundwater models through the user interface ARCVIEW.

5.3 Graphical User Interface ARCVIEW

The graphical user interface (GUI) of the integrated system is customized within ARCVIEW to be the main command control providing the access to various components of the system as shown in Fig. 5.1. The interface allows a user to select and perform the customized functions. It is used not only for displaying the data stored in the database but also for estimating model parameters and executing simulations. The user customized functions are displayed as tool bars or button bars on the ARCVIEW screen.

ARCVIEW (ESRI, 1994) is windows-based GIS software for a desktop computer, and facilitates the organization, display, querying, analysis and publication

of data. There are six specific components in ARCVIEW that are key to an understanding of its operation: PROJECT, VIEW, TABLE, CHART, LAYOUT, and SCRIPT. PROJECT is an ASCII file composed of VIEW, TABLE, CHART, LAYOUT and SCRIPT (Fig. 5.2). VIEW is the main element in ARCVIEW and is an interactive map which allows users to display, explore, query, and analyze geographic data. Actually, it is a collection of geographic features, called themes, which can be an ARC/INFO coverage, an ARCVIEW shapefile, a simple format for storing the locations, attributes of geographic features, or an image data source. TABLE stores attributes of spatial data. A user can add dBASE, INFO or text files to ARCVIEW as tables or can connect to a database server, such as ORACLE, to retrieve records as tables. CHART is a graph of tabular data which provides an additional representation of the attributes of geographic features. LAYOUT generates a map from ARCVIEW. SCRIPT contains AVENUE code to expand the capabilities of ARCVIEW to applications desired by the user.

ARCVIEW has several advantages over other commercial software as the user interface. (1) Its graphic user interface is user-friendly. (2) Its flexibility in linking external software provides as a common platform for an integrated system. (3) It can communicate with ARC/INFO. In this study, ARCVIEW serves as a client and ARC/INFO as a server. ARCVIEW can send requests to ARC/INFO to execute some spatial operation structured by using Arc Macro Language (AML) through the software inter-application communication (IAC). The client and the server can be

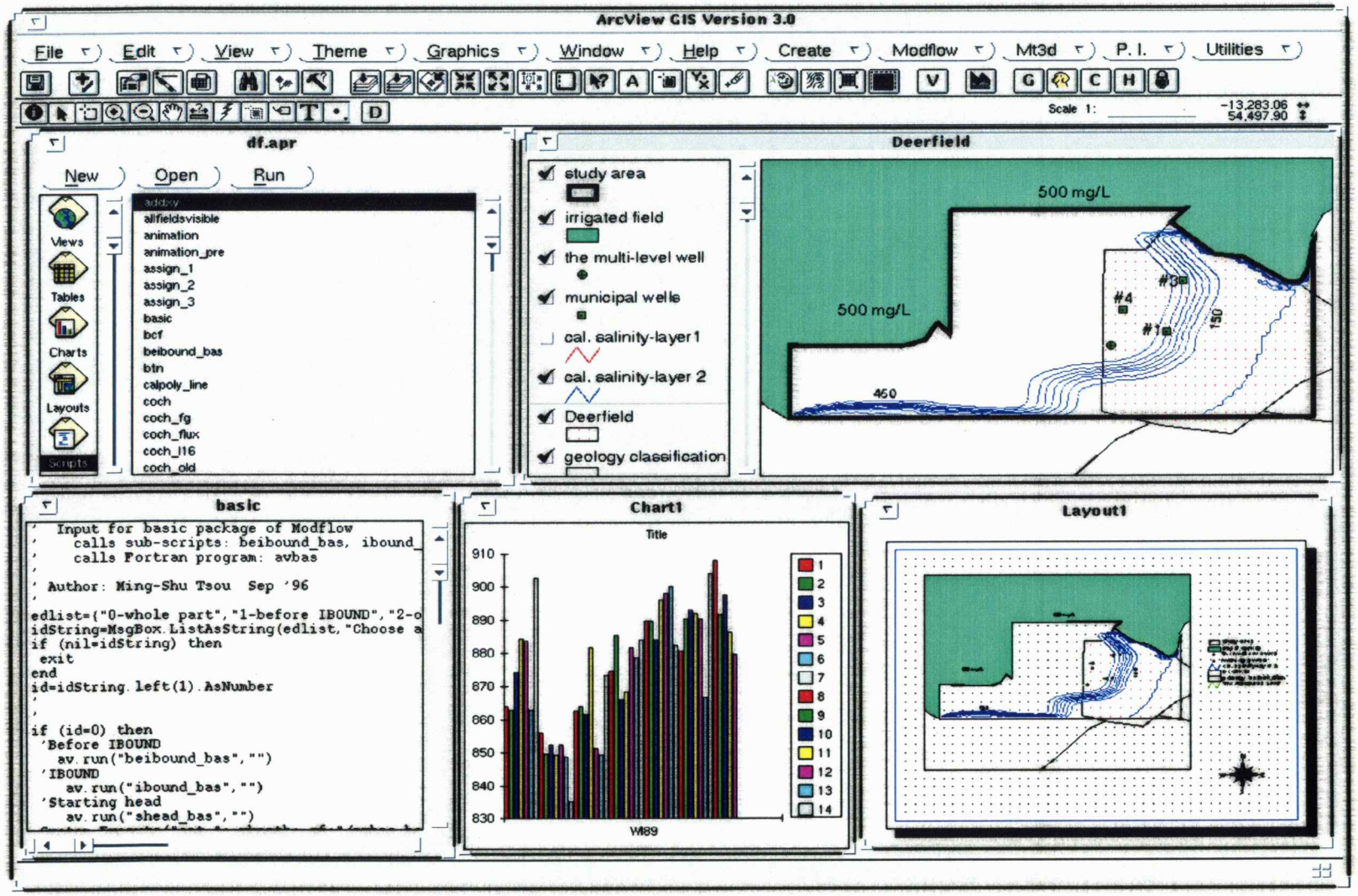

Figure 5.2 Components of an ARCVIEW PROJECT.

placed on different machines of a network if it is desirable. (4) ARCVIEW shares the same tables of attributes with INFO if a coverage is imported.

Figure 5.2 shows the customized user interface composed of a menu bar, a button bar and a tool bar within the ARCVIEW environment. Five menus, "Create", "Modflow", "Mt3d", "P. I." (Parameter Identification) and "Utilities" are added to the existing user interface. Some frequently used functions listed on the menus are also customized as buttons on the second row of the interface. The description of a button or selected menu item is listed in the status bar at the bottom of the screen.

5.4 Modeling Implementation

The procedure of modeling implementation consists of model-grid generation, input data preparation, model calibration, simulation, and display of results in the GIS environment. They are described separately in the following sections.

5.4.1 Model-Grid Generation

Grids of the numerical model are generated as a polygon coverage in the vector-based GIS while points located at the center of a grid cell are represented as a point coverage, called a grid-point coverage in this study. Model parameters are stored at each point. The advantage of a vector-based model for generating grids is that the grid cell sizes can be readily varied by changing the polygons. Grids over the modeling area of interest are generated as a shapefile in two ways. One is to specify the coordinates of the lower left point and upper right point and cell size, while the

other is to create a rectangular region and specify column and row numbers. The grids can also be rotated. Since the groundwater flow model used is based on the assumption that the Cartesian coordinates x, y and z are the principle directions of the hydraulic conductivity tensor, it is necessary to rotate the grids to be parallel to the groundwater flow direction.

5.4.2 Input Data Preparation

Hydrogeologic input data for groundwater models are stored in the coverages of ARC/INFO. They can be transferred to the grid-point coverage by interpolation using TIN (triangular irregular network) in ARC/INFO. Also, users can edit the attributes of the grid-point coverage in graphical form in VIEW or in tabular form in TABLE.

Both MODFLOW and MT3D have a modular structure with different model packages; each package requires a different input data file in a different format. Therefore, the data in the grid-point coverage must be exported from INFO in the required input format to the groundwater model packages through relational queries and by calling external FORTRAN codes in the user interface ARCVIEW.

5.4.3 Model Calibration and Display of Results

The model can be calibrated through a trial-and-error or an automated process. In trial-and-error calibration, the user interface can facilitate the calibration process by

allowing revision parameter values in a spatial display on a computer screen and recomputing the results. The recomputed results can be compared with the measured values by overlaying two respective data layers. Also, the difference between computed and measured values can be displayed as residual contours for identifying areas of large discrepancies for further modification.

In comparison, automated calibration uses the inverse approach. In the integrated system, the geological structure method is used for parameterization so that the lithologic data can be incorporated into the inverse procedure, whereas the software PEST is utilized to conduct the automated calibration. After the automated calibration, the optimized model outputs and model parameters can be shown on the screen.

The final simulated results can be shown as line drawings or in colored grid cells with different overlaying coverages such as city locations, land uses and so on in VIEW. Also, it is convenient to generate a map from LAYOUT by bringing in the VIEW, adding descriptions in the layout, and sending the layout to a printer or a plotter. The selected themes in VIEW can be shown continuously. For example, water level in different years can be selected and shown continuously to observe the changes.

VI. APPLICATION OF THE INTEGRATED SYSTEM TO DEERFIELD GROUNDWATER SYSTEM

The integrated system described in the preceding chapter is applied to evaluate the saline water intrusion in the groundwater system near the City of Deerfield, Kansas. The groundwater system in the general area is described first and is followed by the investigation of the smaller Deerfield groundwater system. A two-layer groundwater model is used to simulate the aquifer system. Model parameters, hydraulic conductivities and specific yield, are estimated using the geologic structure approach in the inverse method (described in Chapter IV) and measured piezometric heads. Dispersivity values used in the conceptual model are also used for the Deerfield groundwater system because of the lack of available field salinity data for model calibration. The computed temporal variations of salinity distribution in the each of the layers of the aquifer with the municipal wells in operation are presented and discussed in the following sections.

6.1 Description of Deerfield Groundwater System

The City of Deerfield depends on the groundwater system underlying the city for water supply. The Deerfield groundwater system is enclosed within the general aquifer area which used in this study which covers parts of Kearny and Finney counties and has an area of 16.5 km by 17.5 km. Figure 6.1 is a GIS overlay of some

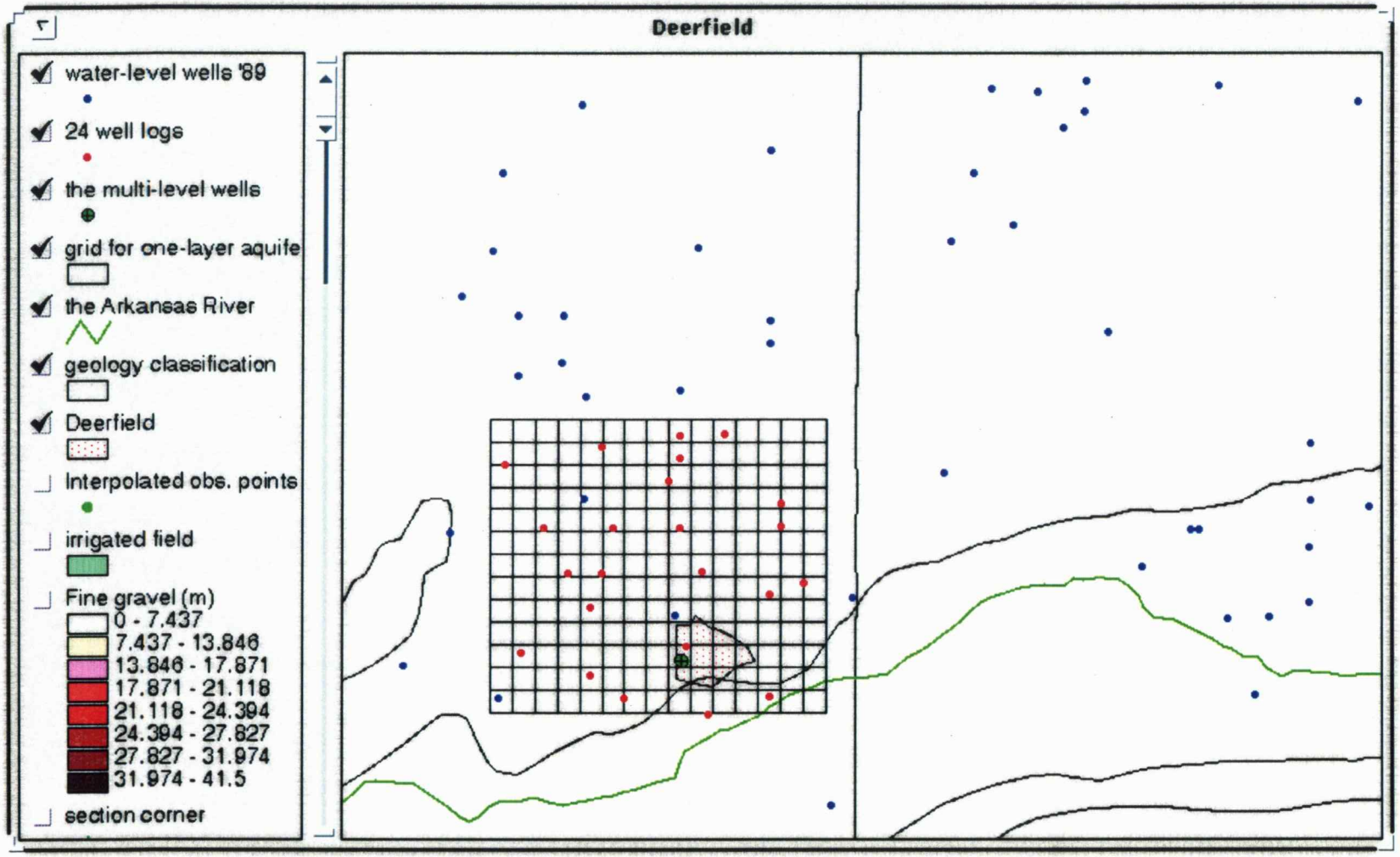

Figure 6.1 The location of water-level wells and lithologic logs.

general features of the area. The map area in the figure is the 16.5 km by 17.5 km aquifer area. The items in the column on the left side of the figure refer to overlay features. The checked items are shown in Figure 6.1.

The City of Deerfield is shown as the small irregular polygon filled with red dots. The Arkansas River is the green line to the south of the city, and Lake McKinney is the black polygon located to the west of the rectangular grid. Irrigation canals (not shown in the figure) direct water from the Arkansas River and Lake McKinney to fields in the area. The blue dots represent locations of 47 wells in the area for which water-level observations are available. The grided area encloses the locations of 24 wells for which lithologic logs exist. The logs are incorporated in calibrating the model along with the piezometric heads interpolated for the grid cells from the 47 water-level wells. The cells are 400-m squares.

In 1989, piezometric heads at the 47 water-level wells were recorded. Some of those observations were reported by local farmers while others were measured by the U.S. Geological Survey and the Division of Water Resources of the Kansas Department of Agriculture. The accuracy of measurements may not be uniform. Nevertheless, the 47 observed values are very valuable for model calibration because no other systematic field data are available. The piezometric head distribution indicates that the groundwater flow has a generally easterly direction.

A previous study have shown that the aquifer system near or in the river valley is an unconfined aquifer with a layered geologic structure composed of a sandy zone

generally underlain by clays and overlying a thicker aquifer of interbeded clay, silt, sand, and gravel. The aquifer system farther away from the valley can be considered as a single unconfined aquifer without the shallow sandy zone. There are 24 lithologic well logs available for the grided area shown in Fig. 6.1. An analysis of the well logs shows that scattered in the aquifer are clay layers or lenses which could retard vertical movement of groundwater.

In 1997, multi-level monitoring wells were installed by the Kansas Geological Survey at a site in Deerfield. The location of the site is shown in Fig. 6.1. Piezometric heads were measured at the well site on June 11, 1997 and July 23, 1997 and are shown in Fig. 6.2 along with specific conductance (SpC) and sulfate concentration determined for water samples from the wells. The dark bands indicate clay layers separating different layers of silt, sand, and gravel. In Fig. 6.2, the top layer is perched water with very high salinity of 1676 mg/L. The salinity decreases to 1037 mg/L from 20 m to about 50 m and further decreases to 530 mg/L below 50 m. The measured piezometric heads and sulfate concentrations suggest that a layered model should be used to simulate the Deerfield groundwater system.

6.2 Modeling Saline Water Migration

A two-layer groundwater model is used to study saline water migration in the Deerfield groundwater system. The contours of piezometric head shown as blue lines in Fig. 6.3 are values interpolated by TIN from the 47 water-level wells shown in Fig.

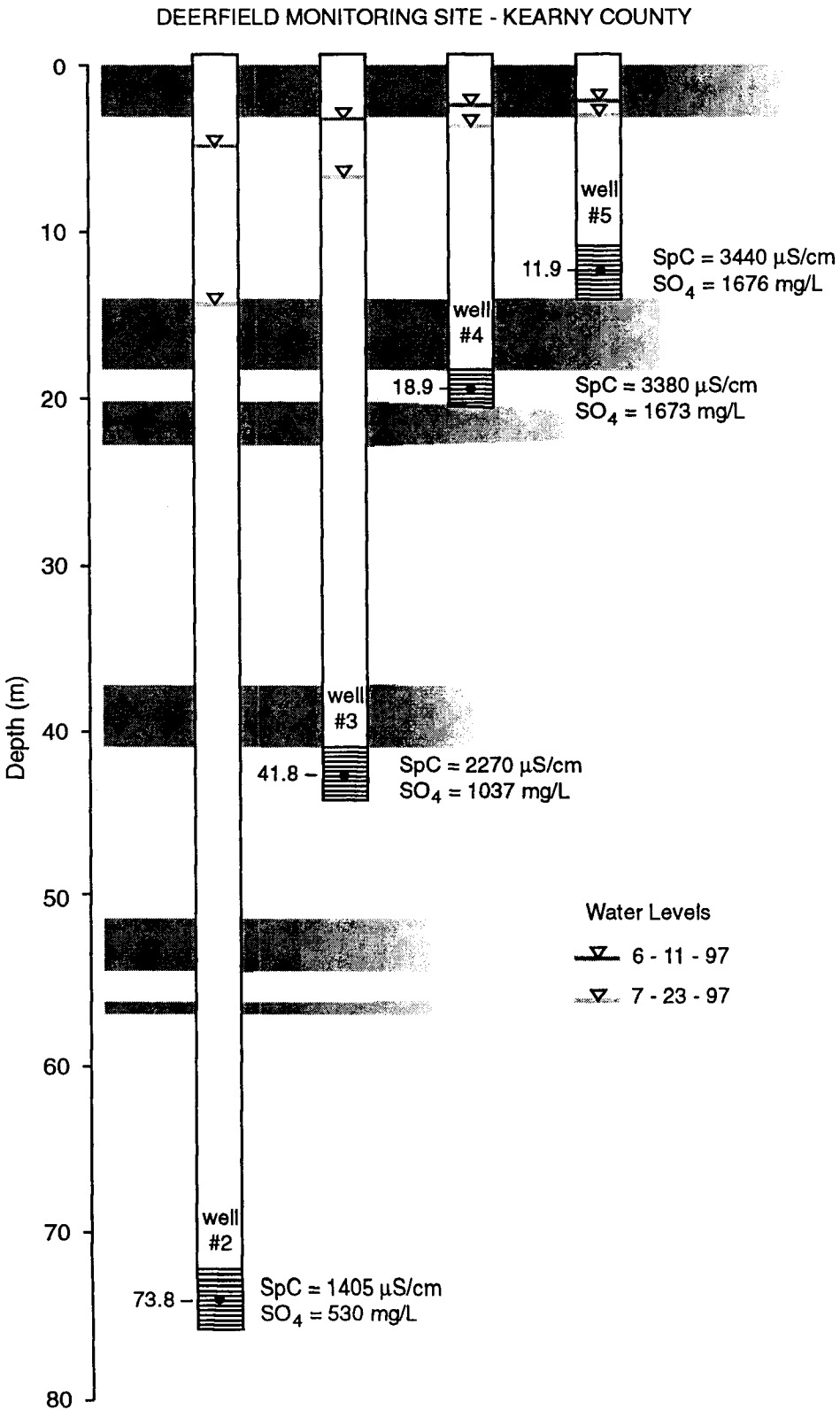

Figure 6.2. Multi-level monitoring wells at Deerfield.

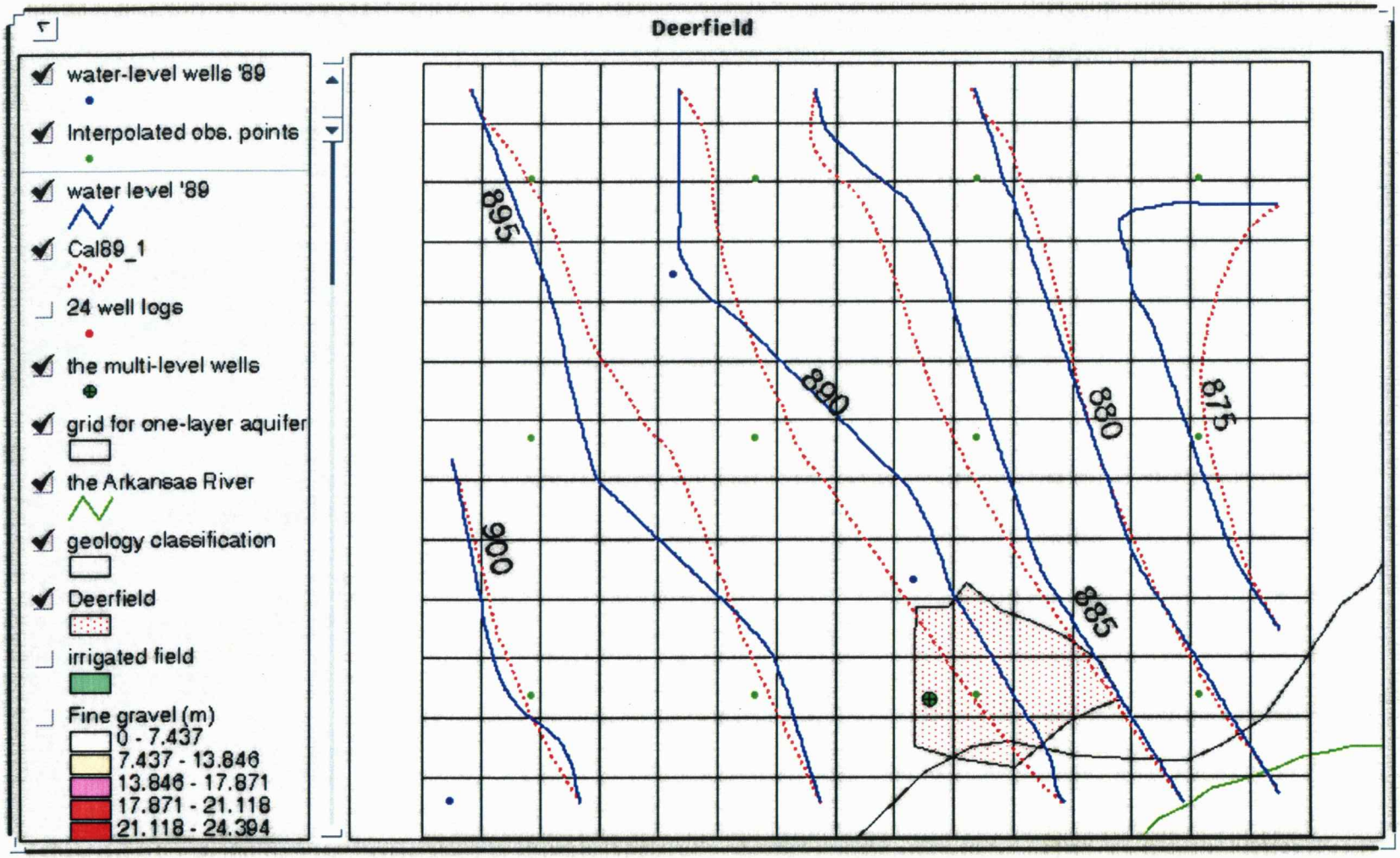

Figure 6.3 The observation points and computed water level.

6.1. The rectangular block has an area of 28.8 km^2 and is selected for model calibration using the interpolated piezometric heads. The 24 well logs in the area are used in the geologic structural method for parameter estimation. The grid system has 400-m square cells that are used in the numerical model for groundwater flow.

6.2.1 Model Parameter Estimation

An analysis of the 24 lithologic well logs is based on the five classifications of the geological material listed in Table 3.1. Based on the well-log data, the thickness of each classified material at each cell can be estimated using the kriging technique. Details of the procedure are Appendix B. An example of the estimated thickness distribution for fine gravel in the area is shown in Fig. 6.4. A scale for different color shades representing thickness ranges is shown in the left column of the figure. The spatial variation in the color shades shows the nonuniform spatial variation of the estimated thickness of fine gravel. Dark shades indicate areas of larger amounts of fine gravel and light shades show locations of low content of fine gravel. The estimated thickness distributions for the other four classifications of lithologic materials are not displayed herein.

The optimal hydraulic conductivity and specific yield of each category are obtained using the inverse method. The optimal parameter values are those values that minimize the sum of deviation squares between the computed piezometric heads shown as red dashed lines and the interpolated values shown as blue lines in Fig. 6.3.

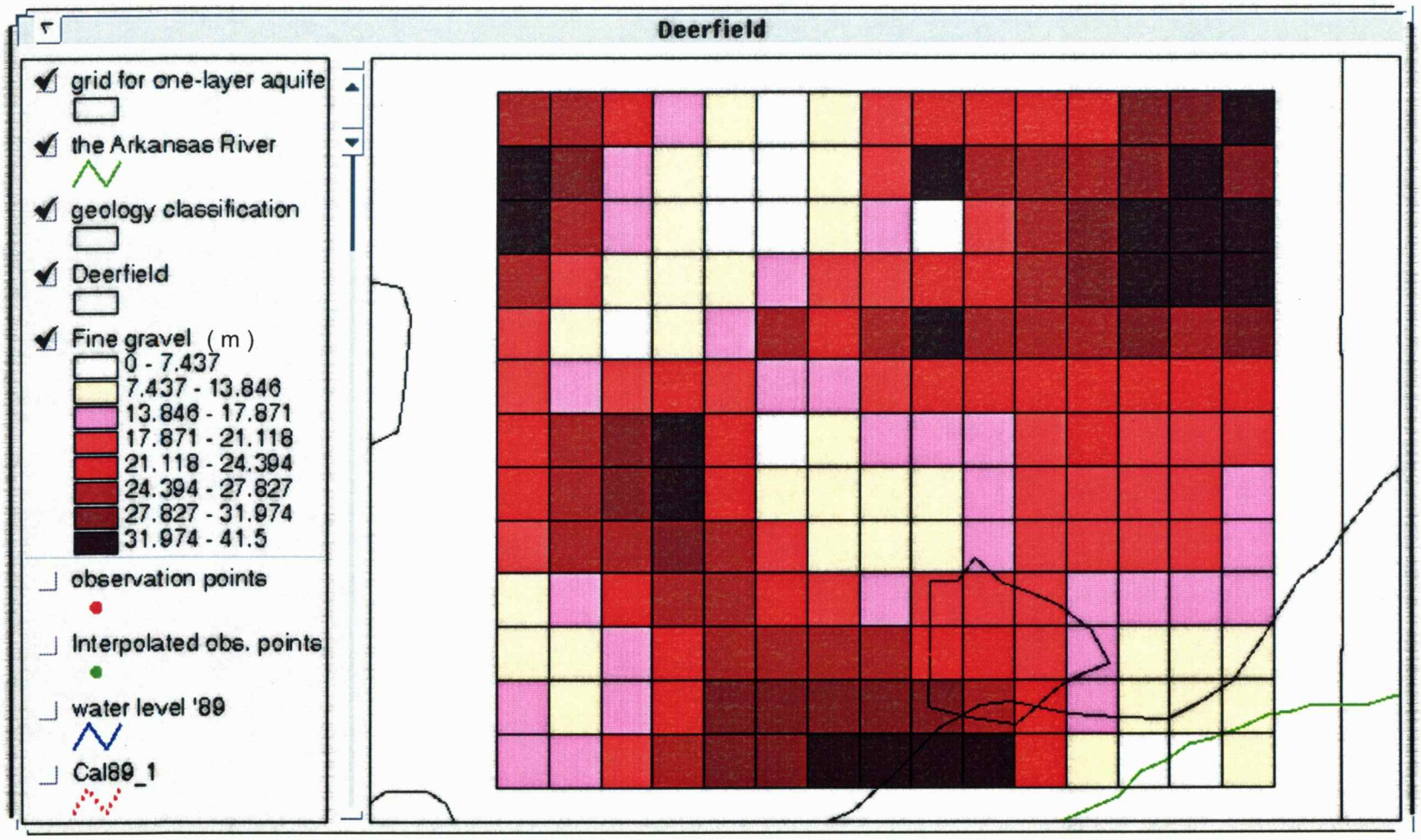

Figure 6.4 The estimated thickness distribution for the fine gravel classification listed in Table 3.1.

A time step of 15 days is used in the numerical solution. The optimal hydraulic conductivity and specific yield for the five classified materials are listed in Table 6.1

6.2.2 Saline Water Migration

A two-layer aquifer model is used for simulating the saline water migration. The area of immediate interest is shown in Fig. 6.5 together with the fields irrigated with Arkansas River water which provides the source of salinity. The ditch irrigated area has a top layer of perched water with high salinity. Below the perched water, two aquifer layers are used for modeling purposes. The first layer water has a salinity lower than that of the perched water but higher than that of the lower second layer. This two-layer model is based on a simplification of the observations from the multi-level monitoring wells in Deerfield. Sulfate concentrations of 1200 mg/L and 500 mg/L are assumed for layers 1 and 2, respectively at the boundaries adjoining the ditch irrigated fields. These values are selected based on the sulfate concentrations from the multi-level well site in Deerfield.

The modeled area is 2.5 km^2 as shown by the thick black line composing the irregular polygon in Figs. 6.5 through 6.9. Grid cells within the modeled area are 25 m squares, a size meeting the requirement for numerical accuracy of the solution. the simulation is conducted for the period 1971-1997 The piezometric head at the boundaries of the study area is assigned to boundary cells using interpolated values of the annual observations of piezometric heads at water-level wells from 1971 to 1997.

Table 6.1 The optimal values of hydraulic conductivity and specific yield for the five classifications of geological materials in the unconfined aquifer.

Geological materials	Hydraulic conductivity (m/day)	Specific yield
Fine gravel and very coarse sand	90.0	0.30
Coarse sand and medium sand	8.64	0.30
Fine sand and silty sand	0.20	0.25
Silt and sandy clay	0.003	0.15
Silty clay and clay	5.3E-5	0.01

The assigned piezometric heads for the boundary cells are assumed to remain constant through the year in the simulation. Since multi-level observations are not available for the two-layer model, the peizometric heads at the boundaries for these two layers are assumed to be the same.

There are four irrigation wells and three municipal wells that pump within the study area. No abandoned irrigation wells are known to exist in the area. However, it is possible that one or more could be present because drilling and plugging records were not required by Kansas until 1975. Although saline water could intrude into the aquifer through the irrigation wells when they were not being pumped, much of the saline water could be recovered during pumping. Therefore, they are not considered as saline water sources in this model.

The green area shown in Fig. 6.5 indicates the source of saline water assumed for this simulation. The water supply for irrigation is seasonal and the pumping may have a substantial local effect on the salinity distribution but would not affect the general trend of salinity distribution. Therefore, in the simulation only the municipal wells are assumed to be operating at a constant rate through the simulation period. The pumpage records for the municipal wells are available only after 1989. For simulating the operation during the 1970s, the annual pumpage is assumed to be one-third of the total pumpage for 1996 and the annual pumpage for 1980s is assumed to be one half. This is based on the generally greater water use per person with time and the population growth in Deerfield.

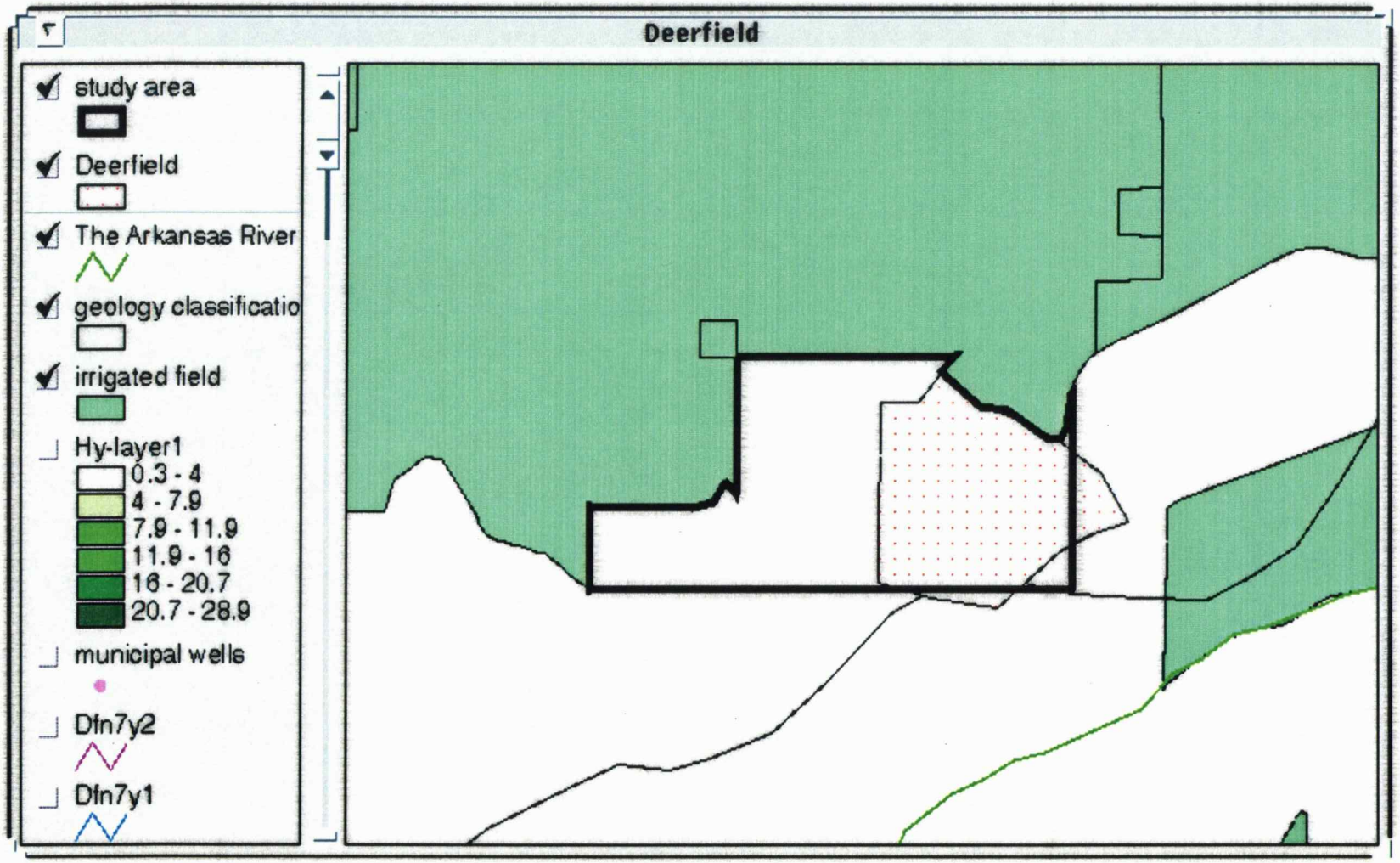

Figure 6.5 Ditch irrigated fields and the study area for saline water migration.

The estimated distributions of hydraulic conductivity for the two layers are shown in Figs. 6.6 and 6.7, respectively. The dark-green shades represents areas of high hydraulic conductivity and the lighter shaded areas have lower hydraulic conductivity. The distributions for the two layers are appreciably different. Most of layer 1 has low hydraulic conductivity whereas the low hydraulic conductivity area in layer 2 is much smaller than that of the layer 1. The distribution of hydraulic conductivity directly affects the distribution of salinity in the study area. The values of the parameters used in the simulation are summarized in Table 6.2.

The computed salinity distributions in the two layers at the end of the 7th year of simulation are shown in Figs. 6.8 and 6.9, respectively. The large area of low hydraulic conductivity in layer 1 apparently causes relatively slower spreading of the saline water than that in layer 2. Although the boundary sulfate concentration is 1200 mg/L, at the end of the 7th year the water in less than half of layer 1 has a sulfate content greater than 800 mg/L. In contrast, over half of the area in the lower layer has water with sulfate concentrations close to the fixed boundary value of 500 mg/L.

A break-through curve for sulfate concentration at the site of municipal well #3 is shown in Fig. 6.10. There is a steep rise in the sulfate content from the end of the 6th year through the 7th year. It takes about seven years for the salinity front to reach the municipal well site.

A plot of the observed sulfate concentration for the public water supply for Deerfield from 1950 through 1997 is shown in Fig. 6.11. From 1950 through 1975,

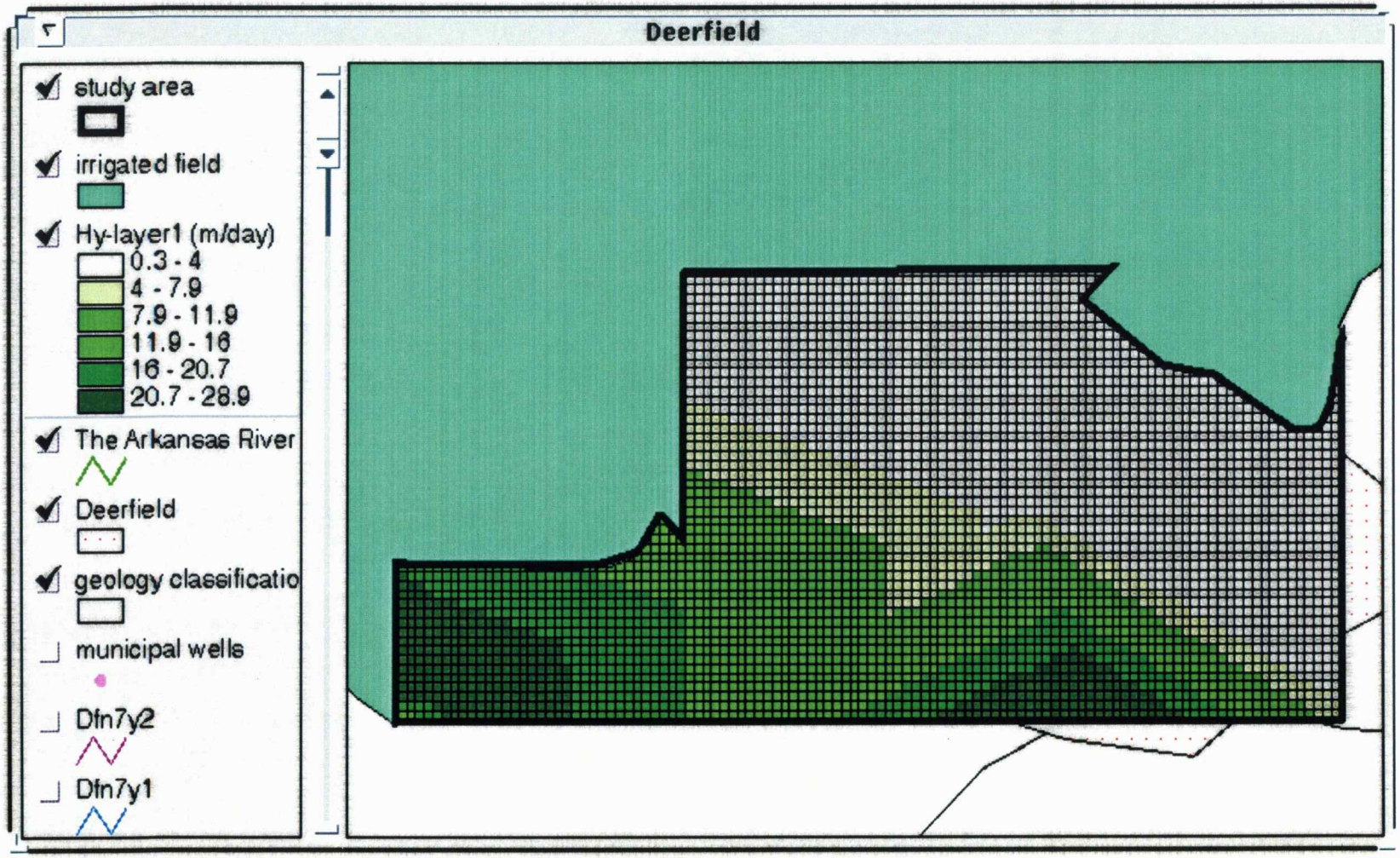

Figure 6.6 The estimated distribution of the horizontal hydraulic conductivity for layer 1.

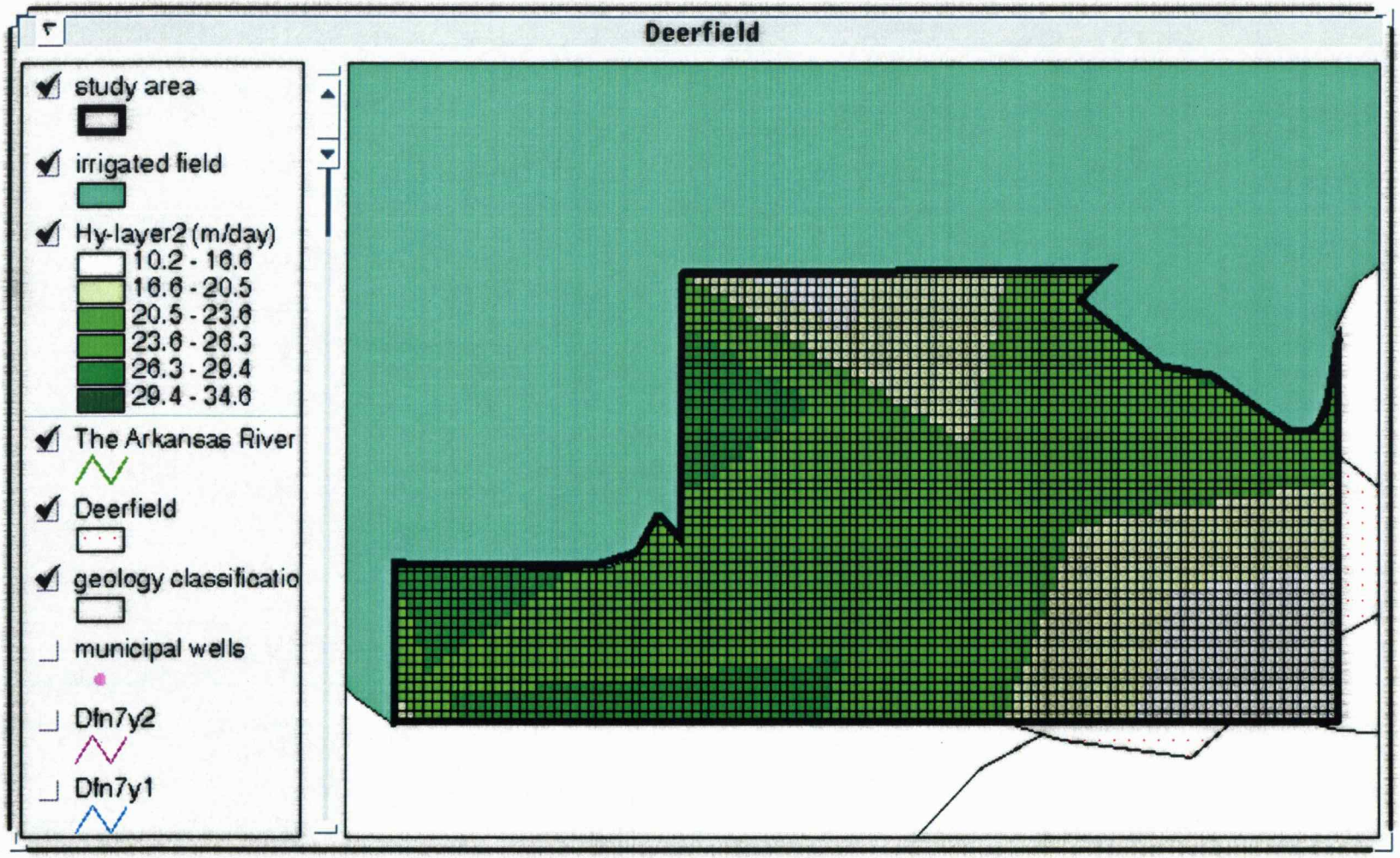

Figure 6.7 The estimated distribution of the horizontal hydraulic conductivity for layer 2.

Table 6-2 : Values of variables and parameters used in the numerical simulation.

Aquifer and other parameters	
horizontal hydraulic conductivity	Fig. 6.6 and Fig.6.7
vertical conductance	0.00003 m^2/day
specific yield	Fig. C.1
storage coefficient	S_c = 0.00002
porosity	θ = 0.25
longitudinal dispersivity	α_x = 5 m
horizontal transverse dispersivity	α_y = 0.5 m
vertical transverse dispersivity	α_z = 0.05
background sulfate concentration for layer 1	800 mg/L
background sulfate concentration for layer 2	100 mg/L
time step	30 days
total simulation time	27 years (1971-1997)

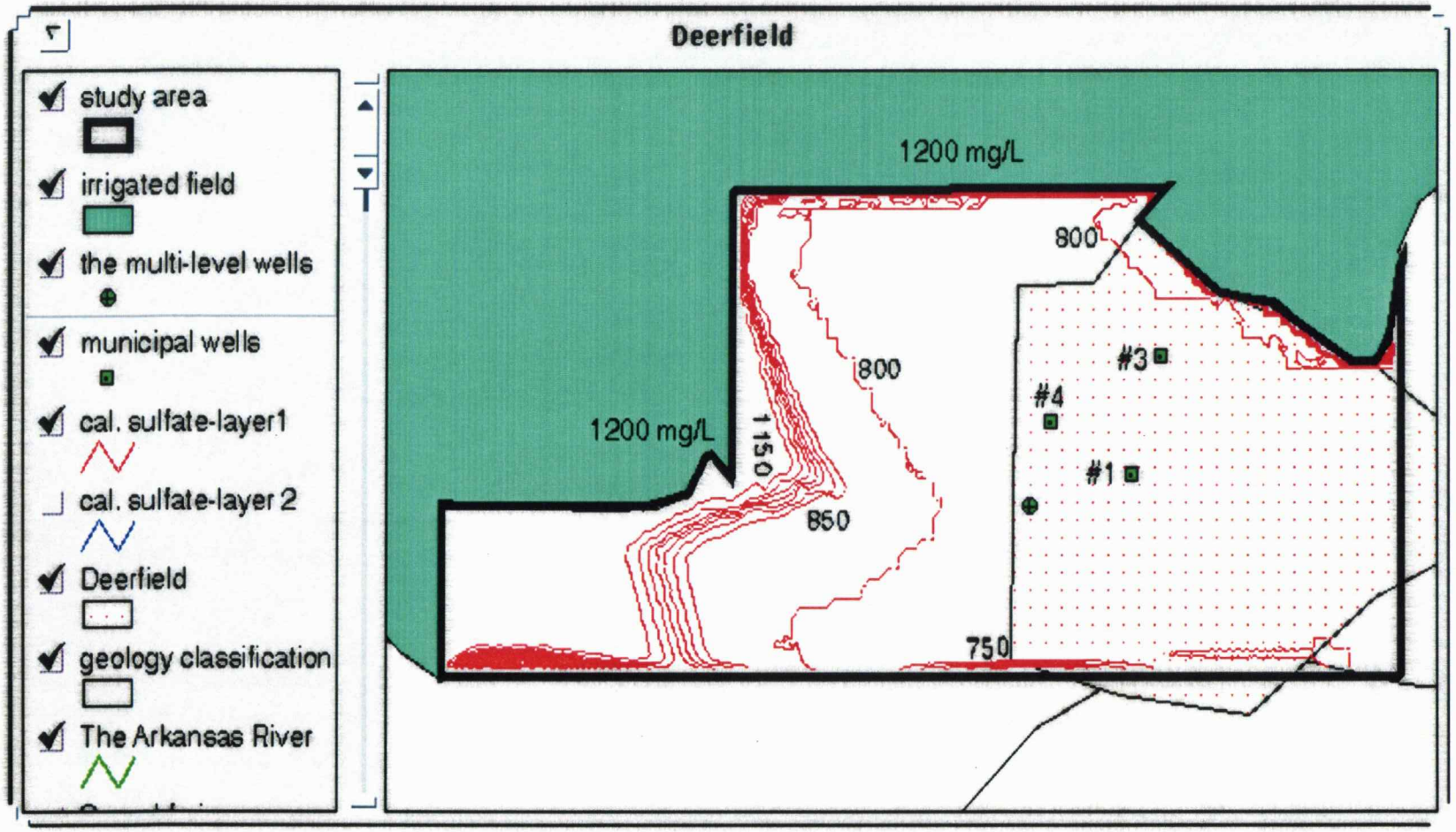

Figure 6.8 Contours of the computed sulfate concentration at the end of the seventh year for layer 1.

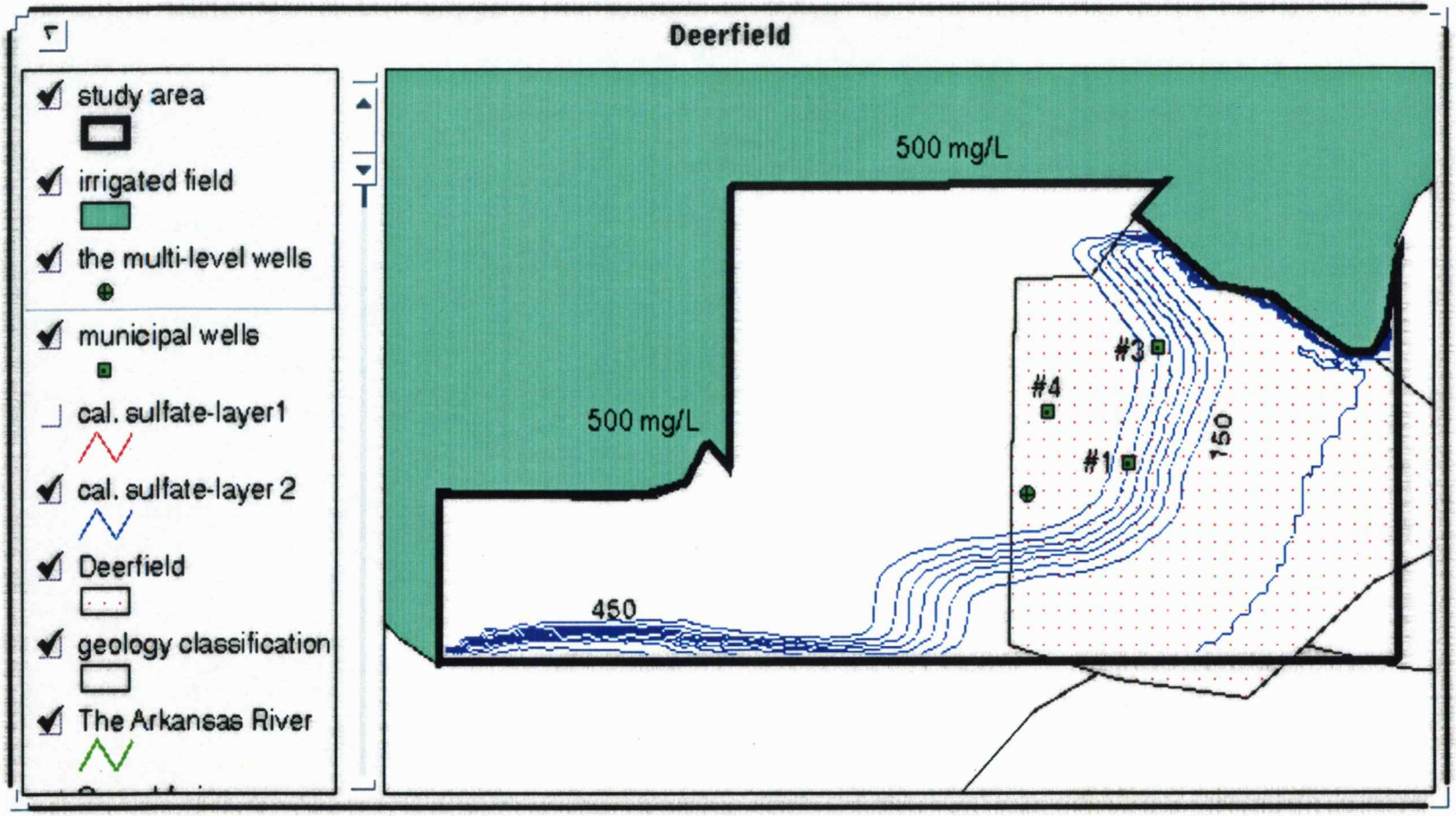

Figure 6.9 Contours of the computed sulfate concentration at the end of the seventh year for layer 2.

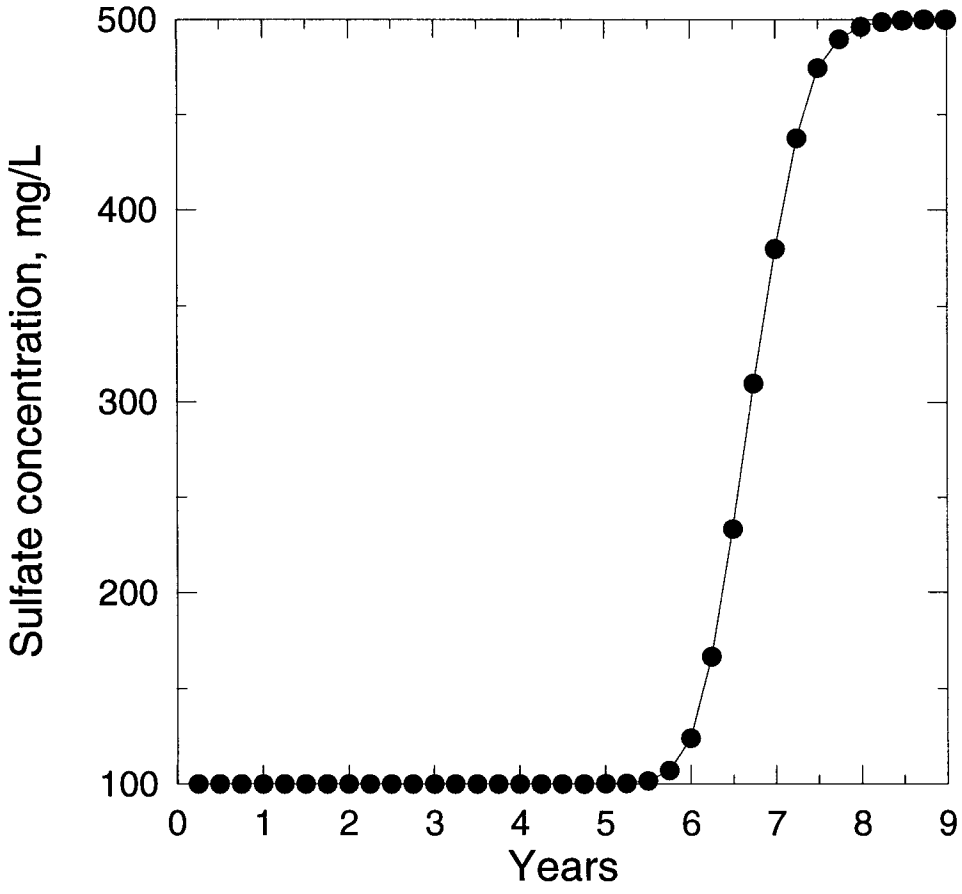

Figure 6.10 The break-through curve at the location of well #3 for layer 2.

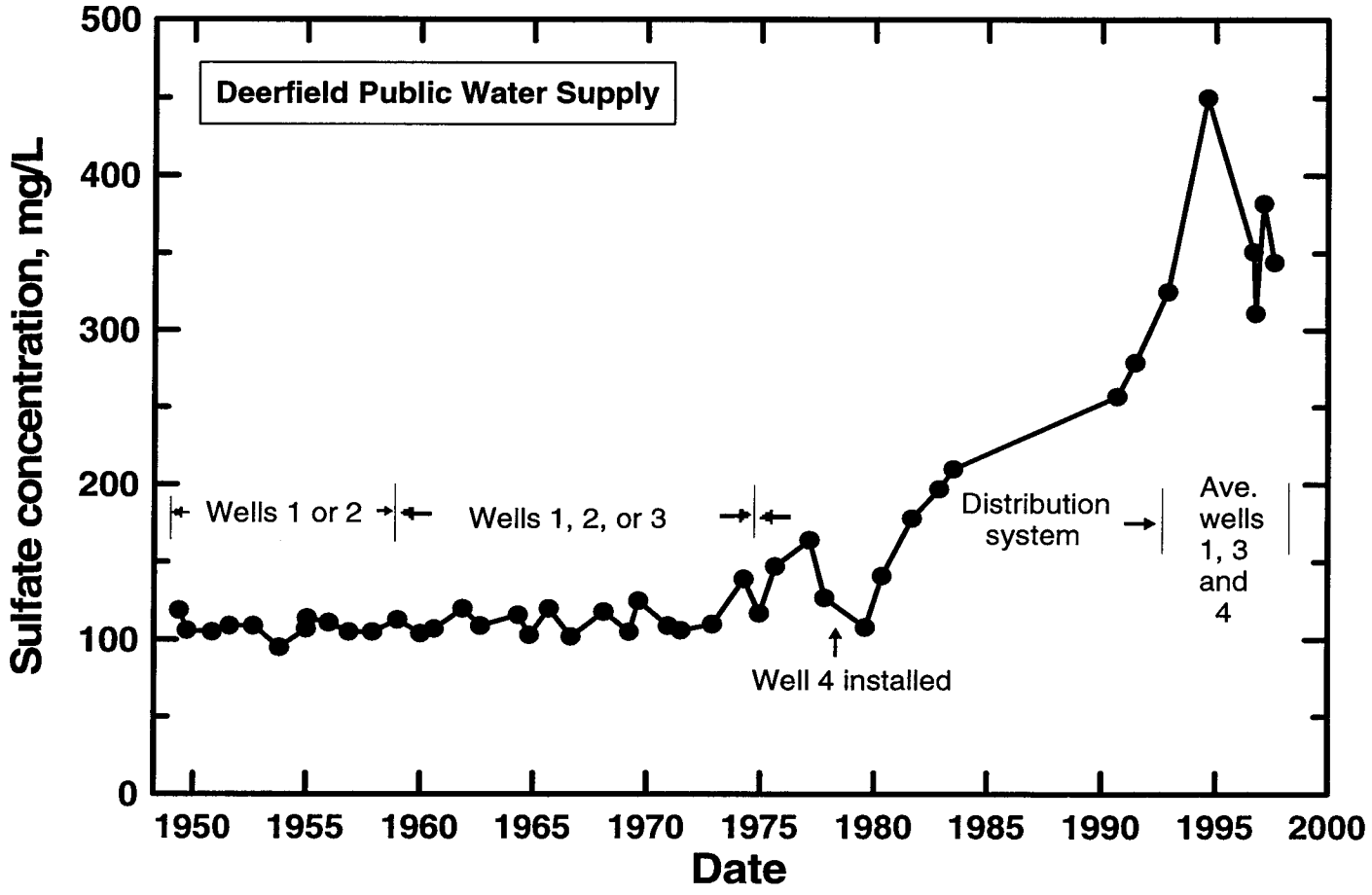

Figure 6.11 Change in sulfate concentration with time for city water-supply wells of Deerfield, Kansas.

water samples were usually annually collected from one of the existing wells. The small variation in sulfate content implies that the salinity distribution in the area where the wells are located was probably uniform. The dramatic increase in the salinity of the public supply waters appears similar to the shape of the break-through curve of Fig. 6.10. Since the municipal water is pumped from the lower layer, the simulated results suggest that the boundary sulfate concentration may not have risen to 500 mg/L until about 7 or 8 years before the early 1980's, in comparison with the assumption of 500 mg/L for 1971. This implication will provide a basis for further examination of a plausible mechanism for the salinity increase in the municipal water supply. The developed model also needs to be validated by additional field data before it can be applied with some certainty for making management decisions.

VII. CONCLUSIONS AND RECOMMENDATIONS

Saline water intrusion in groundwater observed in southwestern Kansas near the Arkansas River is investigated by using mathematical models and available field data to determine the important mechanisms of saline water intrusion and to estimate its effect on fresh groundwater. The results obtained in the study lead to the following conclusions and recommendations.

7.1 Conclusions

1. The results of the conceptual model show that flow of perched saline water through a non-pumping irrigation well is a viable mechanism for intrusion of saline water that can substantially contaminate deeper fresh groundwater. The computed area covered by saline water with a sulfate concentration of 250 mg/L or larger in the sixth layer of the model is approximately 0.25 km^2 at the end of the fifteenth year. This is based on the model assumption of hydraulic conductivities and dispersivities. In the study area, the estimated density of irrigation wells is about four wells per square kilometer. This source of contamination could have substantial effects on the quality of groundwater.

2. An analysis of the lithologic data indicates that clay lenses are extensively distributed in the aquifer near Deerfield. Consequently, the vertical leakage and transverse dispersivity do not significantly affect the numerical simulations. The

spreading of the contaminant source is mainly dominated by the convective process of the groundwater flow. Thus, the selection of the horizontal hydraulic conductivity in the model has a major effect on the results.

3. The model parameters, such as hydraulic conductivity and specific yield, are estimated using the geological structure method through an inverse solution procedure. Their values are directly related to the different geological materials existing in the aquifer determined form lithologic well-log data. Thus, the parameter dimension is simply related to the number of geological materials. The ranges of these parameter values are known for different geological materials and can be used as constraints in the optimal estimation of model parameters. This approach not only includes field geologic information but also reduces the parameter dimension.

4. The GIS-based integrated system for modeling saline water intrusion in groundwater is applied to the groundwater system near the city of Deerfield. Infiltration of saline water from below ditch irrigated fields and non-pumping irrigation wells outside of the model area appear to be the dominant source of contamination that migrates within the aquifer layers into the study area, rather than flow down irrigation wells within the study area. Comparison of the simulation, including the operation of the municipal wells, to observations for the municipal supply waters suggests that the major intrusion of salinity into the lower aquifer outside and near the boundary of the study area did not occur until the mid 1970's.

7.2 Recommendations

1. To mitigate the saline water intrusion through abandoned irrigation wells, it is recommended that the abandoned wells should be plugged to include grouting the annular zone, as well as the inside of the casing. Also, sealing the annular space in newly constructed wells through the low permeability zone would be an important measures for protecting the Ogallala aquifer.

2. The numerical model used in this study involves uncertainties in model parameters, boundary conditions and initial conditions. Systematic data collection including piezometric head and salinity concentration is needed for model validation. The sulfate concentration sampled in the municipal water supply wells may change with sampling time during pumping as well as during seasons of the year. Thus, a time series of sample concentrations would aid in determining average values for comparison with the computed value from the model.

3. Although many lithologic well logs are available for the general study area, the density distribution of the logs is still low that it is very difficult to find an accurate semivariogram model. Additional well logs are needed to reduce the uncertainty in the semivariogram.

4. A recent advance in GIS software is the three-dimensional analysis package now available for use with ARCVIEW. The next step for further developing the integrated system would be to produce a link to this 3-D GIS. The 3-D visualization

of contaminant plume, lithologic, and other spatial data would improve the interactive integrated system for practical use in sophisticated models.

References

Ahlfeld, D. P. and Zafirakou, A., 1994. An algorithm for approximate solution of the groundwater contaminant remediation problem. Computational methods in water resources X, Kluwer Academic Publishers, Netherlands.

Bard, Y., 1974. Nonlinear parameter estimation. Academic Press, San Diego, California.

Blandford, T. N and Huyakorn, P. S., 1990. A modular semi-analytical model for the delineation of wellhead protection areas. U.S. Environmental Protection Agency Office of Ground-Water Protection, Washington, DC.

Bureau of Reclamation, 1993. Arkansas River water management improvement study- Modeling of chloride transport in the Equus Beds aquifer. Technical report. U. S. Department of Interior.

Burrough, P. A., 1986. Principles of geographic information systems for land resources assessment. Clarendon Press, Oxford, Great Britain.

Cooley, R. J., 1979. A method of estimating parameters and assessing reliability for models of steady state groundwater flow: 2. Application of statistical analysis. Water Resources Research, v 15, no. 3, pp. 603-617.

Davis, J. C., 1986. Statistics and data analysis in geology, 2nd ed., John Wiley, New York.

Deutsch, C. and Journel, A., 1992. GSLIB: Geological software library and user's guide. Oxford University Press, New York.

DeVantier, B. A., and Feldman, A. D., 1993. Review of GIS applications in hydrologic modeling. Journal of Water Resources Planning and Management, v. 119, no. 2, pp. 229-245.

Doherty, J., 1994. PEST. Watermark Computing, Corinda, Australia.

Dunlap, L. E., Lindgren, R. J., and Sauer, C. G., 1985. Geohydrology and model analysis of the stream-aquifer system along the Arkansas River in Kearny and Finney counties. southwestern Kansas: U. S. Geological Survey, Water-supply Paper 2253, 52 p.

El-Kadi, A. I., Oloufa, A. A., Eltahan, A. A., and Malik, H. U., 1994. Use of a geographic information system in site-specific ground-water modeling. Ground Water, v. 32, no. 4, pp. 617-625.

Eppstein, M. J. and Dougherty, D. E., 1996. Simultaneous estimation of transmissivity values and zonation. Water Resources Research, v 32, no. 11, pp. 3321-3336.

ESRI, 1994. Introducing ArcView. Environmental Systems Research Institute, Inc. Redland, California.

Fetter, C. W., 1994. Applied hydrogeology. Macmillan College Publishing Company. New York.

Gelhar, L. W., Welty, C., and Rehfeldt, K. R., 1992. A critical review of data on field-scale dispersion in aquifers. Water Resources Research, v 28, no. 7, pp. 1955-1974.

Goodchild, M. F., Parks, B. O., and Steyaert, L. T., 1993. Environmental modeling with GIS. Oxford University Press. New York.

Gutentag, E. D., Lobmeyer, D. H., and Slagle, S. E., 1981. Geohydrology of southwestern Kansas. Kansas Geological Survey Irrigation Series 7.

Harlin, J. M. and Lanfear, K. J., 1993. Proceedings of the Symposium on geographic information systems and water resources. American Water Resources Association.

Keidser, A. and Rosbjerg, D., 1991. A comparison of four inverse approaches to groundwater flow and transport parameter identification. Water Resources Research, v. 27, no. 9, pp. 2219-2232.

Konikow, L. F. and Bredehoeft, J. D., 1978. Computer model of two-dimensional solute transport and dispersion in groundwater. Techniques of Water-Resources Investigations of the U.S. Geological Survey. Book 7, Chapter C2.

LaVenue, A. M. and Pickens, J. F., 1992. Application of a coupled adjoint sensitivity and kriging approach to calibrate a groundwater flow model. Water Resources Research, v 28, no. 6, pp. 1543-1569.

Ma, T., 1996. Geostatistical analysis of field data and numerical solution for saltwater intrusion into the freshwater aquifer in south-central Kansas. Ph.D. Dissertation, University of Kansas.

Maidment, D. R., 1993. GIS and hydrology modeling. in the Proceedings of "Environmental modeling with GIS." edited by Goodchild et al.

Maguire, D. J., 1992. The raster GIS design model - a profile of ERDAS. Computer and Geoscience, v. 18, no. 4, pp 463-470.

Mangold, D. C. and Tsang, C. F., 1991. A summary of subsurface hydrological and hydrochemical models. Review of Geophysics, v. 29, no. 1, pp. 1379-1394.

Marquardt, D. W., 1963. An algorithm for least squares estimation of nonlinear parameters. SIAM Journal of Numerical Analysis, no. 11, pp 431.

McDonald, J. M., and Harbaugh, A. W., 1988. A modular three-dimensional finite-difference ground-water flow model. Techniques of Water Resources Investigations of the United States Geological Survey, Book 6, Chapter A1.

Medina, A. and Carrera, J., 1996. Coupled estimation of flow and solute transport parameters. Water Resources Research, v 32, no. 10, pp. 3063-3076.

Meyer, W. R., Gutentag, E. D., and Lobmeyer, D. H., 1970. Geohydrology of Finney county, southwestern Kansas. USGS Water-Supply Paper 1891.

Morehouse, S., 1992. The ARC/INFO geographic information system. Computer and Geoscience, v. 18, no. 4, pp 435-441.

Neuman, S. P., 1973. Calibration of distributed parameter groundwater flow models viewed as a multiple-objective decision process under uncertainty. Water Resources Research, v 9, no. 4, pp. 1006-1021.

Orzol, L. L. and McGrath, T. S., 1992. Modifications of the U.S. Geological Survey modular, finite-difference, ground-water flow model to read and write geographic information system files. U.S. Geological Survey Open-File Report 92-50.

Redell, D. L. and Sunada, D. K., 1970. Numerical simulation of dispersion in groundwater aquifers. Colorado State University Hydrology paper 41, 79p.

Reeves, M., Ward, D. S., Johns, N. D., Cranwell, R. M., 1986. Theory and implementation for SWIFT II, the Sandia Water-Isolation Flow and Transport Model for Fractured Media. Rep. NUREG/CR-3328 and SAND83-1159, Sandia National Lab., Albuquerque, N. M.

Rifai, H. S., Hendricks, L. A., Kilborn, K., and Bedient, P. B., 1993. A geographic information system (GIS) user interface for delineating wellhead protection areas. Ground Water, v. 31, no. 3, pp. 480-488.

Roaza, H., Roaza, R. M., and Wagner, J. R., 1993. Integrating geographic information systems in ground-water applications using numerical modeling techniques. Water Resources Bulletin, v.29, no. 6, pp. 981-988.

Rushton, K. R. and Redshaw, S. C., 1979. Seepage and groundwater flow-numerical analysis by analog and digital methods. John Wiely and Sons, New York.

Strecker, E. W. and Chu, W., 1986. Parameter identification of a ground-water contaminant transport model. Ground Water, v. 24, pp. 56-62.

Sun, N. Z., 1994. Inverse problems in groundwater modeling. Kluwer Academic Publishers, Netherlands.

Sun, N. Z., Jeng, M. C., and Yeh, W., 1995. A proposed geological parameterization method for parameter identification in three-dimensional groundwater modeling. Water Resources Research, v. 31, no. 1, pp. 89-102.

Tsou, M.-S., and Whittemore, D. O., 1996. Interfacing Geographic information Systems with Groundwater models. EOS, Transactions, American Geophysical Union Fall Meeting, v. 77, no. 46, pp. 264.

Tsou, M.-S., Whittemore, D. O., and Yu, Y.-S.,1997. Development of an interactive integrated groundwater modeling and geographic information system for the upper Arkansas River corridor study. Kansas Geological Survey Open-File Report 97-35.

Tsou, M.-S., 1998. GISFLOW, A GIS-based integrated system for ground-water flow and transport modeling. Kansas Geological Survey Open-File Report No. 98-12.

Tim, U. S., Dharmesh, J., and Liao, H.-H., 1996. Interactive modeling of ground-water vulnerability within a geographic information system environment. Ground Water, v. 34, no. 4, pp. 618-627.

U.S.G.S. Water Resources Data Kansas Water Year 1995. U.S. Geological Survey Water-Data Report KS -95-1.

Wagner, B. J. and Gorelick, S. M., 1987. Optimal groundwater quality management under parameter uncertainty. Water Resources Research, v 23, no. 7, pp. 1162-1174.

Wagner, B. J., 1992. Simultaneous parameter estimation and contaminant source characterization for coupled groundwater flow and contaminant transport modelling. Journal of Hydrology, v. 135, pp. 275-303.

Wang, G.-T. and Yu, Y.-S., 1990. Modeling rainfall-runoff process including losses. Water Resources Bulletin, v. 26, no. 1, pp. 61-66.

Watkins, D. W., McKinney, D. C., Maidment, D. R., and Lin, M.-D., 1996. Use of geographic information systems in ground-water flow modeling. Journal of Water Resources Planning and Management, v. 122, no. 2, pp. 88-96.

Whittemore, D. O., Tsou, M.-S., and Grauer, J., 1996. Upper Arkansas River corridor study: Inventory of available data and development of conceptual models. Kansas Geological Survey Open-File Report 96-19.

Whittemore, D. O., and Butler, J.J., 1997. Invasion of saline Arkansas River water into the Ogallala aquifer. 14th Annual Water and the Future of Kansas Conference Proceedings.

Xiang, Y., Sykes, J. F., and Thomson, N. R., 1992. A composite L_1 parameter estimation for model fitting in groundwater flow and solute transport simulation. Water Resources Research, v 29, no. 6, pp. 1661-1673.

Yeh, W., 1986. Review of parameter identification procedures in groundwater hydrology: the inverse problem. Water Resources Research, v 22, no. 2, pp. 95-108.

Young, D., Grauer, J., and Whittemore, D. O., 1997. Upper Arkansas River corridor study: Progress on lithologic characterization of unconsolidated deposits in the study area with emphasis on Kearny and Finney counties.

Yu, Y. S., 1991. Parameter identification in water resources. Proceedings, the Fourth International Conference on Computing Civil and Building Engineering, Tokyo, Japan, July 29-31, pp. 361-364.

Zheng, C., 1992. A modular three-dimensional transport model for simulation of advection, dispersion and chemical reactions of contaminants in groundwater systems. S. S. Papadopulos & Associates, Inc. Rockville, Maryland.

APPENDIX A

NOTES ON THE INTERACTIVE INTEGRATED SYSTEM

A.1 Introduction

A.1.1 General

The interface is saved as an ARCVIEW project called avgm.apr. The interface is customized in Views, so one can utilize the interface by opening a View. Five menus, "Create", "Modflow", "Mt3d", "P.I.", and "Utilities", are listed on the menu bar. Some functions in the interface are required to link with ARC/INFO. In other words, the interapplication communication between ARCVIEW and ARC/INFO need to be established. For the distinguishing purposes, the symbol (*) is added on the end of a function title, which indicates the requirement of linking with ARC/INFO for this function. For instance, the function title "5. Export and Generate" is followed by (*) in A.2 Create.

In the text, the script is referred to a code written in AVENUE within ARCVIEW. AML is an Arc Macro Language in ARC/INFO. F77 is referred to FORTRAN 77.

A.1.2 Installation

The first step is to open the compressed file avgm.tar.Z in the root directory. The project avgm.apr is in the directory " ~/avgm/work". The avgm1.apr is a backup of the avgm.apr. To launch ARCVIEW and the interface type "arcview avgm&" in the directory " ~/avgm/work". Place the executable files of MODFLOW, MT3D, and

F77 codes within " ~/avgm/f77" in a specific directory which can be reached from any other directory. The executable file of "trcon.f" should only be place in " ~/avgm/work".

A.1.3 Interapplication communication

Interapplication communication (IAC) establishes communication between client and server applications. In the interface, ARCVIEW acts as a client and sends requests to a server ARC/INFO to manipulate spatial analysis which ARCVIEW cannot handle. ARCVIEW communicates with ARC/INFO through Remote Procedure Call on a UNIX platform. The client and server can be on different computers in a network. On the other hand, software such as groundwater models and the parameter estimation program PEST used in the integrated system can be directly called by ARCVIEW since ARCVIEW can send system commands to the UNIX system to execute these files.

A.2 CREATE

When a View is opened, there is a menu "Create" on the menu bar. There are five items, "Grid - input coordinates", "Grid - drag a rectangle", "Grid - variant sizes", "Grid - variant sizes and rotation", and "Export and Generate", under the menu as shown in Fig. A.1.

A.2.1 Grid - input coordinates

One can create a grid shapefile with a homogeneous grid size and a shapefile of grid center points by executing the function. These two shapefiles can also be

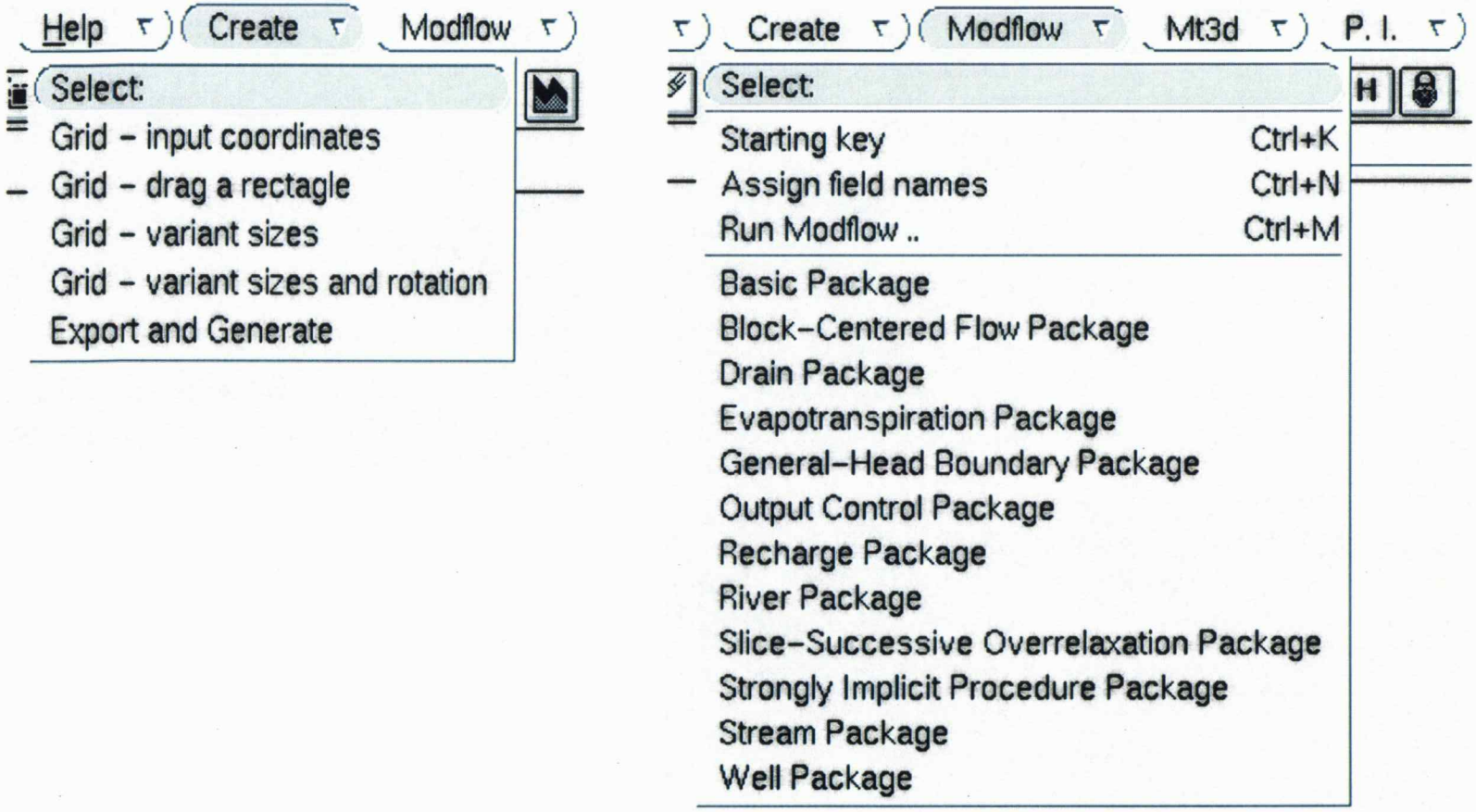

Figure A.1 The items under the menu “Create” and “Modflow”.

obtained in the next three functions. The coordinates of the lower left and upper right corners, and the grid cell width and height must be entered. The script for this function is "mkgrid_cor".

A.2.2 Grid - drag a rectangle

This function allows dragging a rectangle over the desired area to be grided instead of entering the grid corner coordinates. The number of rows and columns must be specified. This function is executed by clicking the button "D" on the tool bar; the related script is "mkgrid_drg".

A.2.3 Grid - variant sizes

This function can create variable grid cell sizes. It needs the lower left coordinate and the number of grid-cell sizes along a row and a column instead of the upper right corner coordinate. In the pop-up menu, there is a line "Widths along a row: 3*1000 7*500" which specifies different widths along a row. "3*1000" is called a set of width, which means there are 3 grid cells with the width 1000 along the row. Each set is separated by a space, so there are two sets of width in this entering. The "2" needs to be entered in the following line. The related script is "mkgrid_var".

A.2.4 Grid - variant sizes and rotation

The method of entering data is the same as for the previous function 3 but the last line "Rotation degree:(number)" is additional. The number, such as "30", means 30 degrees East of North. The grid is created as a "Polygon" rather than "Rect"

(rectangle) used by the previous function, thus it might take more time to create grids than by the function without rotation. The related script is "mkgrid_rot".

A.2.5 Export and Generate (*)

This function exports a grid shapefile to ARC/INFO as a generate file and generates a point and a polygon coverage in ARC/INFO. The shapefile of a grid created by one of the four grid functions must be sent to ARC/INFO and converted a point coverage in order to store the spatial attributes of each cell. Before running the item, IAC must be opened through the item "Open IAC" under the menu "Utilities" (see Section A.6 UTILITIES). In addition, the theme of interest should be active. The related script and AML are "exp_gen" and "gen.aml".

A.3 MODFLOW

This section describes the user interface for the groundwater model MODFLOW. The related hydrogeologic information for the simulation area is stored in a grid point coverage which is generated from menu "Create". The information is transferred into the input files of MODFLOW through the following items. The items under the menu are shown in Fig. A.1.

A.3.1 Starting key

This item assigns global variables based on simulation data files which are initially prepared by the interface. Since ARCVIEW deletes all global variables after closing ARCVIEW, the global variables need to be re-assigned based on the existing

data file after opening ARCVIEW if work is to continue on that simulation case. The first pop-up dialogue involves assigning a directory which will store the simulation data files and the grid point coverage name. The second dialogue assigns field names which are defined in the grid point coverage. The third dialogue reads the file names of the packages used in the simulation case. These file names are stored in the file "modflow.dat" which is the input file for MODFLOW. This function can also be executed through a button with a "lock" symbol in the button bar. The related script is "assign_1".

A.3.2 Assign field names

This function is same as the second dialogue of "Starting key". If the field name of the grid point coverage is re-defined, this item must be run to enter the re-defined name. The related script is "assign_2".

A.3.3 Running Modflow

This function executes MODFLOW. The related script is "MODFLOW".

A.3.4 Basic Package

The Basic Package is the major module that controls some administrative tasks for MODFLOW. The related script and F77 code are "basic" and "avbas.f", respectively.

A.3.5 Block-Centered Flow Package

The field names of related parameters in the grid point coverage need to be defined as the following names:. "sf1" for primary storage coefficient, "hy" for

transmissivity or hydraulic conductivity, "bot" for elevation of the aquifer bottom, "vcont" for vertical hydraulic conductance, "sf2" for second storage coefficient and "top" for elevation of the aquifer top. The primary storage coefficient in the first layer is defined as "sf1_1". This convention is applied to other parameters. The program only searches for the field name with a layer number, so the layer number must be specified in the field name. The related script and F77 code are "bcf" and "avbcf.f", respectively.

A.3.6 Drain Package

The layer in which a drain is located needs to be specified for each stress period. For example, in the third dialogue, "In how many layers is the drain in? 2" and "What layers: 1 3" are shown. This means that the drain is in layer 1 and layer 3. The field names of the drain elevation and conductance should be defined as "drn_1-ele_2" and "drn_1-cond_2". The first number is a stress period and the second is a layer number. The related script and F77 code are "drn" and "avdrn.f", respectively.

A.3.7 Evapotranspiration Package

The field names of "ET surface", "Maximum ET rate", "ET extinction depth" and "layer indicator array" are defined by users in the Basic package or "Assign field names". The related script and F77 code are "evt" and "avevt.f", respectively.

A.3.8 General-Head Boundary

The field names of the GHB head and conductance should be defined as "ghb_1-head_2" and "ghb_1-cond_2". The convention is the same as the Drain

package. The related script and F77 code are "ghb" and "avghb.f", respectively. The revised script and F77 code for the Deerfield area are "ghb_n" and "avghb_n.f".

A.3.9 Output Control Package

In the second dialogue, the number of different time step sets must be entered. One time step set means one "INCODE, IHDDFL, IBUDFL, ICBCFL", so two different sets means that at least one element within "INCODE, IHDDFL, IBUDFL, ICBCFL" is different from another set of "INCODE, IHDDFL, IBUDFL, ICBCFL". The related script and F77 code are "oc" and "avoc.f", respectively.

A.3.10 Recharge Package

The field names of "recharge rate" and "layer indicator array" are defined by users in the Basic package or "Assign field names". The "layer indicator array" is shared with the Evapotranspiration package. The related script and F77 code are "rch" and "avrch.f", respectively.

A.3.11 River Package

The field names of the river head, the riverbed hydraulic conductance and the elevation of the bottom of the riverbed should be defined as "riv_1-stag_2", "riv_1-cond_2" and "riv_1-rbot_2". The convention is same as the Drain package. The related script and F77 code are "riv" and "avriv.f", respectively.

A.3.12 Slice-Successive Overrelaxation Package

This package is a method for solving the groundwater-system equations through iteration in MODFLOW. This interface is prepared for entering the parameter

values to the package. The related script and F77 code are "sor" and "avsor.f", respectively.

A.3.13 Strongly Implicit Procedure Package

Another package for solving the equations in MODFLOW. The related script and F77 code are "sip" and "avsip.f", respectively.

A.3.14 Stream Package

In the second dialogue, "Max. number of segments within a grid cell" must be entered. Generally, one grid cell has only one segment but the cell in which the stream has a tributary or a diversion has three segments. The field names of the stream segment and reach should be defined as "st1-seg" and "st1-reh". The "1" means the main segment within the grid cell. If there is more than one segment existing in the cell, the field names can be defined as "st2-seg" and "st2-reh" and so on. The field names of the stream flow, the stream stage, the streambed hydraulic conductance, the elevation of the bottom of the streambed and the elevation of the top of the streambed should be defined as "st1_1-flow_1", "st1_1-sta_1", "st1_1-cond_1", "st1_1-sbot_1" and "st1_1-stop_1". The first "1" represents the main segment within the cell, the second "1" indicates the stress period 1 and the third "1" means layer 1. The field names of the stream width, the stream slope and the stream roughness should be defined as "st1_1-width", "st1_1-slope" and "st1_1-rough". The first "1" and the second "1" have the same convention as above. The related script and F77 code are "str" and "avstr.f", respectively.

A.3.15 Well Package

The field name of the volumetric recharge rate is defined as "wel_1-q_1". The convention is the same as the Drain package. The related script and F77 code are "wel" and "avwel.f", respectively.

A.4 MT3D

The interface for MT3D is similar to the one for MODLFOW. Four main packages, "Basic Transport Package", "Advection Package", "Dispersion Package" and "Sink and Source Package", are used in the system as shown in Fig. A.2.

A.4.1 Basic Transport Package

The convention for this item is similar to "Block-Center Flow Package". The related script and F77 code are "btn" and "avbtn.f", respectively.

A.4.2 Advection Package

The Advection Package is for solving the solute transport equations in MT3D. This function is for entering parameter values needed in the package. The related script and F77 code are "adv" and "avadv.f", respectively.

A.4.3 Dispersion Package

This function is for entering the longitudinal, horizontal transverse, and vertical transverse dispersivities. The related script and F77 code are "dsp" and "avdsp.f", respectively.

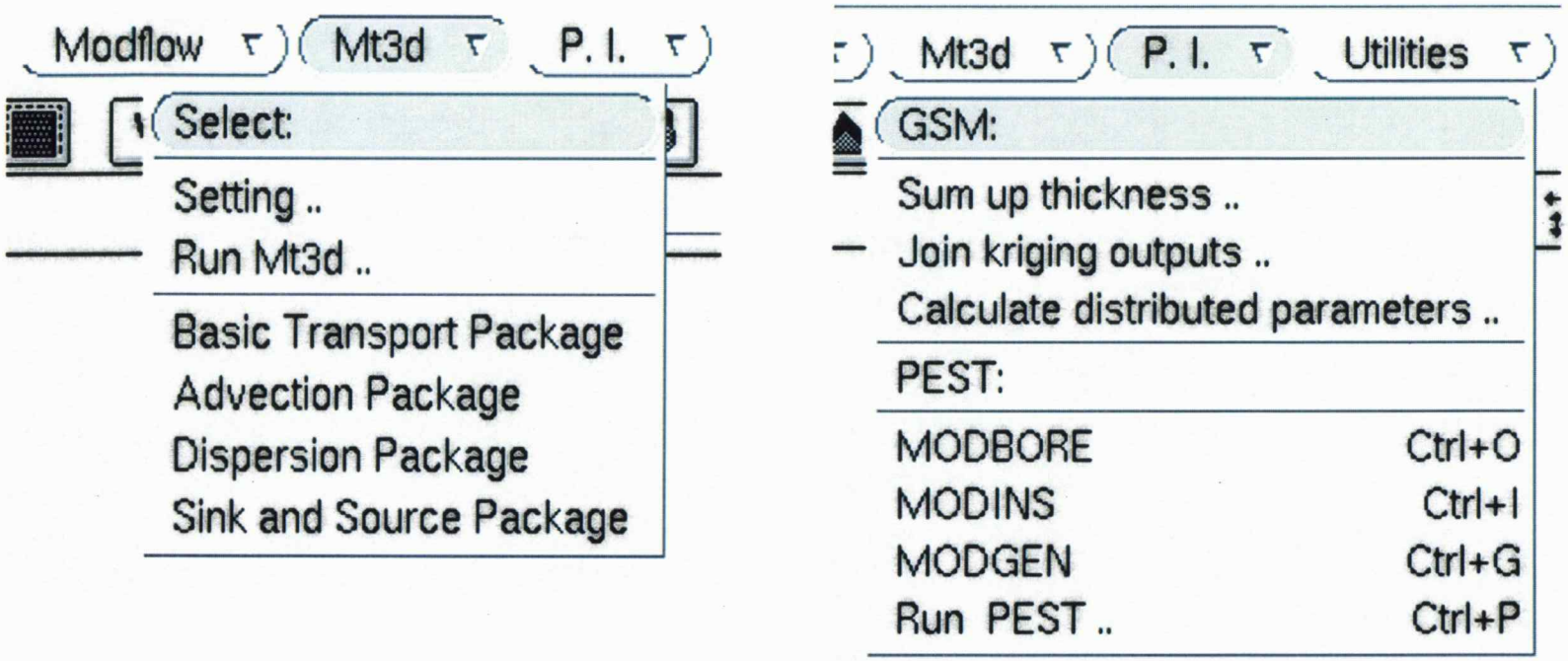

Figure A.2 The items under the menu “Mt3d” and “P. I.”.

A.4.4 Sink and Source Package

This function is for entering the concentration of the sinks and sources. The related script and F77 code are "sas" and "avsas.f", respectively.

A.5 PARAMETER IDENTIFICATION

There are two parts under the menu: one is the geological structure method (GSM) which is for parameterization, the other is a parameter estimation package (PEST) as shown in Fig. A.2. The items “Modbore”, “Modins” and “Modgen” are PEST utilities for MODFLOW and MT3D.

A.5.1 Sum Up Thickness

The different geological materials are classified into five categories. The thickness for each geological material is summed up in a model layer for each well log. A point coverage storing the total thickness of different materials can be generated. The spatial interpolation for each grid cell is computed based on the total thickness of the different materials in each well log. The related script and F77 code are "sum_thk" and "dflog.f", respectively.

A.5.2 Join Kriging Outputs

The outputs of KTB3D (GSLIB) can be placed in the grid cells and shown in the interactive system. The related script and F77 code are "jo_kr" and "trkt.f", respectively.

A.5.3 Distributed Parameters

Based on the interpolation results for each material in each grid cell, the weighted thickness for each grid cell can be calculated and the distributed values for parameters can also be obtained. The corresponding F77 code is "mops.f". The distributed results is joined into the grid cells using "jo_ps" and "trps.f".

A.5.4 Modbore

The point coverage storing the observed piezometric heads needs to be specified. The related script is "modbore".

A.5.5 Modins

A PEST instruction file by reading a output file of Modbore is generated through this function. The related script is "modins".

A.5.6 Modgen

A PEST control file is generated through this function. The related script is "modgen".

A.5.7 Run Pest

The geological structure method is incorporated into PEST by adding the program "mops.f". The related script is "pest".

A.6 UTILITIES

There are nine items, "Open IAC", "Close IAC", "Contour simulation outputs", "Interpolation or Contouring", "Zoning", "Updating zoned parameters",

"Intersect and Grouping", "Pre-Animation", and "Animation" under the menu "Utilities" as shown in Fig. A.3.

A.6.1 Open IAC (*)

This function opens the Interapplication Communication between ARCVIEW and ARC/INFO. One file called "cf" which stores the hostname of the machine, the server id number, and the version number is created after clicking the item. The file in the pop-up file dialog must be selected to make this information available for ARCVIEW. The message such as "Connected to server at pangaea 40000000 1" will be shown in the status bar at the bottom of the screen if the linking is successful. If the linking message doesn't appear in the status bar at the first running, comment out the line " System.Execute("arc" "&ty [iacopen "+wkpath+"cf]" "&") " in the script "iacopen" and recompile the script in order to re-run the function. Then remove the comment indication in front of the line after the second running. ARCVIEW users can share the same ARC/INFO server simultaneously by using the same file "cf". If the ARCVIEW user is not the first one to start the server and wants to share the same server, the same process described above (comment and recompilation) can be used to connect to the same server. The related script is "iacopen".

A.6.2 Close IAC (*)

This function closes the Interapplication Communication. The text "ARC/INFO server is closed" is shown in the dialogue if the operation is successful. The related script is "iacclose".

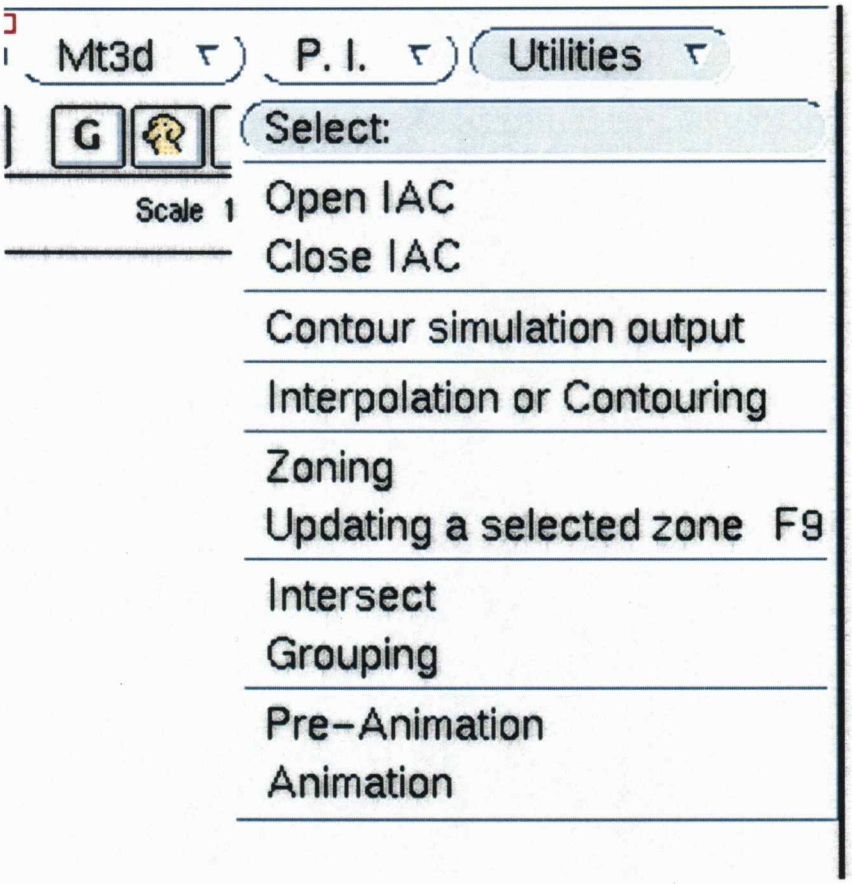

Figure A.3 The items under "Utilities".

A.6.3 Contour Simulation Results(*)

The contours for simulation results of MODFLOW or MT3D can be generated through this item. The related script, aml, and F77 codes are "coch_fg", "coch.aml" and "trcon_for.f" (or "trcon.f"), respectively. The "trcon_for.f" is for formatted outputs whereas "trcon.f" is for unformatted outputs.

A.6.4 Interpolation or Contouring (*)

This function can execute the spatial interpolation and make contours. The related script and amls are "intrp_contour", "tin_con.aml" and "tin_spot.aml".

A.6.5 Zoning and Updating zoned parameters

A zoned parameter can be updated by running "Zoning", creating a polygon to select a zone, and running "Updating zoned parameters" to update the values. The related scripts are "zoning" and "update".

A.6.6 Intersect and Grouping (*)

A stream or well points can be intersected by a grid polygon by running "Intersect" and running "Grouping" to sum or average fields and place them into the grid point coverage. The related scripts and aml are "intersect", "group_int" and "intsect.aml".

A.6.7 Pre-Animation and Animation

The themes which are to be shown for animation are first selected and the display time of each theme can be set in the function "Pre-animation". Run animation the "animation" menu. The related scripts are "animation_pre" and "animation".

APPENDIX B

KRIGING ESTIMATION

In universal kriging, a drift or a trend causes the experimental semivariogram to vary with azimuth. Owing to the absence of a large sample size, the drift is difficult to detect in this study. The omnidirectional search is conducted for semivariograms of the geological material thickness.

The Kolmogorov-Smirnov test for normality is carried out to test the normality hypothesis. The test statistics D is

$$D = \max_{-\infty<x<\infty} [F_n(x) - F_0(x)] \tag{B.1}$$

where $F_n(x)$ is the sample's cumulative distribution function, and $F_0(x)$ is a known normal cumulative distribution function. The results show that at a significant level of 5%, the test statistics, D, for five geological materials are 0.104, 0.165, 0.254, 0.120 and 0.156, which are less than that of 0.278 for a normal distribution. However, the third one, 0.254, is close to 0.278. This one is transformed to a normal score to produce a better kriging result.

The best fitted model is selected by performing the semivariogram model fitting software developed by Jian, Olea and Yu (1995). The weighted least-squares

method and the Akaike information criterion, AIC (Akaike, 1979) are used for selecting the best model. The AIC is

$$\hat{AIC} = n \ln(\frac{R_m}{n}) + 2p \tag{B.2}$$

where n is the number of points in the experimental semivariogram, p is the number of parameters in the model, and R_m is the sum of the squares of the weighted differences. The spherical model is the best semivriogram model for the five materials. The spherical model is expressed as follows

$$\gamma(h) = \begin{cases} C\left(1.5\frac{h}{a} - 0.5\left(\frac{h}{a}\right)^3\right) & , 0 \le h < a \\ C & , h \ge a \end{cases} \tag{B.3}$$

where C, h, and a are the sill, the lag and the range, respectively. The experimental semivariograms and the semivariogram models for the geological materials are shown in Fig. B.1. The thickness distribution for fine gravel is shown in Fig. 6.4. The distributed hydraulic conductivity for the one-layerd aquifer system is shown in Fig. B.2.

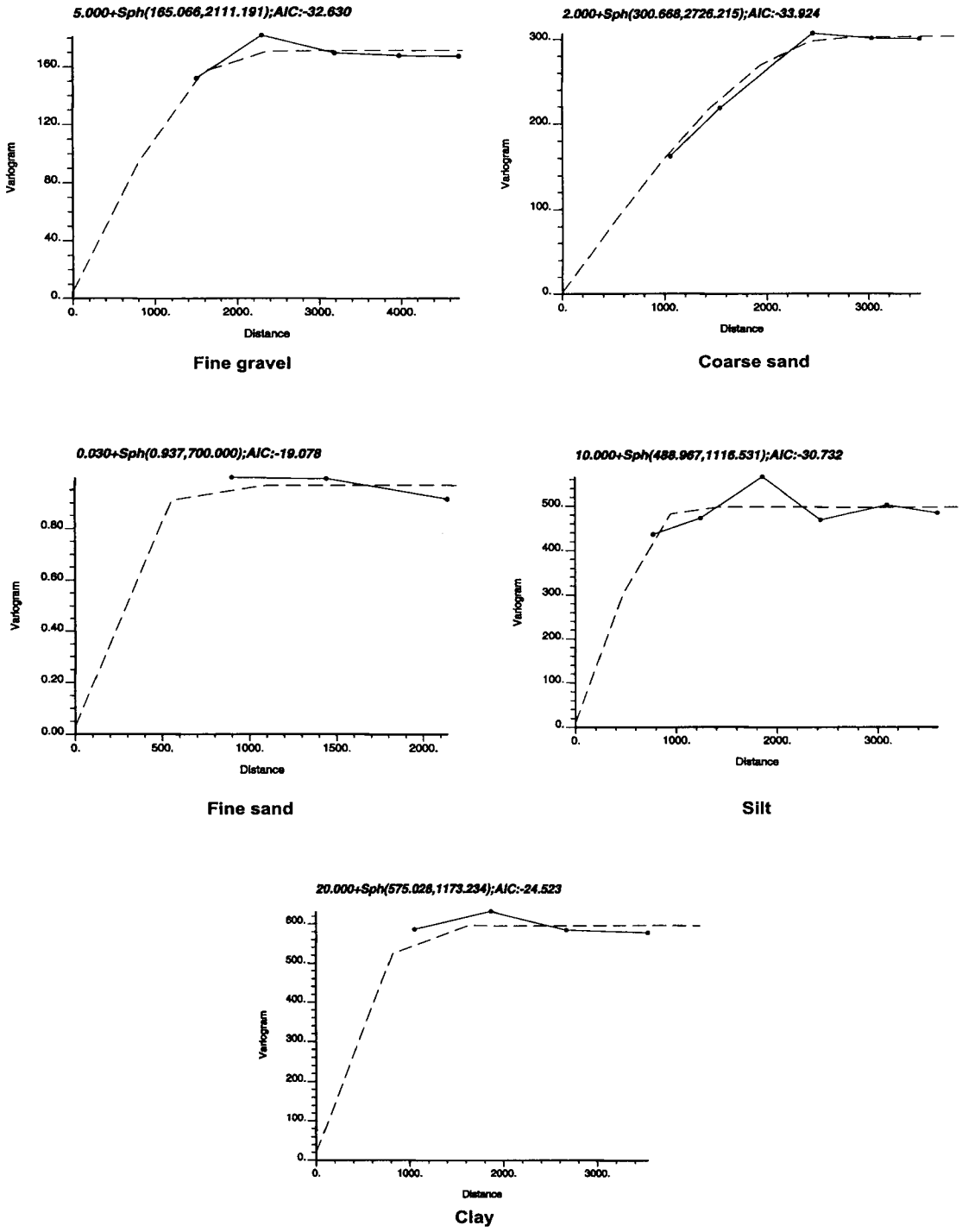

Figure B.1 Experimental semivariograms for the five different geological materials.

----- Theoretical model

• Measurement

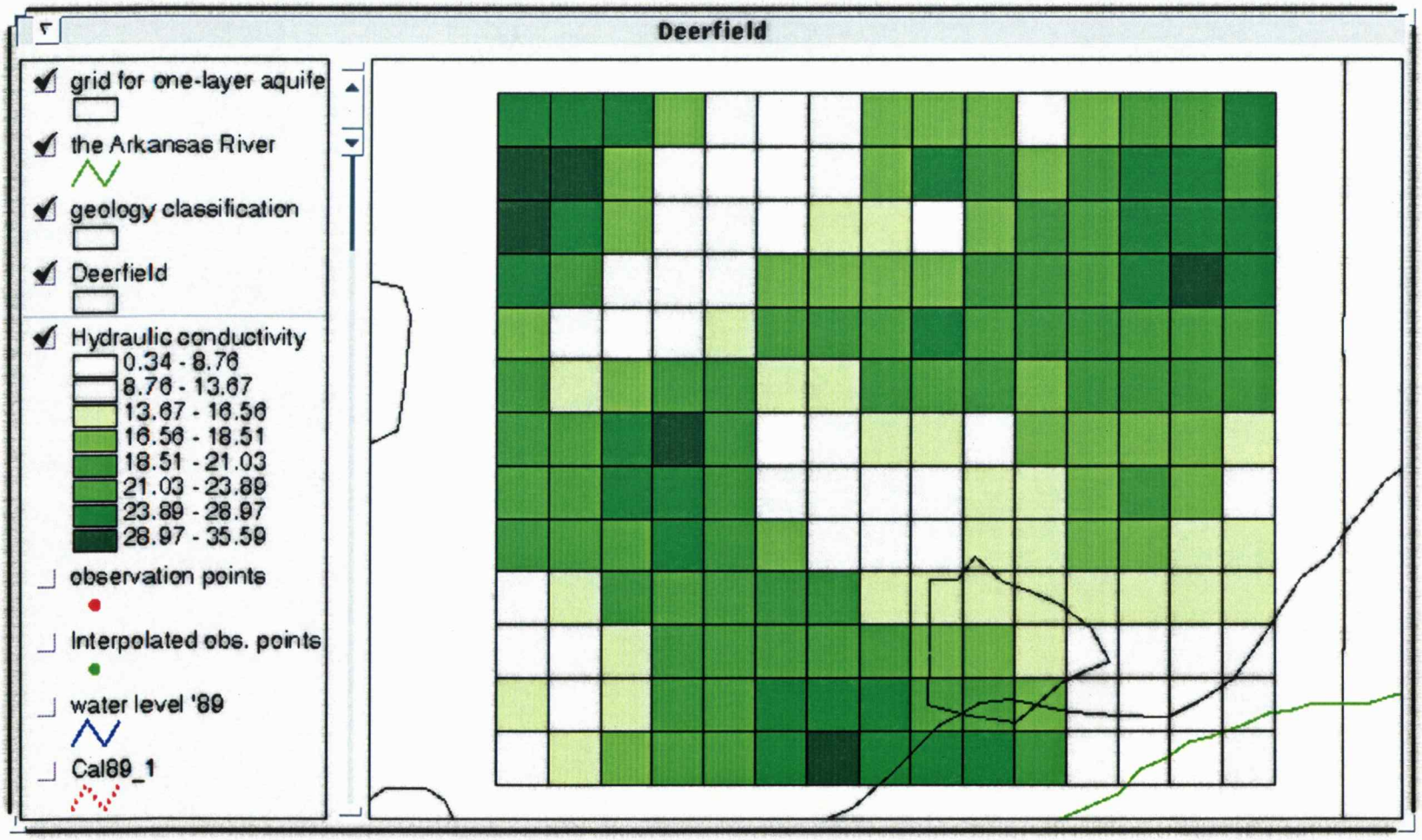

Figure B.2 The estimated distribution of the horizontal hydraulic conductivity for the one-layer model.

APPENDIX C

ESTIMATED SPECIFIC YIELD

In the two-layered model, the upper layer is unconfined layer whereas the lower layer is semi-confined. The estimated specific yields for both layers are shown in Fig. C.1 and Fig. C.2.

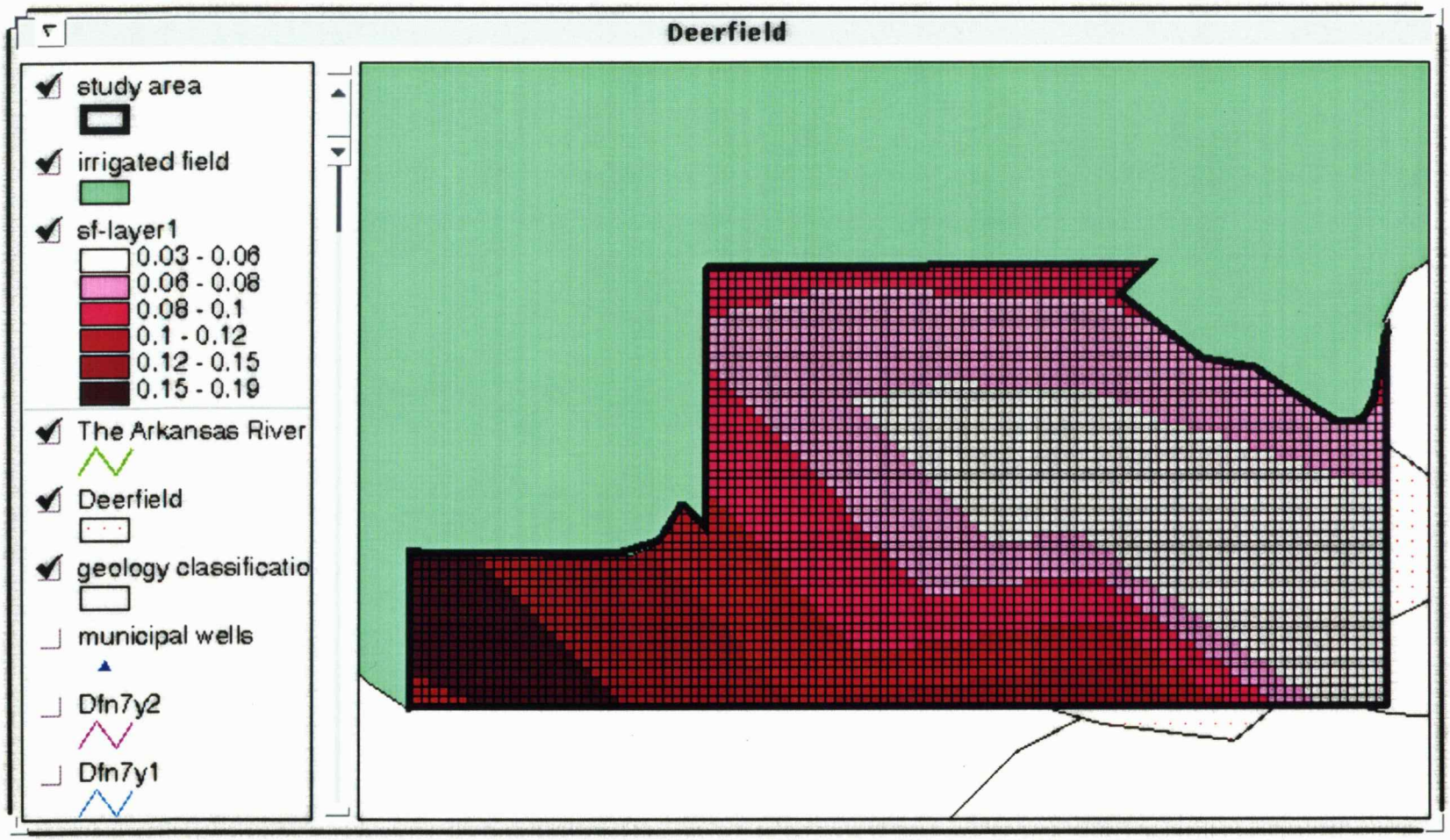

Figure C.1 The estimated distribution of the specific yield for layer 1.

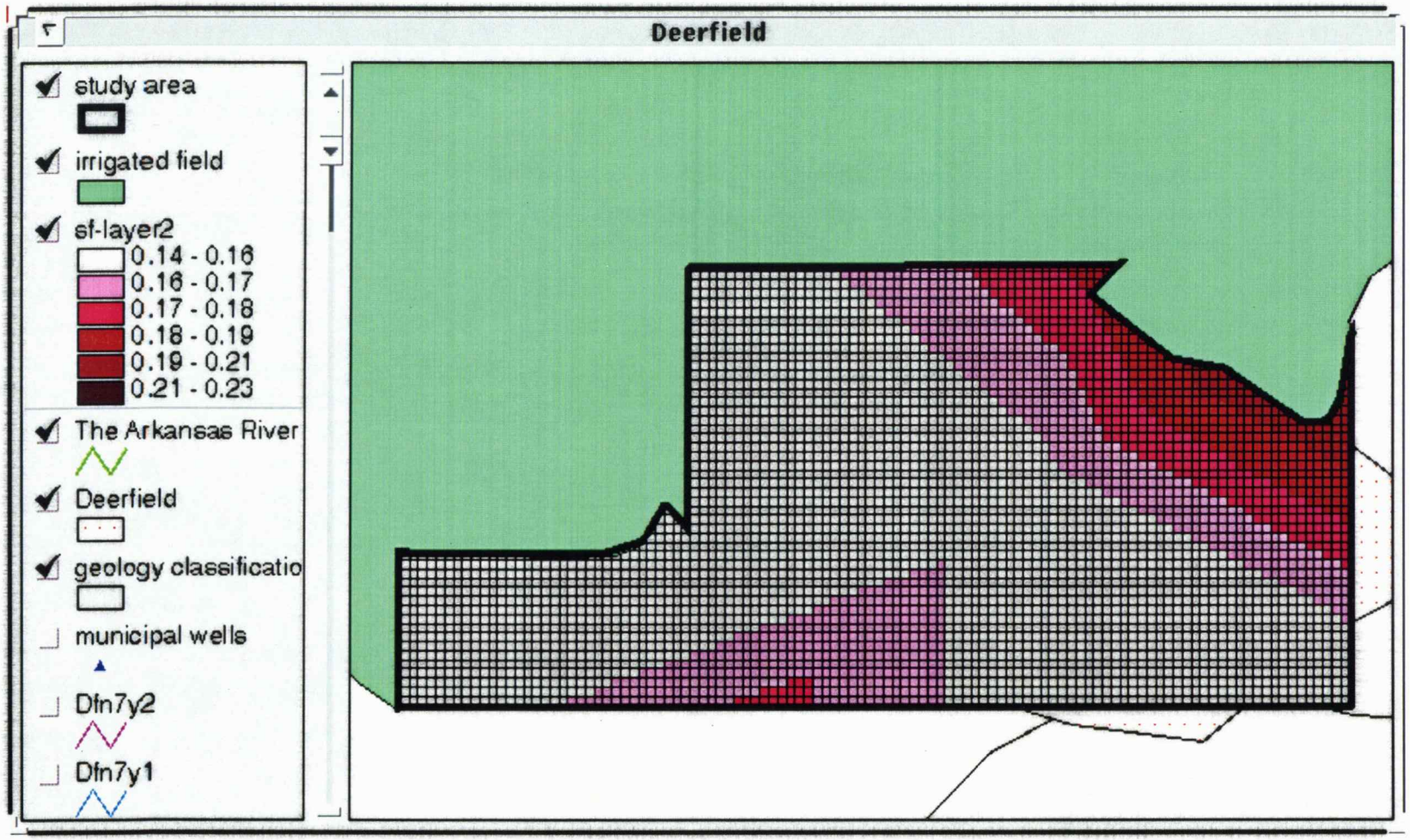

Figure C.2 The estimated distribution of the specific yield for layer 2.